Development and optimization of multidimensional methods based on online comprehensive microscale liquid chromatography and mass spectrometry

Dissertation

zur Erlangung des akademischen Grades eines

Doktors der Naturwissenschaften

– Dr. rer. nat. –

vorgelegt von

Juri Leonhardt

geboren in Osch (Kirgisische Republik)

Fakultät für Chemie

der

Universität Duisburg-Essen

2016

Die vorliegende Arbeit wurde im Zeitraum von Februar 2012 bis September 2016 im Arbeitskreis von Prof. Dr. Torsten C. Schmidt im Fachgebiet Instrumentelle Analytische Chemie (IAC) der Universität Duisburg-Essen durchgeführt.

Tag der Disputation: 21.12.2016

Gutachter: Prof. Dr. Torsten C. Schmidt

                    Prof. Dr. Oliver J. Schmitz

Vorsitzender: Prof. Dr. Christian Mayer

"Die größten Wissenschaftler

sind immer auch Künstler."

Albert Einstein

Table of contents

Summary

The technological progress to more sensitive detection techniques such as mass spectrometry reveals the complexity of samples from fields as diverse as proteomics, genomics, environmental protection and food science. One dimensional liquid chromatography coupled to mass spectrometric detection is a powerful tool for the analysis of such complex samples, but it has limitations in terms of peak capacity. An alternative separation technique with higher peak capacity is comprehensive two dimensional liquid chromatography.

This thesis deals with the development and optimization of multidimensional methods based on microscale comprehensive online liquid chromatography coupled with mass spectrometry. The performance of the microscale two-dimensional system was evaluated by a comparison to a conventional one-dimensional system. For the comparison multi-reference standards as well as samples with a complex matrix (influent of a wastewater treatment plant) were used. An automatic workflow based on Excel macro programming was developed and applied for the visualization of the two- or three-dimensional data sets.

The comparison of the reference standards showed that it is possible to detect more compounds with the conventional one-dimensional approach. In contrast, for the complex sample it was possible to detect and identify two times more compounds with the microscale two-dimensional approach than with the conventional one-dimensional approach.

The comparison showed not only the enormous potential of the two-dimensional system, but also significant technical and methodological weaknesses, including dilution caused by the system, the selection of stationary phases and data evaluation/data visualization. These aspects were addressed in this thesis and possible solutions are presented and discussed in detail.

To counteract dilution caused by the system, a 50 mm long stationary phase based on porous graphitic carbon was used in the first dimension of the microscale system at the beginning. This allowed the injection of large volumes of aqueous samples, which resulted in a better sensitivity. However, significant disadvantages relating to the peak shape of non-polar analytes could be observed. Therefore, a pre-column concept was developed in this work that is based on a serial coupling of a 1 cm short pre-column filled with porous graphitic carbon and an additional main column. The concept evaluation revealed that it is possible to inject large volumes of aqueous samples without significant peak broadening for non-polar analytes.

To evaluate the pre-column concept in the first dimension of the microscale two-dimensional system, a new method for the calculation of the orthogonality and selectivity based on the compound distribution across the separation space was developed. Additionally, the new method was compared with three established methods reported in literature. The orthogonality study of this work showed that the additional selectivity of the serially coupled columns in the first dimension results in a higher orthogonality of the two-dimensional system. In addition, there is now a simple and automatable tool available for method development in the field of two-dimensional separation techniques. The best column combination can be determined based on a few basic measurements and a representative reference standard.

Further technical developments in the field of microscale two-dimensional liquid chromatography could focus on the coupling with ion mobility spectrometry to further increase the analytical information gained from measurement of unknown samples. In that regard, the evaluation of new algorithms for automatic data processing should also be pursued.

Kurzfassung

Der technologische Fortschritt zu empfindlichen Detektionstechniken, wie der Massenspektrometrie, zeigt die Komplexität der Proben aus den analytischen Bereichen Proteomik, Genomik, Umweltschutz und Lebensmittelindustrie. Eindimensionale Flüssigkeitschromatographie gekoppelt mit massenspektrometrischer Detektion bietet ein leistungsstarkes Werkzeug zur Analyse solcher komplexer Proben, hat jedoch Limitierungen im Bereich der Peakkapazität. Eine alternative Trenntechnik mit höherer Peakkapazität ist die umfassende zweidimensionale Flüssigkeitschromatographie.

Diese Dissertation befasst sich mit der Entwicklung und Optimierung multidimensionaler Methoden basierend auf miniaturisierter umfassender online Flüssigkeitschromatographie gekoppelt mit der Massenspektrometrie.

Die Leistungsfähigkeit des miniaturisierten zweidimensionalen Systems gegenüber konventionellen eindimensionalen Systemen wurde mit einer neu entwickelten Methode zum Vergleich solcher Systeme erfolgreich evaluiert. Der Vergleich erfolgte anhand von Multireferenzstandards und Realproben mit komplexer Matrix, hier beispielhaft Kläranlagenzuläufe. Zur automatischen Visualisierung von zwei- bzw. dreidimensionalen Daten wurde ein Workflow auf Basis von Excel Makro-Programmierung entwickelt und angewandt.

Der Vergleich des Referenzstandards, der matrixarme Proben repräsentiert, zeigte, dass der klassische eindimensionale Ansatz in der Lage ist, mehr Komponenten zu detektieren. Bei den komplexen Matrixproben wurden doppelt so viele Analyten mit dem miniaturisierten zweidimensionalen System detektiert und eindeutig identifiziert als mit dem eindimensionalen Ansatz.

Der Vergleich zeigte nicht nur das enorme Potential des zweidimensionalen Systems, sondern auch deutliche technisch-methodische Schwächen auf, zu denen systembedingte Verdünnung, die Auswahl der stationären Phasen und Datenevaluierung/Datenvisualisierung gehören. Diese Aspekte konnten im Einzelnen adressiert, mögliche Lösungen vorgestellt und diese im Detail diskutiert werden.

Um systembedingten Verdünnungen entgegenwirken zu können, wurde in der ersten Dimension zu Beginn eine 50 mm lange stationäre Phase basierend auf graphitisiertem

Kohlenstoff eingesetzt. Diese ermöglichte großvolumige Injektionen wässriger Proben, was sich positiv auf die Sensitivität auswirkte, jedoch deutliche Nachteile bezüglich der Signalform der unpolaren Analyten zeigte.

In dieser Arbeit wurde daher ein Vorsäulen-Konzept erarbeitet, das auf einer seriellen Kopplung einer 1 cm kurzen Vorsäule mit graphitisiertem Kohlenstoff und einer zusätzlichen Hauptsäule basiert. Die Evaluierung zeigte, dass es möglich ist, ohne signifikante Peakverbreiterung unpolarer Analyten, große Volumina wässriger Proben zu injizieren und zu fokussieren.

Um das Vorsäulenkonzept auf der ersten Dimension des miniaturisierten zweidimensionalen Systems bewerten zu können, wurde eine neue Methode zur Bewertung der Orthogonalität/Selektivität auf Basis der Analytverteilung über das zweidimensionale Chromatogramm entwickelt und im Vergleich zu drei etablierten Methoden evaluiert. Die Orthogonalitätsstudie dieser Arbeit zeigte, dass die zusätzliche Selektivität der seriellen Kopplung der Vor- und Hauptsäule auf der ersten Dimension zur besseren Orthogonalität des zweidimensionalen Systems führt. Darüber hinaus steht nun ein einfaches und automatisierbares Tool zur Methodenentwicklung für zweidimensionale Trennsysteme zur Verfügung. Die beste Säulenkombination kann anhand weniger Basismessungen und einem repräsentativen Referenzstandard ermittelt werden.

Die weiteren technischen Entwicklungen im Bereich der miniaturisierten zweidimensionalen Flüssigkeitschromatographie liegen vor allem in der Kopplung mit der Ionenmobilitätsspektrometrie zur Erhöhung der Informationsdichte von unbekannten Proben. Diesbezüglich darf die Evaluierung neuer Algorithmen zur automatischen Datenprozessierung nicht außer Acht gelassen werden.

Chapter 1   Introduction and theoretical background

1.1 Multidimensional chromatography

The technological progress to more sensitive detection techniques like mass spectrometry reveals the complexity of environmental samples [1, 2]. However, the analysis of such complex samples with one-dimensional liquid chromatography has limitations in terms of peak capacity. The definition of peak capacity given by Neue is "*[…] the measure of the number of peaks that can fit into an elution time window t_1 to t_2 with a fixed resolution […] of 1.*" [3]. Therefore, the peak capacity (n_c) of one-dimensional systems can be calculated according to Equation 1-1, where (t_g) is the gradient time and ($\overline{w}$) the mean peak width of all detectable signals.

Equation 1-1 $$n_c = 1 + \frac{t_g}{\overline{w}}$$

In the 1980ies, Giddings introduced the multidimensional chromatography and defined this separation technique as a promising concept to increase the peak capacity [4, 5]. In the early 1990ies, Giddings described the general concept behind multiple dimensions in analytical separations. He postulated, that "*In theory […], multidimensional methods can be developed by combining almost any of the different chromatographic mechanisms or phases, electrophoretical techniques, or field-flow fractionation subtechniques.*" [6]. One of the most important multidimensional methods is two-dimensional liquid chromatography (2D-LC). Figure 1-1 shows that the interest in the field of 2D-LC is steadily increasing from the beginning of the year 2000.
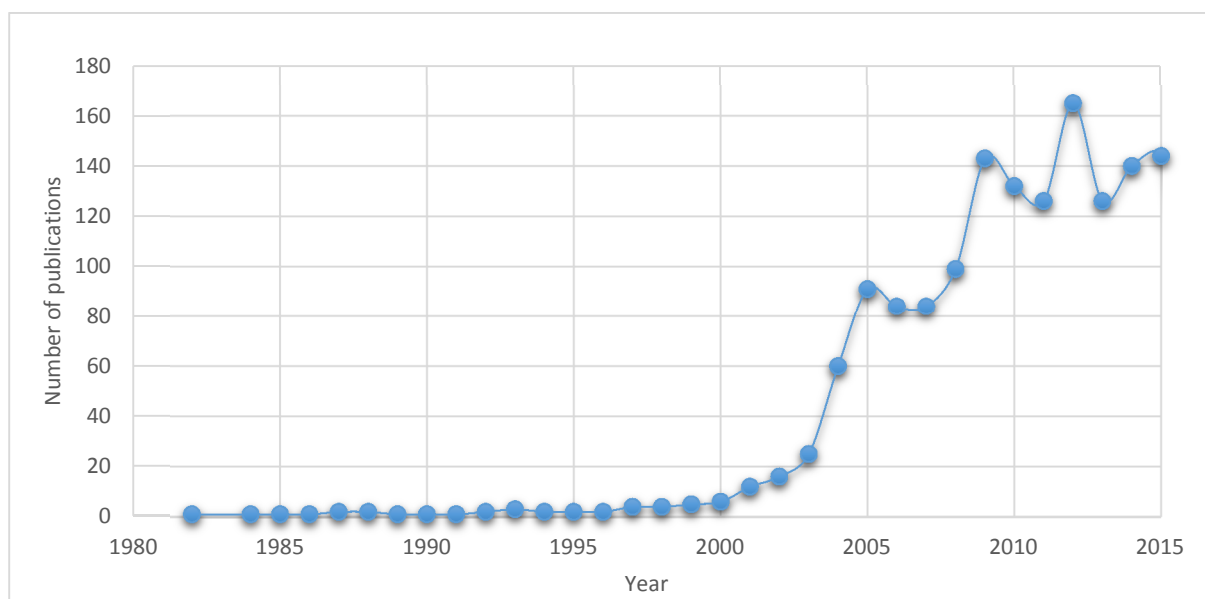
Figure 1-1:   Number of publications since 1982 containing at least one of the topics: "2D-LC", "two-dimensional liquid chromatography", "multidimensional liquid chromatography". Total number of publications: 1,552. Source: Thomas Reuters – Web of Science, https://apps.webofknowledge.com, accessed 29 June 2016.

1.2 Subcategories of 2D-LC

Basically, two-dimensional separation systems can be classified into three main categories. In the heart-cut 2D-LC (LC-LC), typically one fraction of the chromatogram of the separation column of the first dimension is "cut out" and transferred to the column of the second dimension for further separation. The heart-cut technique allows the possibility to analyze the transferred fraction on a phase system with a different selectivity. In optimum, the separation of all co-eluting compounds in this fraction is then possible. For the transfer of the fraction on the second column a simple 6-port two-position valve with a transfer-loop is needed (see Figure 1-2).
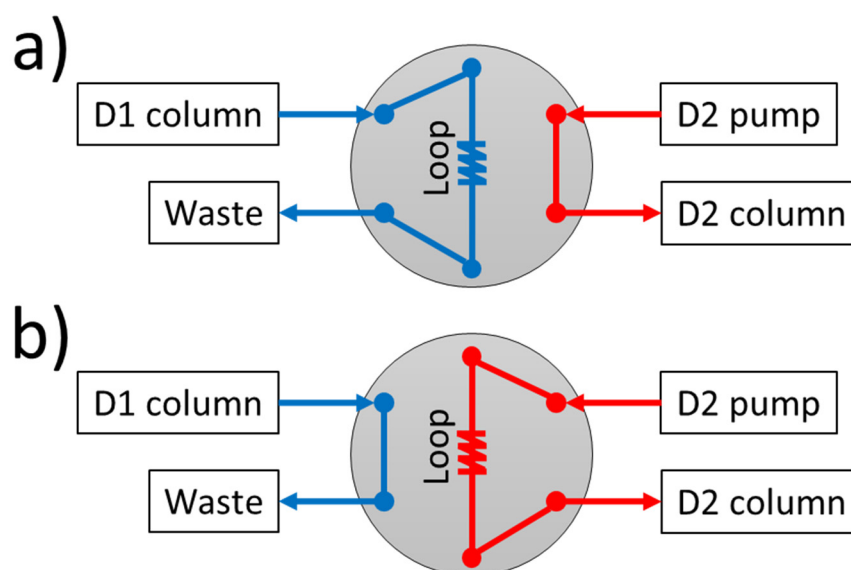
Figure 1-2:   Flow scheme of the heart-cut technique based on a 6-port 2-position valve. Position a): fraction collecting in the loop. Position b): flushing of the fraction stored in the loop on the second column.

To keep the system as flexible as possible, an additional detector after the first column should be used. A comprehensive analysis of the entire chromatogram of the first dimension is not aspired. The total peak capacity ($n_{c,2D}$) of an LC-LC system is the sum of peak capacities of the first (n_{c1}) and second (n_{c2}) dimension. Therefore, the total peak capacity can be calculated by Equation 1-2.

Equation 1-2 $$n_{c,2D} = n_{c1} + n_{c2}$$

A much more complex approach is the so-called comprehensive 2D-LC (LCxLC). In comparison to LC-LC, the complete effluent of the first dimension must be transferred to the second dimension in small fractions for the consecutive separation (Murphy–Schure–Foley criterion) [7]. An additional monitoring detector after the first dimension column is often not used, to reduce the system volume and peak broadening due to the detector (cell). Therefore, it is of decisive importance that a peak eluting from the first column should be cut three to four times (sampling). If the M-S-F criterion is not fulfilled, the chromatogram of the first dimension

cannot be reconstructed from the retention time data of the second dimension. In addition, a lower total peak capacity as theoretically possible will be obtained.

The total peak capacity of an LCxLC system is the product of peak capacities of the first and second dimension, when both dimensions are orthogonal and the loss of peak capacity by sampling can be neglected [5, 8]. Therefore, the theoretical total peak capacity for an orthogonal LCxLC system can be calculated by Equation 1-3. This Equation shows the enormous potential of two-dimensional separation techniques in terms of increasing the peak capacity.

Equation 1-3 $$n_{c,2D} = n_{c1} \times n_{c2}$$

However, it must be noted that it is not possible to achieve a fully orthogonal system in practice, because each separation mechanism is a combination of several interactions [9]. Therefore, the same interactions will partially occur on both dimensions.

A third approach is the multiple or selected heart-cut 2D-LC (sLCxLC) [10, 11]. With this approach it is possible to transfer and analyze several successive fractions of the first dimension with a different selectivity. The total peak capacity of an sLCxLC system is the sum of peak capacities of the first and second dimension, which is dependent on the number of transferred fractions (z) on the second column. Therefore, the total peak capatity can be calculated by Equation 1-4.

Equation 1-4 $$n_{c,2D} = n_{c1} + n_{c2} \times z$$

A combination of sLCxLC and LCxLC is the so called LC+LC, which was recently introduced by Stephan et al. [12] and is based on the early work of Erni and Frei [13]. In this approach the whole eluate of the first dimension is transferred to the second dimension as in the LCxLC, but in significant larger fractions (of four minutes). As a result, peaks of the first dimension are mostly not or only once modulated. Consequently, most of the compounds will be observed in

only one single second dimension chromatogram. Applying the LC+LC approach the two-dimensional separation can be illustrated as a single-dimensional chromatogram.

The peak capacity of an LC+LC system is a product of the peak capacities of both dimensions as for the LCxLC (see Equation 1-3). As a result of the long modulation time, the peak capacity of the first dimension should be corrected by Equation 1-5, where t_{total} is the total analysis time. The peak capacity value of the first dimension is equal to the number of transferred fractions on the second dimension.

Equation 1-5 $$n_{c2} = \left(\frac{t_{total}}{modulation\ time} - 1 \right)$$

The total peak capacity can be calculated according to Equation 1-6.

Equation 1-6 $$n_{c,2D} = \left(\frac{t_{total}}{modulation\ time} - 1 \right) \times n_{c2}$$

However, the online comprehensive 2D-LC is the most sophisticated technique and the development of such systems is not trivial, but it is much more suitable for the analysis of complex samples containing a high number of unknown compounds than the previously mentioned variations LC-LC and sLCxLC. The reason is that there will be no fractions that do not contain signals, which is why each fraction of the first dimension must be transferred to the second dimension for further separation. Therefore, the comprehensive 2D-LC approach is in the focus of this thesis.

1.3 Theoretical background for LCxLC

1.3.1 Operation modes of LCxLC

The comprehensive 2D-LC is subcategorized in different operation modes, which differ in terms of automation degree and total analysis time [14–16].

The first is the offline operating system. The fractions of the first dimension can be easily collected manually or automatically by a fraction collector or trapped on trap columns. The collecting time or modulation time is independent from the separation time of the second dimension. Therefore, the analysis time of the second dimension is unlimited. This approach is very flexible and a dedicated 2D-LC system is not necessary. After the first dimension separation, the system of the first dimension could be used for the second dimension separation, if system parameters like mobile and stationary phase will be changed. Additionally, first dimension fractions could be prepared prior to the analysis on the second dimension. For example, it is possible to evaporate the mobile phase, eliminate incompatible solvents and pre-concentrate the injection solution. Offline systems provide the highest possible separation performance, as a result of the unlimited analysis time on the second dimension. However, this is also the reason for very long analysis time and limited reproducibility.

The second is the online operating system, where the analysis time on the second dimension is linked to the collecting time of one fraction. Online LCxLC requires a high level of automation and a very fast cycle time on the second dimension (< 2 minutes). The run time of the first dimension, which is equal to the total analysis time, should be shorter than 60 minutes. In comparison to offline systems, the online LCxLC consists of two separate liquid chromatography systems connected by a modulation valve, which is the fully automated fraction collecting and transfer unit. The fractions are collected in two or more sample loops with an identical volume or in some cases on trap columns [17]. Because of the high automation degree of online systems, the sample throughput is higher, compared with offline systems. However, the drawback of the high level of automation is the lower peak capacity as well as the possible solvent incompatibility and peak broadening.

The third is the stop-flow operating system, which is a hybrid of the two aforementioned techniques. In general, stop-flow LCxLC operates identical to online LCxLC with the difference that the flow on the first dimension is stopped after the collection of a fraction for

the duration of the analysis on the second dimension. This reduces the complexity of the modulation valve where only one sample loop or trap column for fraction collection is needed. The cycle time of the second dimension is independent of the fraction collection time and first dimension analysis time. However, the flow stop results in additional band broadening on the first dimension. The negative effect on the peak capacity is, however, negligible [16]. The peak capacity as well as the total analysis time is more comparable to offline than online systems.

1.3.2 Online LCxLC modulation

The modulation unit is the heart of any online comprehensive 2D-LC system. The modulation unit is typically based on one or more valves and at least two transfer-loops. The purpose of the modulation is the fractionation of the first dimension eluate and the transfer of the eluate to the second dimension. There are a variety of diverse modulation schemes and instrumental setups [14, 17], but frequently used is the "two-loop"-technique.

Figure 1-3 shows the flow scheme of the two-loop technique based on two synchronously switched 4-port 2-position valves. As the name suggests, the modulation is based on two loops. The loops are filled alternately by switching both valves synchronously. In each valve position, one of the loops is filled with the effluent of the first dimension and the content of the other loop is flushed onto the second dimension column for the further separation. It is also possible to use two trap columns instead of loops in order to obtain an online enrichment or band focusing. However, a suitable elution medum should be used to prevent peak broadening on the second dimension.

Figure 1-3 shows the cycle time limitation of the second dimension of this online LCxLC technique. The cycle time of the second dimension should be equal to or smaller than the filling time of a single loop. If this is not the case, a part of the first dimension eluate is directed into the waste. To avoid this, usually a significantly lower flow rate is adjusted for the first dimension than for the second dimension, where the flow rate should be very fast to achieve the highest possible linear velocity for a fast separation and short cycle time. Therefore, the inner diameter and the length of columns as well as temperature are very important. For the first dimension with low flow rate, a longer column with a smaller inner diameter should be used as for the second dimension. For the second dimension a short column with a larger inner

diameter should be used. The difference of the column inner diameters ($\Delta i.d.$) should be between 0.5 and 1. It can be calculated according to Equation 1-7 where $d_{c,1}$ is the i.d. of the first and $d_{c,2}$ the i.d. of the second dimension column.

Equation 1-7 $$\Delta i.d. = \frac{d_{c,2} - d_{c,1}}{d_{c,2}}$$

For additional increase in linear velocity, the column backpressure should be reduced by using elevated temperature in combination with core-shell or monolithic stationary phases and in consequence higher flow rate. These modifications allow very fast cycle times of less than 60 seconds.
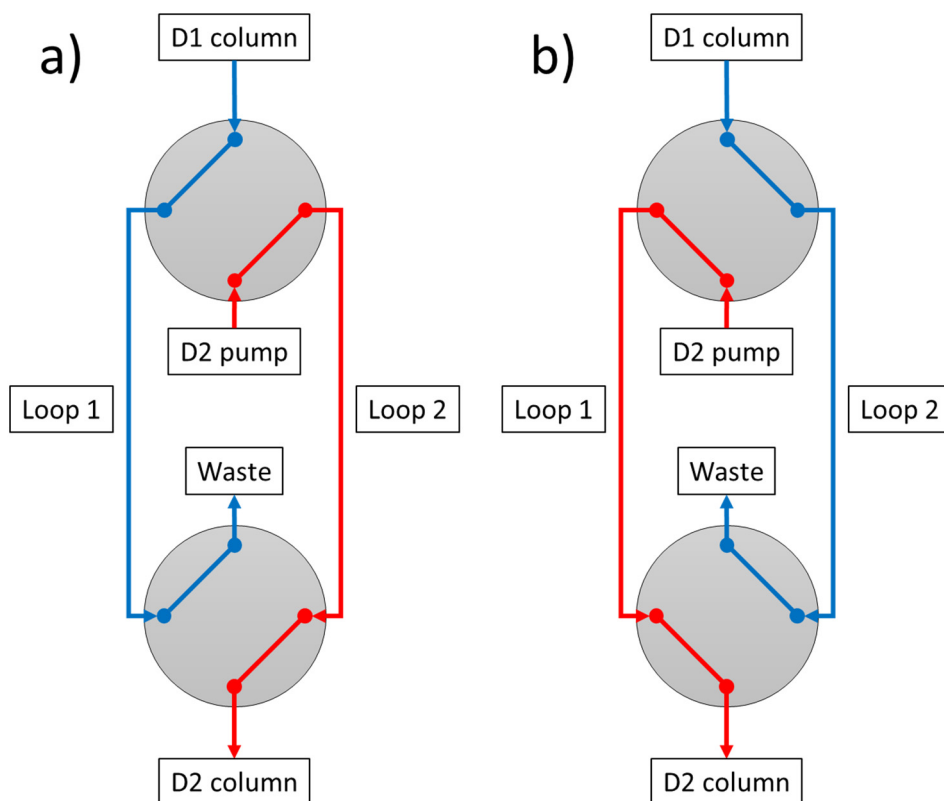
Figure 1-3:   Flow scheme of the two-loop technique based on two synchronously switched 4-port 2-position valves. Position a): fraction collecting in the 1st loop; flushing of the fraction stored in the 2nd loop. Position b): fraction collecting in the 2nd loop; flushing of the fraction stored in the 1st loop.

The major disadvantage of the presented two-loop technique is the synchronization of the two valves.

The two-loop technique can also be constructed with different instrumental setups. One of the frequently used is based on a 10-port 2-position valve that was used for all 2D-LC experiments in this work. The operation principle is the same but the synchronization of two valves is no longer needed, because only one valve is sufficient for the modulation as shown in Figure 1-4.
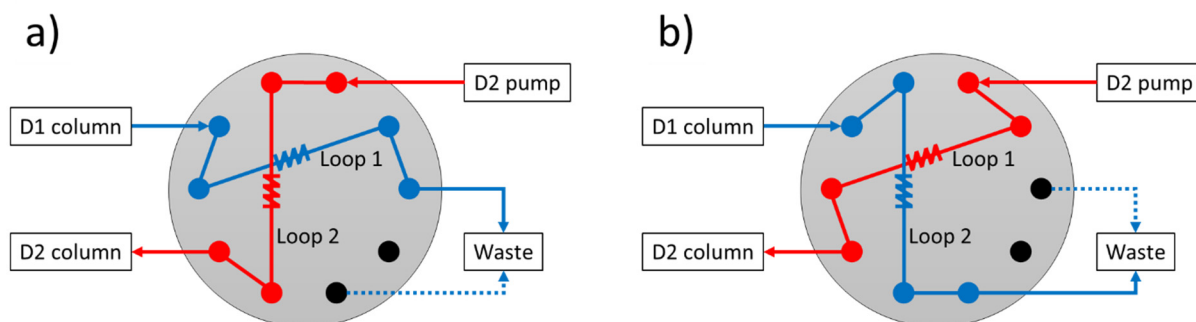
Figure 1-4:   Flow scheme of the two-loop technique based on a 10-port 2-position valve. Position a): fraction collecting in the 1st loop; flushing of the fraction stored in the 2nd loop. Position b): fraction collecting in the 2nd loop; flushing of the fraction stored in the 1st loop.

1.3.3 Visualization

The visualization of two-dimensional data is typically based on a workflow as shown in Figure 1-5. At first it must be noted that an additional detector on the first dimension is unusual. As a result, the information contained in the first dimension chromatogram must be reconstructed from the 2nd dimension chromatograms. Therefore, it is necessary to sample every first dimensional peak at least 3-4 times (Murphy–Schure–Foley criterion) to conserve the separation information by the modulation [7]. The chromatographic parameters of the first dimension should be adjusted to obtain signals, which are not too sharp and not unnecessary broad to fulfil the sampling criterion. This fraction-wise scanning process is shown in Figure 1-5 a), where each fraction is transferred and separated consecutively on the 2nd dimension.
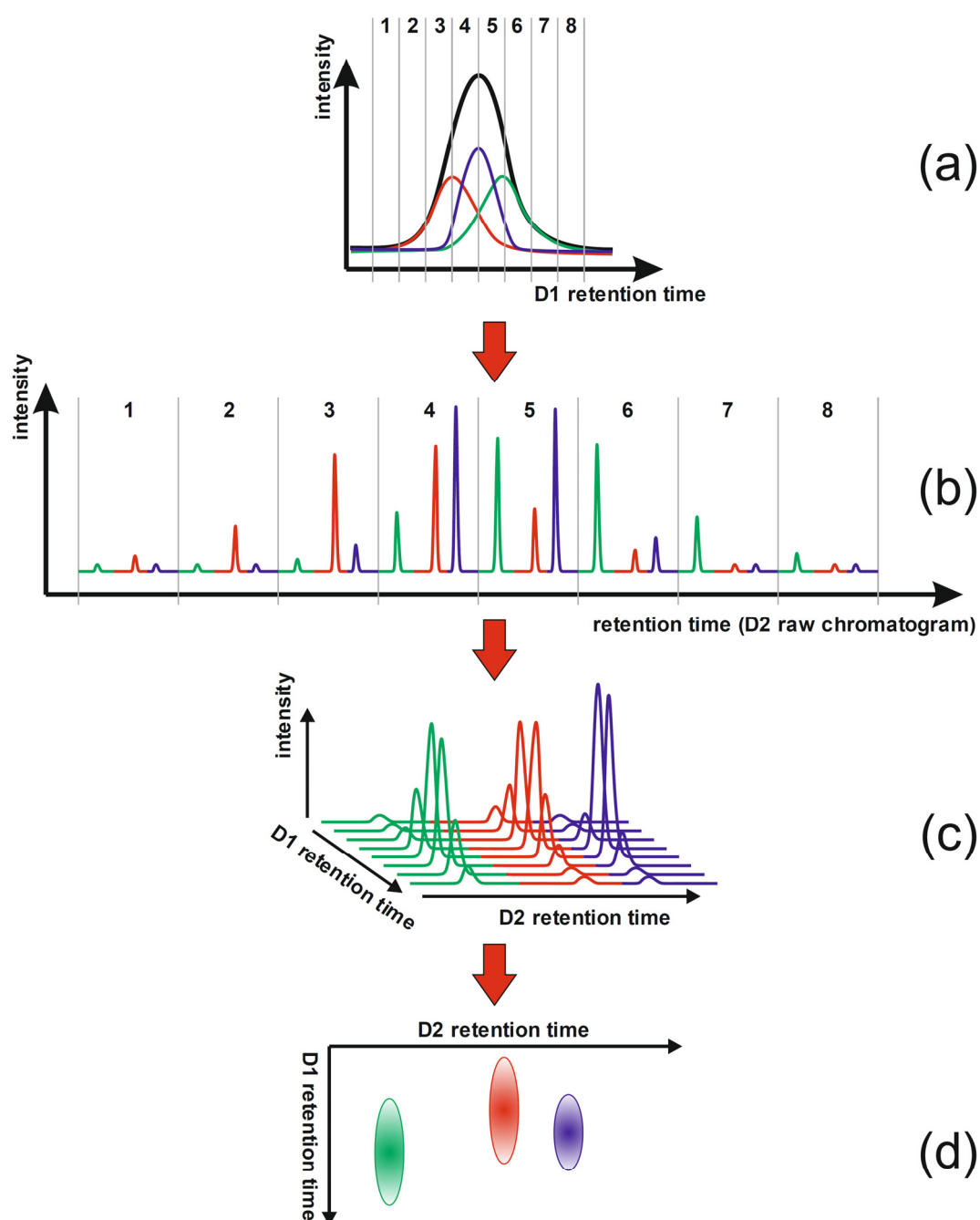
Figure 1-5:   Schematic illustration of the workflow for data visualization of two-dimensional data. a) a small chromatogram segment of the first dimension and the fractionation in eight fractions. Black line: chromatogram signal or total ion current (TIC) signal. Red, blue and green lines: co-eluting compound signals. b) raw data chromatogram of the second dimension. Signal of fraction-wise separation and consecutive detection. c) alignment of the pre-processed single second dimension runs. d) visualization as a two dimensional contour-plot. The figure is reprinted from [18] and is based on Scheme 1 in [19].

The 2nd dimension detector acquires consecutively signals from the separation of every transferred fraction in one raw chromatogram. Figure 1-5 b) shows the resulting raw chromatogram of the two-dimensional separation containing the information of both dimensions. The evaluation of raw chromatograms is not effective, so the individual chromatograms of the second dimension must be rearranged to a side-by-side matrix (Figure 1-5 c)). Fraction numbers should be used for the first dimension axis. For the second dimension axis, the retention time of each single chromatogram can be recalculated based on the modulation time interval. Finally, the raw data matrix can be used to create a 2D contour or color plot (see Figure 1-5 d)) as well as 3D plots. For a detailed statistical data evaluation a 2D dot plot (apex plot) containing only the information of the fraction number of the first and the retention time of the second dimension is more useful (see Figure 1-6).
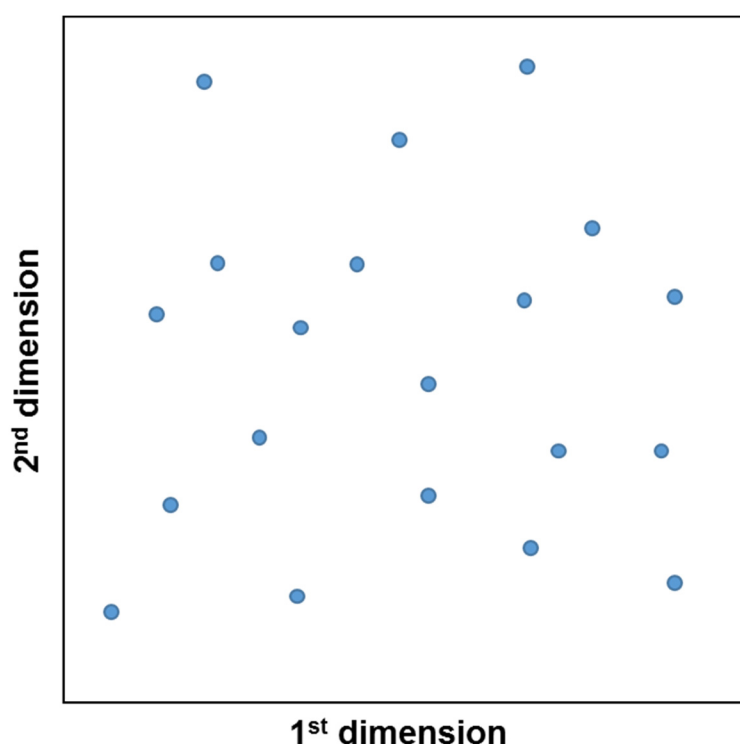
Figure 1-6:   Schematic illustration of a 2D dot plot (apex plot).

1.3.4 Orthogonality

The term "orthogonality" is well known and defined in the field of mathematics or statistics and means "perpendicular" or "independent". In the field of separation science it is used to show different retention mechanisms of the first and the second dimension [20, 21]. It includes

aspects of independency of dimensions, peak capacity, separation space and peak spreading. Therefore, an orthogonal system will be obtained when the retention mechanisms of both dimensions are statistically independent.

An orthogonal system is characterized by an even and random distribution of compounds across the two dimensional separation space [22]. This case can be only observed if the sample contains a sufficiently high number of compounds with independent compound properties [23] and when the retention mechanisms are independent. In most cases, this is not given and therefore, the theoretically possible orthogonality of 100% is difficult to achieve.

A poor orthogonality is often given by line formation or local clustering of peaks and therefore low distribution across the separation space [22]. The reason for the line formation is the high similarity of separation mechanisms in both dimensions. The peak clustering is mostly based on the similarity in chemical properties or structure.

To achieve the highest possible orthogonality for an online LCxLC system, the selectivity of stationary phases of both dimensions plays a decisive role. Therefore, different separation mechanisms should be used. However, it must be ensured that the majority of compounds can be retained by both mechanisms. In the literature different column combinations can be found, which have already been investigated [24–27]. In general, there are six groups of column combinations: IECxNP, IECxRP, SECxRP, HILICxRP, NPxRP and RPxRP. The most frequently used combinations are NPxRP or HILICxRP, as a result of different separation mechanisms and therefore a good basis for a high orthogonality. However, the mobile phases of these combinations are often incompatible, which results in peak broadening [27, 28]. This is the reason why much more RPxRP combinations are used in the last years [27, 29–32]. In general, it can be assumed that such a combination has a limited selectivity as a result of the same separation mechanisms in both dimensions. But this is not necessarily true, if two RP phases with different selectivities can be chosen [27]. The major reason for different selectivity can be explained with secondary retention interactions like hydrogen bonding, dipole-dipole, etc. [9, 33–35]. Additionally, the selectivity can be influenced by the temperature and mobile phase [36–38].

Furthermore, the selectivity and therefore the orthogonality can be increased by gradient elution for both dimensions. However, to avoid peak broadening effects it must be ensured that the mobile phases are compatible and the transfer volume to the second dimension (loop volume)

is not too large. Peak broadening effects can be minimized by applying several techniques, which are discussed in detail in Chapters 4 and 5.

For determination of the orthogonality value, there is a variety of different methods [39–43], which have been discussed in several reviews [14, 15, 27, 44, 45]. However, a universal "Swiss army knife" method for all possible application does not exist. A further detailed discussion and a comparison of the frequently used methods is given in Chapter 6.

1.4 Practical problems of online comprehensive 2D-LC

1.4.1 Mobile phase

In order to achieve the highest possible orthogonality, stationary phases as well as the mobile phases of both dimensions should exhibit a different selectivity. However, limited solvent miscibility and additionally negative solvent strength effects may affect the selectivity, retention stability and peak shape. According to a recently published review [46] and a technical note [47] the mobile phases of the following combinations are compatible: RPxRP, RPxIEC, HILICxRP, SECxRP, SECxNP, SECxIEC and IECxNP. However, the question about the solvent compatibility cannot be answered easily. Rather, there are a variety of factors that are decisive with regard to compatibility of the mobile phases. This includes the elution mode (isocratic or gradient elution) and mobile phase composition on the respective dimension as well as the transfer volume (modulation volume) for the second dimension. The best solvent compatibility can be achieved with the smallest transfer volume possible and isocratic elution on both dimensions with an equal mobile phase composition (e.g., the same portion of the organic solvent).

For a successful coupling of fully aqueous systems like IECxSEC or aqueous-based first dimension separation like IECxRP or SECxRP, only the miscibility and pH compatibility of mobile phases, as well as the solubility of analytes in both solvent systems should be considered.

More complex is the coupling of solvent systems containing aqueous and organic solvents on both dimensions in full gradient mode, which is frequently used in online LCxLC. In this case, the composition of the transfer solution as well as the gradient start conditions of the second

dimension should be investigated additionally. For the same solvent conditions of the transfer volume and gradient start point of the second dimension, larger transfer volumes can be used, because the peak broadening is minimized. Otherwise, smaller transfer volumes should be used to avoid the peak broadening.

An NPxRP system is often described as orthogonal [48], but unfortunately the solvent systems are not compatible. Organic mobile phase, which is the weakest eluent in normal phase chromatography, is the strongest in reversed phase chromatography. Therefore, an injection of fractions containing a high percentage of organic solvents eluting from the NP phase could lead to distorted or split peaks on an RP column [28]. Accordingly, the transfer volume should not be too high to minimize these effects.

According to the literature [46, 47], mobile phases of RPxRP systems are compatible. However, using full gradient mode for both dimensions, the concentration and the amount of the organic solvent within a single fraction increases corresponding to gradient conditions of the first dimension. Thus, fractions containing a high percentage of organic solvents will be injected into aqueous start conditions of the second dimension, which might lead to distorted or split peaks. One possible solution is the reduction of the transfer volume, resulting in a larger dilution on the second dimension column and an improvement of the peak shape. However, the reduction of the transfer volume results automatically in a shorter modulation time on the second dimension (cycle time needs to be reduced) or lower flowrate on the first dimension. Both factors have a strong impact on the overall system efficiency and should be evaluated. An alternative approach is the online dilution of the transfer solution prior the injection and separation on the second dimension column. Depending on dilution degree, a flow splitter could be used to reduce the transfer volume to the second dimension. However, the online dilution leads to other disadvantages, such as loss in sensitivity or more complex system configuration. Another approach is the so-called "shift gradient" mode, where the start and end point of the second dimension gradient varies depending on the gradient of the first dimension. This ensures that the start point of the second dimension gradient contains an equal portion of organic solvent as in the transferred fraction. Additionally, a better coverage of the separation space could be achieved [49]. The main problem of shift gradients is the continuous retention time shift to shorter retention time for a first dimensional signal which is transferred within several consecutive fractions on the second dimension. Large retention time shifts could lead to incorrect data interpretation of 2D-LC plots (see reference [50] Figure S2).

1.4.2 Signal intensity loss caused by the modulation

In order to conserve the first dimensional separation, the peak profile of the first dimension should be sampled 3-4 times according to the M-S-F criterion [7]. In reverse, this means that a peak of the first dimension is cut into 3-4 smaller signals with significantly reduced intensity from the second dimension. Additionally, a further dilution can be observed, especially when a larger column inner diameter is used for the second dimension than for the first dimension. Thus, it is possible that a signal can be detected in the first, but not in the second dimension, if a detection in the first dimension is used.

In order to counteract these problems, new techniques are necessary to inject large volumes of sample on the first dimension. An additional pre-concentration of the sample by SPE is also helpful and counteracts the described effects.

1.4.3 Flow rate and hyphenation to mass spectrometry

To keep the transfer volume of the first dimension as small as possible and to avoid peak broadening effects, the cycle time of the second dimension should be very fast. For a cycle time less than a minute, very high flow rates up to 5 mL min^{-1} have been reported in the literature to achieve a high linear velocity and therefore a very short gradient delay time, if a column i.d. of 4.6 mm is used [27].

The comprehensive 2D-LC was mainly developed for the analysis of very complex samples containing thousands of compounds. Therefore, high resolution (time of flight) mass spectrometry with MS/MS functionality should be used for the detection. For the hyphenation electrospray ionization (ESI) as well as atmospheric pressure chemical ionization (APCI) can be used. The optimum flow rate range of these MS sources is < 1 mL min^{-1} for ESI and < 2 mL min^{-1} for APCI. Therefore, often flow splitters are used to reduce the very high solvent load. In reverse, this means a loss in absolute analyte mass and therefore a loss in intensity.

Another aspect, which cannot be disregarded, is the very high amount of toxic solvent waste produced at such high flow rates, which is typically not recycled.

1.4.4 Microscale online LCxLC

In order to reduce the amount of toxic solvent waste and to achieve a splitless hyphenation to mass spectrometry, a microscale online LCxLC system can be used [51]. The concept of a microscale LCxLC is based on the reduction of inner diameters of the columns and transfer capillaries as well as the concomitant reduction of flow rates. For the first dimension of such a system, a nano-LC with column inner diameter < 100 μm and flow rate < 1 μL min^{-1} can be used. Proceeding from the setup of the first dimension, micro-LC with column inner diameter < 500 μm and flow rate < 100 μL min^{-1} can be used on the second dimension. Especially for the second dimension, the reducing of the column inner diameter and lower flow rate has several advantages. The reduced flow rate results in less toxic solvent waste and the system can be hyphenated splitless to a mass spectrometric detector. Additionally, the sensitivity can be increased by decreasing of the solvent load into the ion source. The reduced analyte dilution in columns with smaller inner diameter can additionally increase the sensitivity, if the same injection volume could be used as for conventional columns. However, it is recommended to adjust the injection volume to avoid peak broadening.

Another advantage of the reduced flow rate and column inner diameter is the very high linear velocity, which leads to a very short cycle time in the second dimension.

Such a microscale online LCxLC system was developed for the first time by Haun and Leonhardt et al. [2] and is the basis of this thesis.

1.5 Scope of the thesis

The aim of this thesis was the comparison of the microscale online LCxLC system to a conventional one-dimensional system and the optimization of the miniaturized approach with regard to sensitivity and orthogonality. Figure 1-7 visualizes how the different Chapters contribute to the overall goal of the thesis highlighted with the discussed system components.
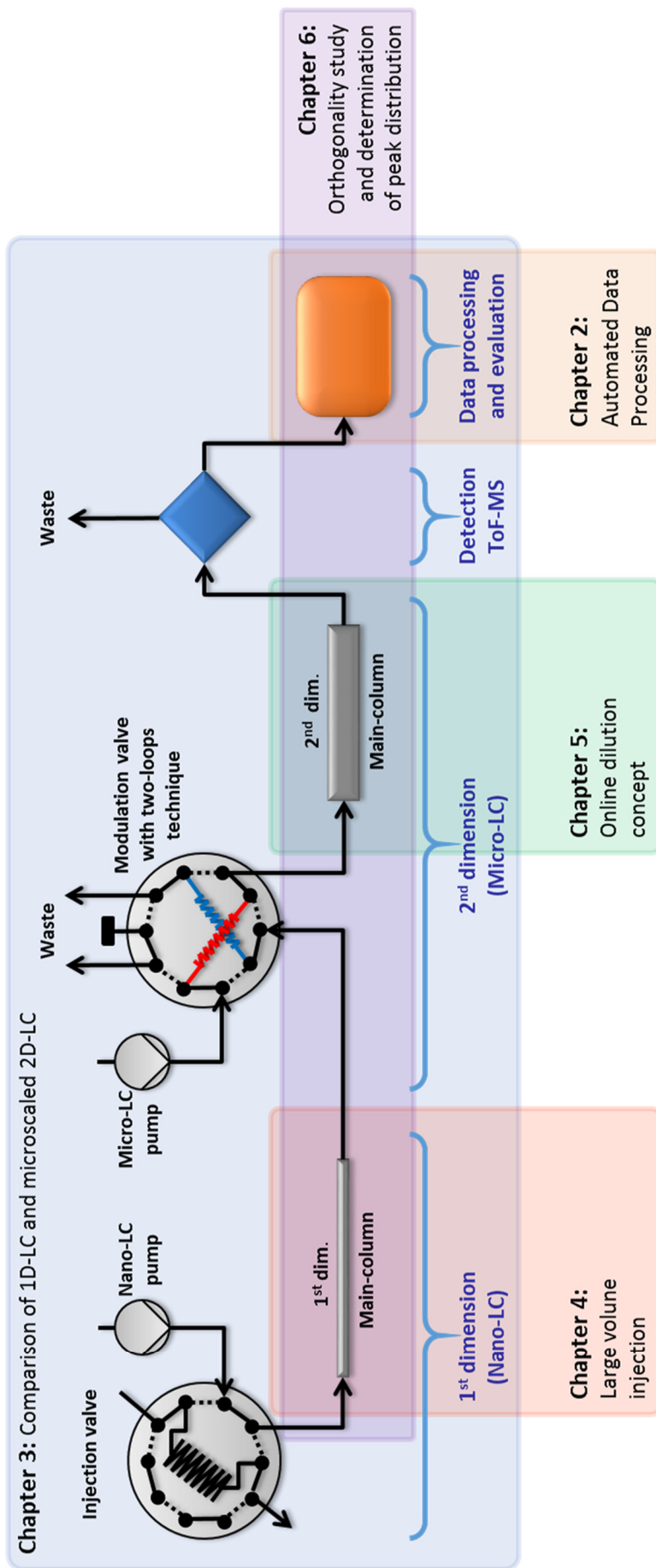
Figure 1-7:   Graphical overview of the contents of this thesis.

As is shown in Figure 1-7, automated data processing as well as visualization is the main aspect of Chapter 2. Due to the lack of commercially available software, data visualization for the microscale 2D-LC-MS was not possible. Therefore, an automated data processing workflow has been developed to transfer the raw data chromatogram, for example the total ion current (TIC), into a data matrix which can be used for a graphical data evaluation. For this purpose, a program code was developed to convert the acquired raw data to a data matrix. The program code as well as the exact description is discussed in Chapter 2.

The functionality of the developed microscale LCxLC was already demonstrated [2]. However, the comparison to a conventional one-dimensional system was not carried out. Therefore, Chapter 3 deals with the comparison of microscale 2D-LC and a conventional 1D-LC system as shown in Figure 1-7. Since the 2D-LC was developed for the analysis of complex samples, a standard routine 1D-LC method for the analysis of complex samples was chosen for the comparison. The comparison is based on a suspected-target screening and the number of identified compounds.

The microscale 2D-LC system offers significant advantages, but there are also some problems related to the limited injection volume or strong interaction of non-polar compounds with the 50 mm long PGC (porous graphitic carbon) phase on the first dimension. As shown in Figure 1-7, Chapter 4 is dealing with the optimization of the first dimension. It describes a concept where the injection volume of aqueous samples can be significantly increased, to counteract the dilution caused by the modulation and to increase the sensitivity on the second dimension. This concept is based on a short PGC pre-column, which does not minimize the strong interactions with non-polar components, but the elution time in comparison to the 50 mm long PGC phase.

As discussed in Section 1.4.1, the solvent compatibility of both dimensions is a general problem, which applies not only to the miniaturized approaches. Chapter 5 presents a concept which can minimize the peak broadening resulting from an injection of incompatible solvents. This concept is demonstrated by an injection of a solution with high organic content on an RP column under aqueous conditions. According to Figure 1-7, Chapter 5 is related to the optimization of the second dimension of the microscale 2D-LC.

Chapter 6 deals with the orthogonality study of column combinations for the microscale 2D-LC system in consideration of the aforementioned concepts and the general questions regarding the orthogonality determination. There is a variation of different methods for the determination of

the orthogonality with advantages and disadvantages. Especially the compound distribution across the separation space is often neglected, which questions the information of the orthogonality. Three frequently used methods will be discussed and a new concept for compound distribution is presented, which allows to find out the optimal column combination for a two-dimensional system.

1.6 References

1. Leonhardt J, Teutenberg T, Tuerk J, Schlüsener MP, Ternes TA, Schmidt TC. A comparison of one-dimensional and microscale two-dimensional liquid chromatographic approaches coupled to high resolution mass spectrometry for the analysis of complex samples. Anal Methods; 2015;7(18):7697–706

2. Haun J, Leonhardt J, Portner C, Hetzel T, Tuerk J, Teutenberg T, Schmidt TC. Online and Splitless NanoLC × CapillaryLC with Quadrupole/Time-of-Flight Mass Spectrometric Detection for Comprehensive Screening Analysis of Complex Samples. Anal Chem; 2013;85(21):10083–90

3. Neue UD. Peak capacity in unidimensional chromatography. J Chromatogr A; 2008;1184(1–2):107–30

4. Giddings JC. Two-dimensional separations: concept and promise. Anal Chem; 1984;56(12):1258–70

5. Giddings JC. Concepts and comparisons in multidimensional separation. J High Res Chromatog; 1987;10(5):319–23

6. Giddings CJ. Use of Multiple Dimensions in Analytical Separations. In: Cortes HJ (editor). Multidimensional chromatography - Techniques and applications. New York and Basel: Marcel Dekker, Inc.; 1990, pp. 1–28.

7. Murphy RE, Schure MR, Foley JP. Effect of Sampling Rate on Resolution in Comprehensive Two-Dimensional Liquid Chromatography. Anal Chem; 1998;70(8):1585–94

8. Davis JM, Stoll DR, Carr PW. Effect of first-dimension undersampling on effective peak capacity in comprehensive two-dimensional separations. Anal Chem; 2008;80(2):461–73

9. Snyder LR, Dolan JW, Carr PW. A new look at the selectivity of RPC columns. The hydrophobic subtraction model evaluates the selectivity of HPLC reversed-phased columns so that researchers can choose a suitable substitute or a sufficiently orthogonal second column. Anal Chem; 2007;79(9):3254–62

10. Groskreutz SR, Swenson MM, Secor LB, Stoll DR. Selective comprehensive multi-dimensional separation for resolution enhancement in high performance liquid chromatography. Part I: Principles and instrumentation. J Chromatogr A; 2012;1228:31–40

11. Wang S, Qiao L, Shi X, Hu C, Kong H, Xu G. On-line stop-flow two-dimensional liquid chromatography-mass spectrometry method for the separation and identification of triterpenoid saponins from ginseng extract. Anal Bioanal Chem; 2015;407(1):331–41

12. Stephan S, Jakob C, Hippler J, Schmitz OJ. A novel four-dimensional analytical approach for analysis of complex samples. Anal Bioanal Chem; 2016;408(14):3751–9

13. Erni F, Frei R. Two-dimensional column liquid chromatographic technique for resolution of complex mixtures. J Chromatogr A; 1978:561–9

14. François I, Sandra K, Sandra P. Comprehensive liquid chromatography: Fundamental aspects and practical considerations-A review. Anal Chim Acta; 2009;641(1-2):14–31

15. Guiochon G, Marchetti N, Mriziq K, Shalliker RA. Implementations of two-dimensional liquid chromatography. J Chromatogr A; 2008;1189(1-2):109–68

16. Kalili KM, de Villiers A. Systematic optimisation and evaluation of on-line, off-line and stop-flow comprehensive hydrophilic interaction chromatography × reversed phase liquid chromatographic analysis of procyanidins, Part I: Theoretical considerations. J Chromatogr A; 2013;1289:58–68

17. Francois I, Sandra K, Sandra P. History, evolution, and optimization aspects of comprehensive two-dimensional liquid chromatography. In: Mondello L (editor). Comprehensive chromatography in combination with mass spectrometry. Hoboken, NJ: Wiley; 2011, pp. 281–330.

18. Haun J; 2014. Miniaturized online comprehensive two-dimensional liquid chromatography. Doctoral thesis, University of Duisburg-Essen

19. Adahchour M, Beens J, Vreuls RJ, Brinkman UA. Recent developments in comprehensive two-dimensional gas chromatography (GC × GC). I. Introduction and instrumental set-up. TrAC-Trend Anal Chem; 2006;25(5):438–54

20. Marriott PJ, Schoenmakers P, Wu ZY. Nomenclature and conventions in comprehensive multidimensional chromatography- an update. LC GC Eur; 2012;25(5)

21. Gilar M, Olivova P, Daly AE, Gebler JC. Orthogonality of separation in two-dimensional liquid chromatography. Anal Chem; 2005;77(19):6426–34

22. Gilar M, Fridrich J, Schure MR, Jaworski A. Comparison of orthogonality estimation methods for the two-dimensional separations of peptides. Anal Chem; 2012;84(20):8722–32

23. Giddings JC. Sample dimensionality: A predictor of order-disorder in component peak distribution in multidimensional separation. J Chromatogr A; 1995;703(1-2):3–15

24. Dugo P, Cacciola F, Kumm T, Dugo G, Mondello L. Comprehensive multidimensional liquid chromatography: Theory and applications. J Chromatogr A; 2008;1184(1-2):353–68

25. Dugo P, Cacciola F, Donato P, Mondello L. Comprehensive two-dimensional liquid chromatography applications. In: Mondello L (editor). Comprehensive chromatography in combination with mass spectrometry. Hoboken, NJ: Wiley; 2011, pp. 391–427.

26. Dugo P, Cacciola F, Donato P, Mondello L. Comprehensive two-dimensional liquid chromatography combined with mass spectrometry. In: Mondello L (editor). Comprehensive chromatography in combination with mass spectrometry. Hoboken, NJ: Wiley; 2011, pp. 331–390.

27. Stoll DR, Li X, Wang X, Carr PW, Porter SEG, Rutan SC. Fast, comprehensive two-dimensional liquid chromatography. J Chromatogr A; 2007;1168(1–2):3–43

28. Haun J, Teutenberg T, Schmidt TC. Influence of temperature on peak shape and solvent compatibility. Implications for two-dimensional liquid chromatography. J Sep Sci; 2012;35(14):1723–30

29. Stoll DR. Recent progress in online, comprehensive two-dimensional high-performance liquid chromatography for non-proteomic applications. Anal Bioanal Chem; 2010;397(3):979–86

30. Li D, Jakob C, Schmitz O. Practical considerations in comprehensive two-dimensional liquid chromatography systems (LCxLC) with reversed-phases in both dimensions. Anal Bioanal Chem; 2015;407(1):153–67

31. Hájek T, Jandera P, Stanková M, Cesla P. Automated dual two-dimensional liquid chromatography approach for fast acquisition of three-dimensional data using combinations of zwitterionic polymethacrylate and silica-based monolithic columns. J Chromatogr A; 2016;1446:91–102

32. Vanhoenacker G, Vandenheede I, David F, Sandra P, Sandra K. Comprehensive two-dimensional liquid chromatography of therapeutic monoclonal antibody digests. Anal Bioanal Chem; 2015;407(1):355–66

33. Hetzel T, Teutenberg T, Schmidt TC. Selectivity screening and subsequent data evaluation strategies in liquid chromatography: the example of 12 antineoplastic drugs. Anal Bioanal Chem; 2015;407(28):8475–85

34. Croes K, Steffens A, Marchand D, Snyder L. Relevance of π–π and dipole–dipole interactions for retention on cyano and phenyl columns in reversed-phase liquid chromatography. J Chromatogr A; 2005;1098(1):123–30

35. Markopoulou C, Tweedlie T, Watson D, Skellern G, Reda H, Petersson P, Bradstock H, Euerby M. A study of the relative importance of lipophilic, π-π And dipole-dipole interactions on cyanopropyl, phenyl and alkyl LC phases bonded onto the same base silica. Chromatographia; 2009;70(5-6):705–15

36. Chen Y, Mant CT, Hodges RS. Temperature selectivity effects in reversed-phase liquid chromatography due to conformation differences between helical and non-helical peptides. J Chromatogr A; 2003;1010(1):45–61

37. Dolan JW. Temperature selectivity in reversed-phase high performance liquid chromatography. J Chromatogr A; 2002;965(1-2):195–205

38. Heinisch S, Rocca JL. Sense and nonsense of high-temperature liquid chromatography. J Chromatogr A; 2009;1216(4):642–58

39. Nowik W, Héron S, Bonose M, Nowik M, Tchapla A. Assessment of two-dimensional separative systems using nearest-neighbor distances approach. Part 1: Orthogonality aspects. Anal Chem; 2013;85(20):9449–58

40. Gilar M, Olivova P, Daly AE, Gebler JC. Orthogonality of separation in two-dimensional liquid chromatography. Anal Chem; 2005;77(19):6426–34

41. Camenzuli M, Schoenmakers PJ. A new measure of orthogonality for multi-dimensional chromatography. Anal Chim Acta; 2014;838:93–101

42. Dück R, Sonderfeld H, Schmitz OJ. A simple method for the determination of peak distribution in comprehensive two-dimensional liquid chromatography. J Chromatogr A; 2012:69–75

43. Zeng ZD, Hugel HM, Marriott PJ. A modeling approach for orthogonality of comprehensive two-dimensional separations. Anal Chem; 2013;85(13):6356–63

44. Schure MR, Davis JM. Orthogonal separations: Comparison of orthogonality metrics by statistical analysis. J Chromatogr A; 2015;1414:60–76

45. Gilar M, Fridrich J, Schure MR, Jaworski A. Comparison of orthogonality estimation methods for the two-dimensional separations of peptides. Anal Chem; 2012;84(20):8722–32

46. Jandera P. Comprehensive Two-Dimensional Liquid Chromatography - Practical impacts of theoretical considerations. A review. Cent Eur J Chem; 2012;10(3):844–75

47. Carr PW, Stoll DR; 2015. Two-Dimensional Liquid Chromatography - Principles, Practical Implementation and Applications. http://www.agilent.com/cs/library/primers/public/5991-2359EN.pdf. Accessed 9 October 2016

48. Jandera P. Column selectivity for two-dimensional liquid chromatography. J Sep Sci; 2006;29(12):1763–83

49. Li D, Schmitz OJ. Use of shift gradient in the second dimension to improve the separation space in comprehensive two-dimensional liquid chromatography. Anal Bioanal Chem; 2013;405(20):6511–7

50. Stoll, Talus ES, Harmes DC, Zhang K. Evaluation of detection sensitivity in comprehensive two-dimensional liquid chromatography separations of an active pharmaceutical ingredient and its degradants. Anal Bioanal Chem; 2015;407(1):265–77

51. Uclés MA, Herrera LS, Reichert B, Lozano FA, Hernando GMD, Fernández-Alba AR. Microflow liquid chromatography coupled to mass spectrometry -An approach to significantly increase sensitivity, decrease matrix effects, and reduce organic solvent usage in pesticide residue analysis. Anal Chem; 2015;87(2):1018–25

Chapter 2   Raw signal processing

2.1 Introduction

Due to the lack of suitable software, data visualization was not possible. Therefore, an automated data processing workflow was developed to convert the raw data chromatogram into a data matrix, which can be used for a graphical data evaluation.

The microscale 2D-LC system is based on syringe pumps with a defined and therefore limited pump volume. While conventional pumps can provide the flow without interruption, syringe pumps must be stopped and re-filled if the pump volume is exhausted. The flow rate of the second dimension (micro-LC) can be adjusted up to 50 µL min^{-1}. The piston stroke volume of the pump (pump channel A and pump channel B) is approximately 650 µL. Therefore, the maximum uninterrupted run time at these conditions is 13 minutes. After this time, the pump must be re-filled. This limitation makes it impossible to provide continuous flow for the complete run time of the first dimension, which is usually longer than 13 minutes. For the first dimension (nano-LC) the limited stroke volume is not a problem since flow rates lower than 1 µL min^{-1} are typically used. As described recently, the overall run-time of the first dimension was 104 minutes. This means that the pump of the second dimension must be stopped and re-filled in total 8 times. Figure 2-1 exemplarily shows gradient profiles of the first and second dimension of a 2D-LC system for continuous flow pumps (Figure 2-1 a and b) and stop flow syringe pumps (Figure 2-1 a and c). Due to the pump stop it is not possible to create only one raw data chromatogram, which can be processed. Rather, a data set of several raw files (number of raw files is equal to the number of re-fill steps) containing the complete 2D-LC run is obtained, which is a major problem for commercially available 2D-LC software. This was the reason for the development of own scripts or programs.
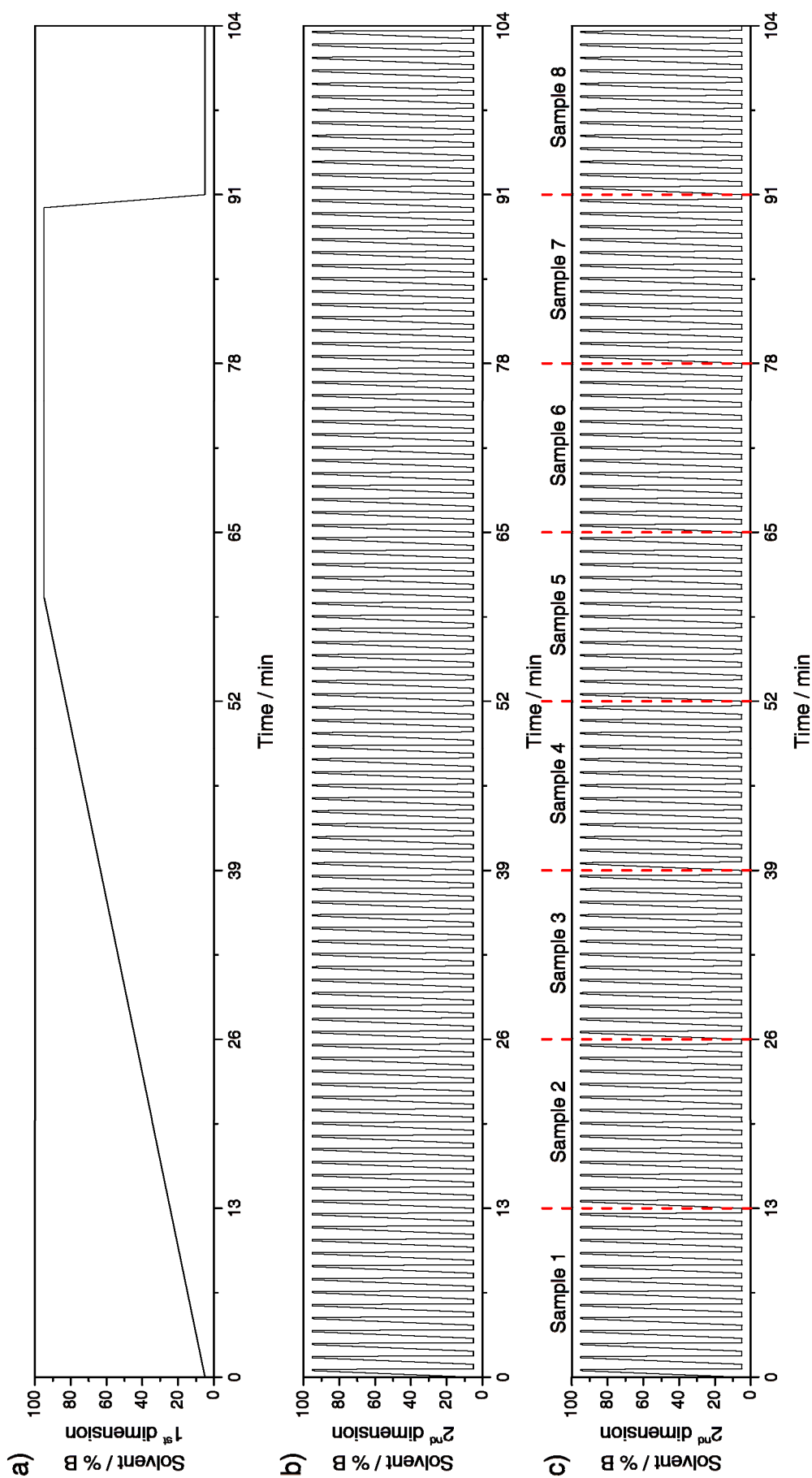
Figure 2-1:   Gradient profiles of a) the first dimension, b) the second dimension for continuous flow pumps and c) second dimension for syringe pumps with limited stroke volume. Red lines represent the pump re-fill of the second dimension.

2.2 Procedure for data processing

For data set raw signal processing to a data matrix, Microsoft Excel 2010 with Visual Basic for Applications 7.0 as well as Microsoft Excel 2013 with Visual Basic for Applications 7.1 was used and for data visualization OriginLab Pro versions 8.6 and higher were used.

The workflow for data processing is given in Figure 2-2 for an example with a total 2D-LC run time of 104 minutes, modulation time of 1 minute and pump re-fill time after 13 minutes. Therefore, the data set contains 8 raw data files and each of them contains information of 13 fractions.

At first all raw files of one data set (Sciex data set is equal to one WIFF file) should be exported as ASCII (*.txt) files (Figure 2-2 1 and 2). Now, 8 raw files containing the complete 2D-LC run are obtained (Figure 2-2 3). Each of these files needs to be processed sequentially (Figure 2-2 4). The process is starting with the load of the 1st raw file, the script filters the raw signal in one minute intervals and copies the data into the data matrix sequentially from the 1st to the 13th fraction (Figure 2-2 5). Following, the 2nd file is loaded and processed with the same procedure. After the processing of all 8 raw files a full data matrix of the complete 2D-LC run (Figure 2-2 6) is obtained, which can be used for the visualization with Excel or OriginLab (Figure 2-2 7).
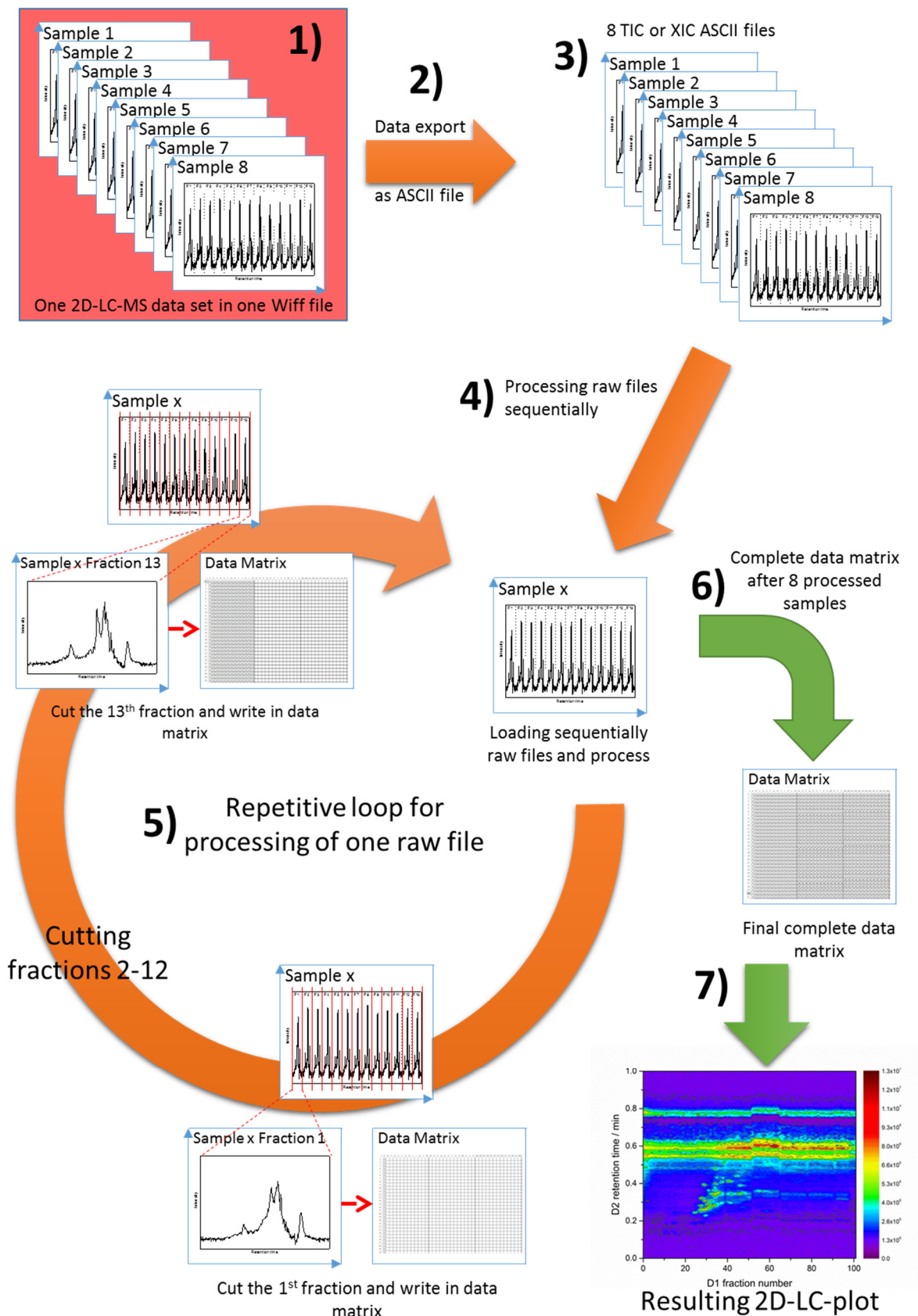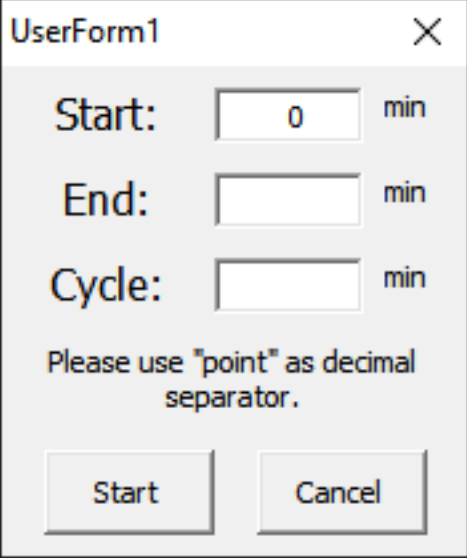
Figure 2-2:   Schematic illustration of the workflow for raw data processing.

Instruction for the use of the script:

1. Export the raw signal (TIC, XIC, UV …) as ASCII files.

2. Delete the head rows inside the ASCII file, if available. File must contain only raw data values.

3. Number the files according to the sequence (example: 1_run, 2_run, 3_run …). This is very important for the automated file import and processing.

4. Copy all files of one sample to the same folder. All files inside this folder will be imported and processed. Do not include files of other data sets or samples!

5. Open the Excel file containing the script with Excel 2010 or higher.

6. Click on Start button, select the file folder as well as the first file, and confirm.

2.3 Script code with explanations and comments

Module	Script	Explanations and comments
User Interface	 Start input box = „TextBox1_start" End input box = „TextBox2_end" Cycle input box = „TextBox3_period" Start button = „CommandButton1" Cancel button = „CommandButton2"	Start input box: Please enter the start time of the single run; default=0 End input box: Please enter the end time of a single run Cycle input box: Please enter the cycle or modulation time in minutes. Use point as decimal separator Start button: initialize the data processing Cancel button: Cancel the data processing

User Interface code	`Public Sub CommandButton1_Click()`
	`bCancel = False`
	`Me.Hide`
	`End Sub`
		Code for start button

	`Public Sub CommandButton2_Click()`
	`bCancel = True`
	`Me.Hide`
	`End Sub`
		Code for cancel button

	`Public Sub TextBox1_start_Change()`
	`Dim t_start As Variant`
	`t_start = TextBox1_start.Value`
	`End Sub`
		Code for start input box

	`Public Sub TextBox2_end_Change()`
	`Dim t_end As Variant`
	`t_end = TextBox2_end.Value`
	`End Sub`
		Code for end input box

	`Public Sub TextBox3_period_Change()`
	`Dim t_period As Variant`
	`t_period = TextBox3_period.Value`
	`End Sub`
		Code for cycle input box

| Main code for signal processing. | Public bCancel As Boolean
Sub DataImport()

    Dim ws2 As Worksheet
    Dim irow As Integer
    Dim pcol As Long
    Dim m As Variant
    Dim run_start As Variant
    Dim run_end As Variant
    Dim run_period As Variant
    Dim sheetIndex As Variant
    Dim t_start As Variant
    Dim t_end As Variant
    Dim t_period As Variant
    Dim X As String   'Status bar
    Dim SBar As String   'Status bar
    Dim fraction As Integer

    fraction = 0

    'Enable Status bar
    X = "Please wait ..."
    SBar = SBar & X
    Application.StatusBar = "Data import is active.   " & SBar

    'Disable Screen update.
    Application.ScreenUpdating = False

    'Enable point as decimal separator
    Application.UseSystemSeparators = False
    Application.DecimalSeparator = "."
    Application.ThousandsSeparator = ","

    'Initialize User Interface
    UserForm1.Show

    If bCancel = True Then Exit Sub

    'Write "1st Dim./2nd Dim." in cell D2
    Sheets("DataMatrix").Select
    Range("a2").Value = "1st Dim./2nd Dim."
    Range("a2").Select
      With Selection
        .HorizontalAlignment = xlCenter
        .VerticalAlignment = xlBottom
        .WrapText = False
        .Orientation = 0
        .AddIndent = False
        .IndentLevel = 0
        .ShrinkToFit = False | Cancel button value.
Script name.

Variable definitions.

Set fraction count to 0.
Enable Status bar to confirm that Excel is processing.

Disable screen update to increase speed.

Enable point as decimal separator.

Initialize User Interface.

If canceled, stop process.
Select sheet "DataMatrix" and write "1st Dim./2nd Dim." in cell D2.
Text format. |

	``.ReadingOrder = xlContext
    .MergeCells = False
  End With

'Cutting process of imported files
  run_start = UserForm1.TextBox1_start.Value
  run_end = UserForm1.TextBox2_end.Value
  run_period = UserForm1.TextBox3_period.Value

  Range("M1").Value = "Start="

  Range("N1").Value = run_start

  Range("P1").Value = "End="

  Range("Q1").Value = run_end

  Range("S1").Value = "Period="

  Range("T1").Value = run_period

  strExt = "*.txt"
  ZuÖffnendeDatei = Application.GetOpenFilename("Text_files ("
& strExt & "), " & strExt, _
              Title:="Folder selection, please select only the first
file …")
  If ZuÖffnendeDatei = False Then Exit Sub

  'Select only the first file, other files will be imported
automatically.
  strPath = CurDir & "\"
  If strPath = "" Then
    Exit Sub
  Else
    ChDir strPath
    strFile = Dir(strPath & strExt)
    Do While Len(strFile) > 0
      Workbooks.OpenText   Filename:=strPath   &   strFile,
DataType:=xlDelimited, _
        TextQualifier:=xlDoubleQuote,
ConsecutiveDelimiter:=True, _
        Tab:=True, Semicolon:=False, Comma:=False, _
        Space:=True,   Other:=False,
trailingMinusNumbers:=False

      Sheets(1).Move
After:=ThisWorkbook.Sheets(ThisWorkbook.Sheets.Count)

      sheetIndex = Worksheets(ActiveSheet.Name).Index
      'MsgBox ("sheetIndex_" & sheetIndex)``` | Cutting process of imported files.

Write "Start=" in cell M1.
Write start input box value in cell N1.
Write "End=" in cell P1
Write end input box value in cell Q1.
Write "Period=" in cell S1.
Write cycle input box value in cell T1.

Open window to select the raw files.

If cancel, stop the process.

Start import data loop Import raw data. X-value = column A; Y-value = column B.

Rename sheet to ASCII raw file name. |

```‘Sheet modification and data processing```	
``` ‘Copy x-values for further calculation```	Copy x-values to column D.
``` Columns("A:A").Select```	
``` Selection.Copy```	
``` Columns("D:D").Select```	
``` ActiveSheet.Paste```	
``` Range("A1").Select```	
``` ‘Column names```	Write column names.
``` Range("A1").Select```	
``` ActiveCell.FormulaR1C1 = "x old"```	Cell A1 = "x-old".
``` Range("B1").Select```	
``` ActiveCell.FormulaR1C1 = "y old"```	Cell B1 = "y-old".
``` Range("C1").Select```	
``` ActiveCell.FormulaR1C1 = "diff"```	Cell C1 = "diff".
``` Range("D1").Select```	
``` ActiveCell.FormulaR1C1 = "x new"```	Cell D1 = "x new".
``` Range("E1").Select```	
``` ActiveCell.FormulaR1C1 = "y new"```	Cell E1 = "y new".
``` Range("A2").Select```	
``` 'Auto-Zero for UV data```	Auto-Zero for UV data, please exclude this step for MS data.
``` Range("C2").Select```	
``` ActiveCell.FormulaR1C1 = "=0" ‘without substraction,``` ```for MS data```	Code for MS data.
``` ‘ActiveCell.FormulaR1C1 = "=RC[-1]*(-1)" 'with``` ```substraction for UV-data```	Code for UV data.
``` Range("E2").Select```	Activate and deactivate by add or delete " ‘ " before "ActiveCell. For…"
``` ActiveCell.FormulaR1C1 = "=RC[-3]+R2C3"```	
``` Range("E2").Select```	
``` Selection.AutoFill Destination:=Range("E2:E50000"),``` ```Type:=xlFillDefault```	
``` Range("E2:E50000").Select```	One of the options must be activated.
``` Range("F1").Select```	
```‘Interpolation of the raw data```	Data interpolation (to 50000 data points) as a result of non-constant time steps for MS data.
``` 'Calculation of dx```	
``` Range("F1").Select```	
``` ActiveCell.FormulaR1C1 = "Time-new"```	
``` Range("g1").Select```	
``` ActiveCell.FormulaR1C1 = "Intensity-new"```	
``` Range("i2").Select```	Number of data points should be selected in dependence of the run time.
``` ActiveCell.FormulaR1C1 = "xmin"```	
``` Range("i3").Select```	
``` ActiveCell.FormulaR1C1 = "xmax"```	
``` Range("i4").Select```	
``` ActiveCell.FormulaR1C1 = "n"```	
``` Range("i5").Select```	

ActiveCell.FormulaR1C1 = "dx" Range("j2").Select ActiveCell.FormulaR1C1 = "=RC[-6]" Range("j3").Select ActiveCell.FormulaR1C1 = run_end Range("j4").Select ActiveCell.FormulaR1C1 = "50000" Range("j5").Select ActiveCell.FormulaR1C1 = "=(R[-2]C-R[-3]C)/R[-1]C"	Lowest time value. Highest time value. Number of data points. New time between two data points.
'Calculation of new x-values Range("f2").Select ActiveCell.FormulaR1C1 = "=RC[-2]" Range("f3").Select ActiveCell.FormulaR1C1 = "=R[-1]C+R5C10" Range("f4").Select ActiveCell.FormulaR1C1 = "=R[-1]C+R5C10" Range("f4").Select Selection.AutoFill Destination:=Range("f4:f50002"), Type:=xlFillDefault Range("f4:f50002").Select	Calculation of the new x-values.
'Interpolation of the new y-values Range("g2").Select ActiveCell.FormulaR1C1 = _ "=TREND(INDEX(C[-2],MATCH(RC[-1],C[-3],1),1):INDEX(C[-2],MATCH(RC[-1],C[-3],1)+1,1),INDEX(C[-3],MATCH(RC[-1],C[-3],1),1):INDEX(C[-3],MATCH(RC[-1],C[-3],1)+1,1),RC[-1])" Range("g2").Select Selection.AutoFill Destination:=Range("g2:g50002") Range("g2:D50002").Select Range("E2").Select	Interpolation of new y-values based on the raw y-values. For a good correlation the number of data points should be very high.

'Filter loop
For m = run_start To run_end – run_period Step run_period
'MsgBox ("Ergebnis L:" & run_period)
 	
   'Definition of filter borders (variabel)
   t_min = m
   t_max = t_min + run_period
 	
'MsgBox ("Ergebnis t_min:" & t_min)
'MsgBox ("Ergebnis t_max:" & t_max)
 	
   'Set filter properties
      Sheets(sheetIndex).Select
      Range("f1:g50500").Select
      Selection.AutoFilter
	Cutting of the raw signal with the filter function. Based on the input values "Start", "End" and "Cycle", filter settings were chosen. Filter shows values between Criteria1=lower border and Criteria2= Upper border. Both borders areincreased automatically after

Code	Description
`ActiveSheet.Range("$f$1:$g$50500").AutoFilter Field:=1, Criteria1:=">=" & t_min, _` `        Operator:=xlAnd, Criteria2:="<" & t_max`	every loop cycle by the cycle input value.

`'Copy filtered/showed values`
`Range("f1:g50500").Select`
`Selection.Copy`
	Copy the filtered values.

`'Create a new sheet`
`fraction = fraction + 1`
`Sheets.Add After:=Sheets(Sheets.Count)`
`ActiveSheet.Name = "Fraction_" & fraction`
	Set fraction number. Create a new sheet for the current cycle. Format: "Fraction_#".

`Range("A1").Select`
`Selection.PasteSpecial                Paste:=xlPasteValues,`
`Operation:=xlNone, SkipBlanks _`
`    :=False, Transpose:=False`
`Range("B1").Select`
`Application.CutCopyMode = False`
	Select cell A1 and paste values of the current cycle.

`Range("B1").Select`
`ActiveCell.Value = t_min`
`'MsgBox ("t_min" & t_min)`
	Write cycle start time in cell B1 (min).

`'Copy (intensity) y-values`
`Range("b1:b50020").Select`
`Selection.Copy`
`Sheets("DataMatrix").Select`
	Copy Intensity values of the current cycle for the transfer into the Data Matrix.

`pcol       =       1       +       ActiveSheet.Cells(16, 300).End(xlToLeft).Column`	Determine the last free column in row 16.

`Range(Cells(2, pcol), Cells(2, pcol)).Select`
`Selection.PasteSpecial                Paste:=xlPasteValues,`
`Operation:=xlNone, SkipBlanks _`
`        :=False, Transpose:=False`
	Select the second row in last free column and paste the copied y-values.

`Sheets(sheetIndex).Select`
`ActiveSheet.Range("$a$1:$b$2030").AutoFilter Field:=1`
`Selection.AutoFilter`
	Select the raw data and reset the filter settings.

`Next m`	Start new loop for the next cycle/fraction.

`    strFile = Dir() 'next file`
`  Loop`
`End If`
	Start new loop and select the next raw ASCII file.

`Range("a1").Select`	

	'Change status bar massage Application.StatusBar = "Data import is finished!"	If all raw ASCII files are processed, set a new message at the status bar. "Data import is finished!"
	'Enable system used decimal separator Application.UseSystemSeparators = True	Enable system used decimal separator.
	'Enable screen update Application.ScreenUpdating = False	Enable screen update.
	Sheets("DataMatrix").Select Range("V1").Value = "DataLocation=" Range("W1").Value = strPath Range("A1").Select	Select the DataMatrix sheet and write "DataLocation=" in cell V1 and the data location in cell W1.
	'Show massage MsgBox ("Data import is finished!")	Show the message "Data import is finished!".
	'Disable status bar Application.StatusBar = False	Disable the status bar.
	End Sub	End of the code.

Chapter 3   A comparison of one-dimensional and microscale two-dimensional liquid chromatographic approaches

The interest in two-dimensional liquid chromatography separations is growing every year together with the number of open questions on the benefits of multidimensional systems in comparison to one-dimensional liquid chromatography. In order to solve some of these open questions this work presents a comparison of one-dimensional and microscale two-dimensional liquid chromatography coupled to high resolution mass spectrometry for targeted analysis in wastewater. The comparison is based on the evaluation of a reference standard mixture containing 99 compounds and a real wastewater sample. For the evaluation and compound identification three different criteria were chosen. At first, a deviation of ± 5 ppm from the exact mass was defined as acceptable to include the compound for further evaluation. To eliminate false positive results, a maximum retention time deviation of less than 2.5% for each compound of the reference standard and the compounds detected in the wastewater sample was defined for a positive identification as a second criterion for 1D-LC and the second dimension of 2D-LC. In the third step, fragment information from MS/MS experiments was used for further identification of compounds in wastewater. Additionally, the influence of a higher mass accuracy of 1 ppm on the number of identified compounds in comparison to a mass accuracy of 5 ppm was investigated. The results showed that the number of identified compounds was higher by a factor of three in the wastewater sample when using the microscale 2D-LC approach. Moreover, a higher reliability for compound identification is obtained when using retention time and MS/MS information as identification criteria instead of only applying high mass accuracy of 1 or 5 ppm.

3.1 Introduction

One-dimensional liquid chromatography (1D-LC) coupled to mass spectrometric detection is a powerful tool for the analysis of complex environmental samples that might contain several thousands of different components [1, 2]. However, the analysis of such complex samples with one-dimensional liquid chromatography has limitations in terms of peak capacity [3]. Alternative analysis techniques with higher peak capacity are therefore deemed necessary to resolve as many compounds as possible. In that regard, two-dimensional liquid chromatography (2D-LC), which is well established in several analytical fields including proteomic and genomic research [4], might also be a powerful tool for the comprehensive analysis of environmental samples.

In general two main variations of 2D-LC are applied. The first one is the heart-cut or selective two-dimensional technique (LC-LC, sLCxLC), which allows to cut one [5] or a few selected [6, 7] fractions of the effluent of the first dimension that are then transferred to a second column. The second technique is the comprehensive 2D-LC (LCxLC) [5, 8, 9] where the whole eluate of the first dimension column (D1) is transferred in small fractions to the second dimension column (D2). Such multidimensional approaches offer the possibility to separate complex samples on stationary phases with different selectivity.

In contrast to 1D-LC, 2D-LC is often associated with very long analysis times of several hours or even days if offline LCxLC is applied [10]. Moreover, a more complex system configuration is needed if online LCxLC is used. A further disadvantage is the dilution introduced by the modulation between the first and second-dimension of an online LCxLC system. Furthermore, very fast cycle times of less than 1 min are necessary for the second dimension separation which often results in high flow rates up to 5 mL min^{-1} [11–13]. Such high flow rates are not compatible with electrospray ionization (ESI) MS detection. Therefore, flow splitters are used to minimize the solvent load that is introduced into the ESI source [14].

In order to provide a splitless hyphenation with mass spectrometry, a microscale online LCxLC system was developed in a previous work [15]. That system was based on nano-LC in first and micro-LC in second dimension. The flow rate for the second dimension separation was adjusted to 40 μL min^{-1}, which is compatible to ESI-MS. For miniaturized systems, however, the injection volume needs to be reduced, which also reduces the absolute mass injected onto the

first dimension column. In this view, it must be critically asked whether a two-dimensional separation with a higher peak capacity is generally favorable for the analysis of complex samples. Although a higher peak capacity might be obtained for a two-dimensional separation, the total number of detected peaks may be lower when compared to a one-dimensional separation. The reason is that the mass spectrometer, which separates the analytes according to their mass-over-charge ratio, is capable of detecting and distinguishing peaks that are not totally resolved chromatographically.

In this context, a comparison between one-dimensional and microscale comprehensive two-dimensional liquid chromatography coupled to high resolution mass spectrometry was performed. First of all, a reference standard mix containing 99 target compounds was analyzed to obtain the retention time and additional MS/MS information. In the second step, a native wastewater sample was analyzed on the basis of a suspected target screening. A small part of the data set was already used to demonstrate the capability of the miniaturized 2D-LC system in a previous work [15].

Three different criteria for analyte identification were defined for both approaches. First of all, the accurate mass and a mass accuracy of less than ± 5 ppm were chosen. As second and third criteria retention time deviations and MS/MS information were defined and applied to increase the reliability of analyte identification. For each step, the total number of detected peaks was compared. To our knowledge this is the first comprehensive comparison of 1D- and 2D-separations for complex environmental samples.

3.2 Experimental section

3.2.1 Solvents and additives

Ultra-pure water (J. T. Baker, LC/MS reagent grade) was purchased from Mallinckrodt Baker (Griesheim, Germany). Acetonitrile and methanol were both LC-MS Optigrade from Promochem (LGC Standards, Wesel, Germany). All LC eluents were acidified by adding 0.1% formic acid (FA) by volume (puriss. p. a., ~ 98%, Sigma-Aldrich, Schnelldorf, Germany).

3.2.2 Multi-component reference mix and wastewater sample

Overall 99 substances were included in the reference mix to obtain information for a suspected target screening of a wastewater sample. This mixture contained 3 corrosion inhibitors, 4 metabolites of sulfonamide antibiotics, 6 mycotoxins, 72 pharmaceuticals (antibiotics, cytostatics, psychotropics and contrast media) as well as 14 pesticides. A detailed list of all components is provided in chapter appendix Table S 3-2. The resulting multi-component mix containing 1 µg mL^{-1} of each target analyte was prepared in acidified (0.1% FA) water - acetonitrile (95:5, v:v).

To investigate the applicability of the comparison, a real wastewater sample (200 mL) was taken after the first sedimentation step of a municipal wastewater treatment plant. The sample preparation steps are given in chapter appendix.

Prior to injection, the multi-component reference mix as well as the wastewater sample were filtered through a 0.2 µm CHROMAFIL RC 20/25 disposable syringe filter (Macherey-Nagel, Düren, Germany).

3.2.3 1D-HPLC instrument

The conventional 1D-LC separations were performed on an Agilent 1260 HPLC system (Agilent Technologies, Waldbronn, Germany). This instrument was equipped with an Agilent 1260 pump (Model Number G1311B), an autosampler (Model Number G1367E) and column oven (Model Number G1316A).

The separation was carried out on a Luna C18(2) column (150 mm x 2.0 mm i.d., 3 µm particles, Phenomenex, Aschaffenburg, Germany). The injection volume was 20 µL and corresponds to 6% of the column void volume. The flow rate was 200 µL min^{-1} and the oven temperature was set to 30 °C. The mobile phase consisted of acidified (0.1% FA) water (eluent A) and acetonitrile (eluent B). A solvent gradient was applied according to the following program: 3 min hold at 2% B, in 15 min 2-98% B, 6 min hold at 98% B, in 0.5 min 98-2% B, re-equilibration for 5.5 min (~4 column void volumes).

3.2.4 2D-HPLC instrument

The separations with on-line comprehensive 2D-LC were performed on an Eksigent NanoLC-Ultra 2D pump system (Sciex, Dublin, CA). This HPLC system contained a column oven compartment with two integrated ten port two-position valves and two binary-gradient pneumatic pumps which are able to generate a maximum backpressure of 680 bar (10 kpsi). The system was controlled by the Eksigent software version 3.12.1. The modification of this system to work in comprehensive mode is described by Haun et al. [15].

For the first dimension (D1) separation a commercially available Hypercarb column (50 mm x 0.1 mm i.d., 5 µm particles, Thermo Fisher Scientific, Dreieich, Germany) was used. This stationary phase contained porous graphitic carbon (PGC) and was selected because of its high retentivity towards polar compounds [16]. The flow rate was adjusted to 200 nL min^{-1} and the oven temperature was set to 60 °C. The mobile phase consisted of acidified (0.1% FA) water (% A) and methanol (% B). The injection volume on the D1 column was 1.57 µL. A solvent gradient was applied according to the following program: 8 min hold at 1% B, in 45 min 1-99% B, 35 min hold at 99% B, in 5 min 99-1% B, re-equilibration for 16 min (~11 column void volumes).

For the second dimension (D2) separation a superficially porous 2.6 µm SunShell C18 particle (ChromaNik Technologies, Osaka, Japan) packed by Grace Davison (Worms, Germany) into a 50 mm x 0.3 mm i.d. hardware, was used. The flow rate was 40 µL min^{-1} and the oven temperature was set to 60 °C. The mobile phase consisted of acidified (0.1% FA) water (% A) and acetonitrile (% B). A solvent gradient was applied according to the following program: 3-97% B in 0.5 min, 0.1 min hold at 97% B, in 0.1 min 97-3% B, re-equilibration at 3% B for 0.3 min (~6 column void volumes). The complete gradient cycle time took 1 min and was usually repeated without flow-stop until the end of the D1 program. The transfer volume on the D2 column was 300 nL. Additional information on the choice of the inner diameter of the columns can be found in chapter appendix.

Different solvents for the first and second dimension were used to increase the selectivity of the phase system. Acetonitrile was used in the second dimension because it has a much lower viscosity maximum than methanol. This is an important prerequisite in order to increase the flowrate as much as possible to achieve a very fast cycle time of 60 seconds in the second

dimension. A slightly elevated temperature of 60 °C was used to reduce the viscosity maximum when a solvent gradient is applied. This is also very important because the column was operated near the maximum pressure of the pumps around 680 bars. During one analysis 104 gradient runs were performed. At a temperature of 60 °C the column is run nearly at constant pressure which greatly reduces the risk of a rapid column degradation. Increasing the temperature above 60 °C will decrease the column lifetime and also poses a risk to the modulation valves which are only specified to a maximum temperature of 60 °C.

3.2.5 MS instrumentation

For the mass spectrometric detection a Sciex (Darmstadt, Germany) hybrid HRMS system (TripleTOF 5600) with a DuoSpray ion source and a TurboIonSpray probe for ESI experiments was used. For the 1D-LC experiments with flow rates of 200 µL min^{-1}, the standard probe was used. To minimize the dead volume and to avoid severe band broadening after the second dimension column of the 2D-LC, the standard emitter tip (i.d. 130 µm) of the source was replaced by an emitter with an i.d. of 50 µm. MS data acquisition was controlled with Sciex Analyst TF 1.5.1 and the data were analysed using Sciex PeakView 1.2.0.3 and MultiQuant 2.1.1742.0. The data acquired by the 2D-LC approach had to be manually evaluated due to the lack of commercially available 2D software packages.

3.2.6 MS parameters

A suspected target screening approach with information dependent acquisition (IDA) [17, 18] was performed to obtain additional structural information. With this combination it is possible to detect a broad *m/z* range and afterwards to generate one or more product ion spectra of the most abundant precursor ions. The cycle time of such an IDA experiment depends on the selected *m/z* range and the defined number of precursor ions with a constant dwell time. The important MS parameters are listed in Table S 3-3. All measurements were performed in positive electrospray ionization (ESI +) mode.

Ions 214.090 Da (n-butyl benzenesulfonamide, plasticizer) and 221.190 Da (butylated hydroxytoluene, antioxidant) are both well-known contaminants in the field of LC-MS and were excluded for all IDA experiments. Dynamic background subtraction was enabled.

3.3 Results and discussion

3.3.1 Comparison of a reference standard mix and a wastewater sample

For the comparison of the 1D- and 2D-LC approach, a multi-component reference mix and a native wastewater sample were analysed with both approaches using high resolution mass spectrometry. The resulting total ion current (TIC) chromatograms are shown in Figure 1-3.
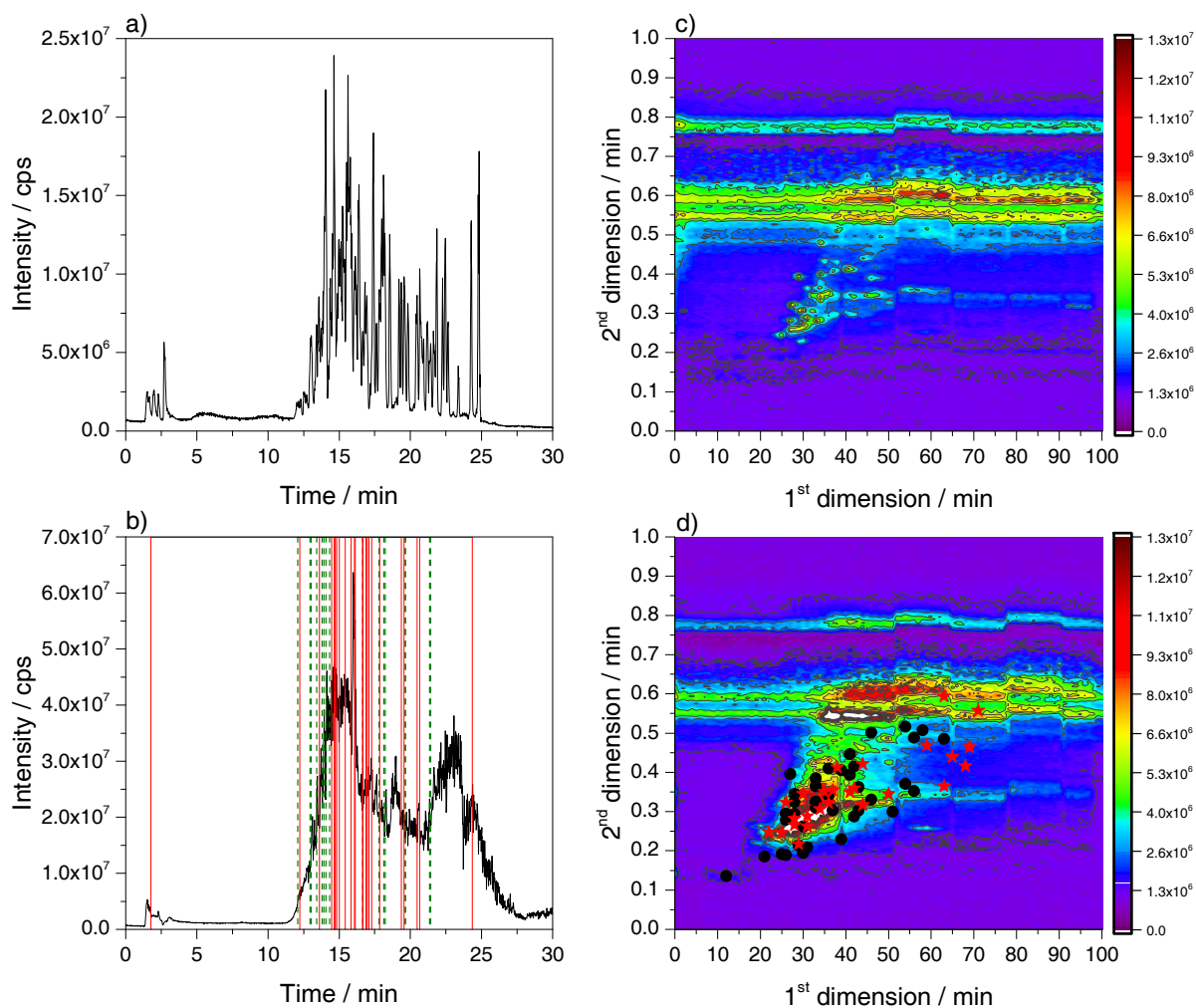
Figure 3-1:   Total ion current chromatograms of a standard mixture and a native real wastewater sample. (a) standard mixture using 1D-HPLC-MS; (b) wastewater sample using 1D-HPLC-MS (red solid lines = detected target compounds without MS/MS spectra; green dashed lines = detected target compounds with MS/MS spectra); (c) standard mixture using 2D-nLC x μLC-MS; (d) wastewater sample using 2D-nLC x μLC-MS (red stars = detected target compounds without MS/MS spectra; black dots = detected target compounds with MS/MS spectra). 2D-LC plots are zoomed in and redrawn with permission from Haun J, Leonhardt J, Portner C, Hetzel T, Tuerk J, Teutenberg T, Schmidt TC (2013) Anal Chem 85(21):10083–10090. Copyright 2013 American Chemical Society.

While for the standard mixture of the 1D separation distinct peaks can be seen in the TIC, a single merged peak is obtained for the wastewater sample (Figure 1-3 a and b). Here, the peaks

cannot be resolved chromatographically, therefore mass spectrometry is required to obtain a separation in the *m/z* dimension. The observed single merged peak is a result of a co-elution of hundreds of compounds and underlines the complexity of the sample. It also clearly demonstrates that one-dimensional LC approaches will not provide the necessary resolution. The 2D-plots (Figure 1-3 c and d) show that the peaks are distributed over the chromatographic space. Nonetheless, there are regions with low and high peak density. The horizontal lines, which spread over the whole chromatographic run in D1 at a retention time in D2 of 0.5 and 0.6 min, resulted from the high content of the organic modifier at the end of the solvent gradient and the fast re-equilibration. In contrast to these signals that can be attributed to solvent effects, there is a horizontal signal at 0.34 min during the solvent gradient in D2, which occurs in fractions 30 to 70 in the reference standard as well as the wastewater sample. In this area, ions with *m/z* 648.3925, 670.3753 and 692.3902 could be observed and were assigned to Triton X detergents [19]. Because of the fact that these ions are also present in the reference standard, they might be introduced by a contamination of the solvent reservoirs. Although the elution profile in D1 is very broad and covers 40 fractions, the retention time in D2 is constant. This underlines that although the elution strength of the transfer solvent continuously increases during the gradient run in D1, this has no effect on the retention on the D2 column. This is an important result because it underlines that the retention time obtained on the D2 column does not depend on the fraction of the organic modifier transferred from the D1 column to the D2 column. The additional solid and dashed lines as well as stars and dots that are also highlighted in Figure 1-3 will be discussed later in Section 3.3.6.

3.3.2 Analyte identification by 5 ppm criterion in reference standard

On the basis of the molecular formula an exact monoisotopic mass and therefore the molecular formula of the protonated molecule $[M+H]^+$ can be calculated. For the identification of detected signals with a high resolution mass spectrometer, a maximum deviation of ± 5 ppm is often used as a criterion for compound identification in targeted analysis [20]. A difference of less than 5 ppm between calculated and accurately measured *m/z* values is then taken as the major criterion for the presence of an analyte with the assumed sum formula. Applying this criterion

it was possible to detect all chosen 99 components both with the 1D- and 2D-LC approach (for more information see Table S 3-4).

3.3.3 Modulation and the associated loss of intensity

The modulation process of the 2D-LC approach reduces the absolute peak intensities obtained after the second dimension separation. This negative effect is the result of the dilution when a one-dimensional peak is sampled in a number of fractions. For many compounds, at least five fractions per peak were obtained. By combining the effect of the lower injection volume (20 µL for 1D-LC and 1.57 µL for 2D-LC) which is applied onto the D1 column and the modulation, the peak area of a 2D-F2 signal in Figure 3-2 a is reduced by a factor of 86. Theoretically, the same factor would be expected for the differences in signal intensity between 1D-LC and 2D-LC. Interestingly, the absolute signal intensity is only reduced by a factor of 10 for the 2D-LC approach in comparison to the 1D-LC approach as is shown exemplarily for carbamazepine in Figure 3-2 a.

Furthermore, the sensitivity and the detection limit do not necessarily depend on the absolute intensity, but on the signal-to-noise ratio (S/N-ratio). Due to the minimized solvent input into the ESI-MS source, a lower dispersion by extra column volume and higher chromatographic efficiency of the 2D-LC system, the noise is substantially lower than for 1D-LC. The S/N-ratio is only 1.5 times smaller for carbamazepine in 2D-LC compared with 1D-LC. A similar observation was made for other target analytes (data not shown here).

A further visual inspection of the MS/MS spectra in Figure 3-2 b and c shows nearly the same pattern and a slightly higher intensity for the 2D-LC spectrum. This example underlines that the influence of the modulation and the strongly reduced injection volume on the identification of targets is very low.
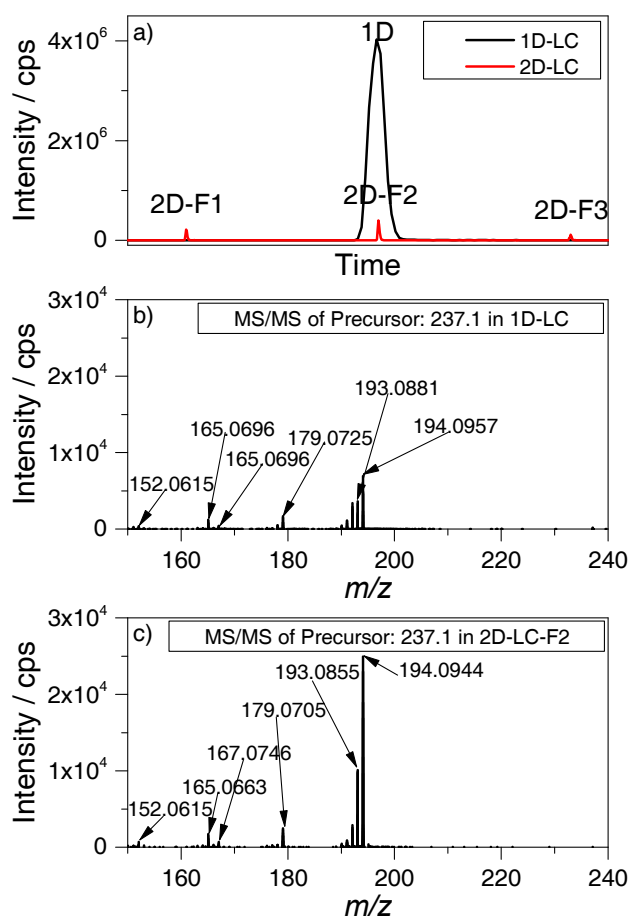
Figure 3-2:   (a) Comparison of the absolute signal intensity of carbamazepine (XIC *m/z* 237.1022) for 1D-LC and 2D-LC approaches as an overlay. F1 to F3 in 2D-LC are three fractions that contain the corresponding target. Intensity: 1D-LC = 4,026,237 cps, 2D-LC-F2 = 399,951 cps; signal-to-noise ratio: 1D-LC = 596, 2D-LC-F2 = 391; Factor Intensity: 10.1; Factor signal-to-noise: 1.5; (b) MS/MS-spectrum of the precursor-ion *m/z* 237.1 in 1D-LC; (c) MS/MS-spectrum of the precursor-ion *m/z* 237.1 in 2D-LC fraction 2.

3.3.4 Influence of mass accuracy on number of identified analytes

A suspected target screening was applied to the wastewater sample to reveal the number of detected compounds in both approaches. When using the 5 ppm criterion, 48 positive hits were obtained for the 1D-LC approach, while 65 positive hits were found for the 2D-LC approach.

However, analyte identification which is only based on the accurate mass can lead to a high number of false positive results when a suspected target screening is applied. For the comparison of the 1D-LC and 2D-LC approaches a deviation of ± 5 ppm was chosen. For a general unknown screening, often a higher mass accuracy is required [21] to reduce the number of possible molecular formula which can be assigned to the molecular mass. Therefore, the question arises whether a smaller deviation of 1 ppm will lead to the elimination of false positive results. Figure 3-3 shows the total number of detected compounds if the deviation is reduced from 5 ppm to 1 ppm in steps of 1 ppm.
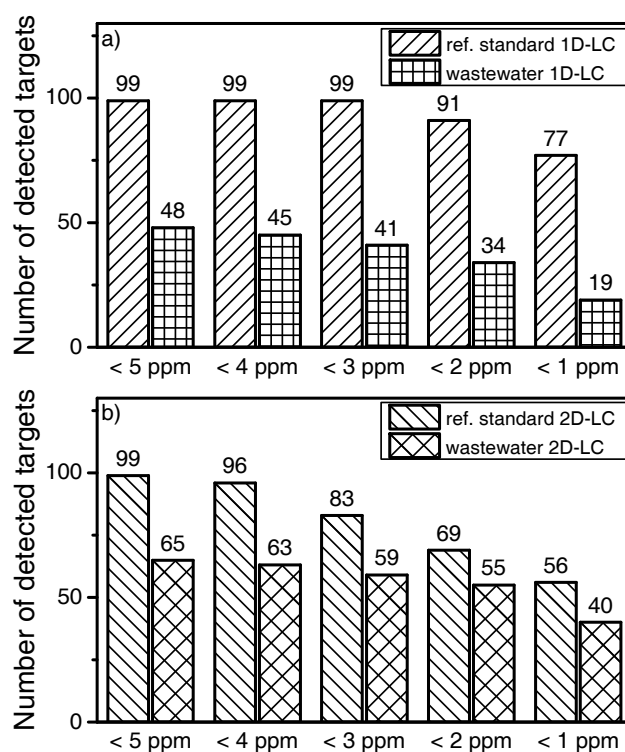
Figure 3-3:   Number of detected targets versus a variable mass accuracy of 5 ppm to 1 ppm in multi-component standard and a real wastewater sample in the 1D-LC (a) and 2D-LC (b) approach.

By reducing the mass accuracy from 5 ppm to 3 ppm for 1D-LC, the total number of detected targets of the reference standard remains constant at 99. If a deviation of 1 ppm is chosen, 78% of all targeted compounds can still be identified. For the wastewater sample, a higher mass

accuracy leads to a more pronounced effect on the absolute number of excluded compounds. For a deviation of 1 ppm, the number of identified compounds is reduced by 60% when compared with a deviation of 5 ppm.

By reducing the mass accuracy from 5 ppm to 1 ppm for 2D-LC, the total number of detected targets of the reference standard decreases continuously. If a deviation of 1 ppm is chosen, 57% of all compounds can still be identified. For the wastewater sample and a higher mass accuracy of 1 ppm the number of identified compounds is reduced by 38% in comparison to a deviation of 5 ppm.

The results underline that already a small deviation of the accuracy of the mass spectrometer can lead to a preliminary exclusion of contained compounds in the sample or reference standard by using a too strong criterion. In this case 22 targets of the reference standard and 29 possible hits of the wastewater sample could be lost in the 1D-LC approach. In the 2D-LC approach, 43 targets of the reference standard and 25 possible hits of the wastewater sample might not be assigned. To avoid the exclusion of such a high number of targets, a mass accuracy of $\pm$ 5 ppm was therefore chosen.

3.3.5 Retention time stability

To use the retention time of the analyte as an additional identification criterion and to exclude false positive hits, the retention time stability needs to be evaluated. A margin of $\pm$ 2.5% was used for the deviation of the retention time measured in the sample from the retention time measured in the reference standard.

To evaluate the retention time stability as an additional criterion for analyte identification, all detected targets that fulfilled the $\pm$ 5 ppm for standard and sample and $\pm$ 2.5% retention time stability criteria were plotted against each other in Figure 3-4 for both approaches.
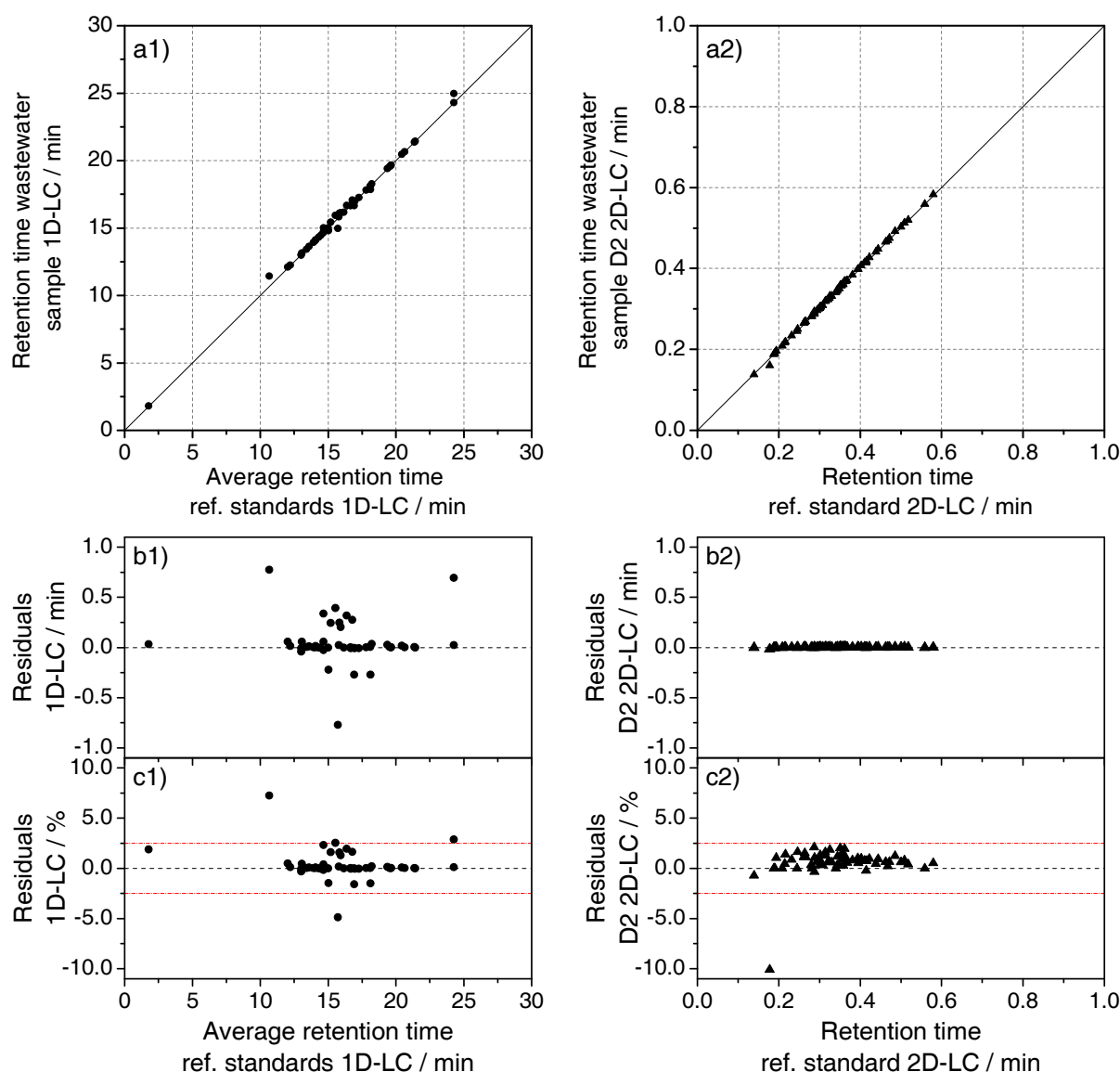
Figure 3-4:   Number Comparison of retention times measured for the reference standard and the wastewater sample for 1D-LC (a1) and 2D-LC (a2) including the absolute (b1 and b2) and relative (c1 and c2) residuals on the basis of mass accuracy of ± 5 ppm and retention time deviation of ± 2.5% (left: 1D-HPLC-MS (48 components), right: 2D-nLC x μLC-MS (65 components)). The residuals are differences between measured retention time in wastewater sample and reference standard mix.

For the 1D-LC approach, 44 of 48 possible targets fulfil the additional retention time criterion of ± 2.5% with a highest absolute deviation of 0.77 min and the coefficient of determination is

R^2=0.9988. For the 2D-LC approach, 64 of 65 possible targets fulfil the same criterion with a maximum absolute deviation of 0.02 min on the second dimension column and an R^2 of 0.9997. Although the R^2-values show a very high correlation for both approaches, they contain no information about the scattering. Therefore, the residuals are also included in Figure 3-4. Data evaluation shows that the absolute deviation for the 2D-LC approach is much lower, by a factor of 100. However, as is shown by the relative deviation depicted in Figure 3-4 c, the majority of targets has a deviation smaller than ± 0.5% for the 1D-LC approach, while most compounds are spread from 0% to 2.0% for the 2D-LC approach. Although the relative deviation is higher for the 2D-LC approach, it has to be considered that the available solvent gradient window on the D2 column is only 30 seconds long. In contrast, the gradient window for the 1D-LC approach extends to 1,440 seconds (24 minutes).

The results clearly point out that the retention time criterion should also be considered for a suspected target screening. Higher deviations in the retention time for the same *m/z* value could be a hint for false positive hits.

At this point we would also like to discuss the approach of retention time predictions on the basis of octanol-water partition coefficients (log P). This strategy has been proposed for non-target analysis in order to confirm a sum formula on the basis of the accurate mass and a defined mass accuracy. It can be seen from the plot in Figure S 3-1, that there is no correlation when the retention factor is plotted against the log P and thus, the proposed criterion is neither applicable for a suspected-target nor non-target screening approach.

3.3.6 Implication of peak width and cycle time on MS/MS spectra

A further exclusion of false positive hits could be achieved by MS/MS spectra of the detected targets. This information can be obtained by data dependent MS/MS experiments.

The identification of compounds in the wastewater sample on the basis of the three selected criteria (mass accuracy of 5 ppm, retention time deviation lower than 2.5% and confirmation by MS/MS spectra) shows that only 16 targets will be identified using the 1D-LC approach and 31 targets will be identified using the 2D-LC approach. The higher reliability by applying additional criteria for analyte identification always results in a lower number of identified peaks.
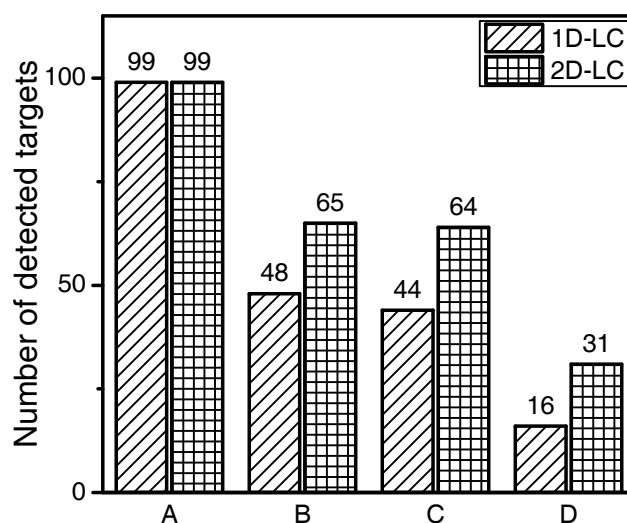
Figure 3-5:   Overview of the identified analytes by 1D-HPLC-MS and 2D-nLC x µLC-MS.
Detailed list of detected targets is given in Table S 3-5. (A) Detected targets in ref. standard by
< 5 ppm; (B) Detected targets in wastewater sample by < 5 ppm; (C) Detected targets in
wastewater sample by < 5 ppm and retention time < 2.5%; (D) Detected targets in wastewater
sample by < 5 ppm, retention time < 2.5% and MS/MS hit.

It can be deduced from Figure 3-5 that the total number of identified peaks is always higher for
the 2D-LC approach when the wastewater sample is analysed. Furthermore, it can be observed
that the number of excluded targets in Figure 3-5 increased by a factor of 2.7 for the 1D-LC
approach and a factor of 2.1 for the 2D-LC approach when the additional MS/MS criterion was
applied. However, this does not allow the conclusion that the excluded targets are false positive
hits. It rather points to a limitation in the mass spectrometer and the chosen mass spectrometric
parameters, especially the number of MS/MS experiments which can be made within one cycle.
On closer inspection of the data it can be seen that not every precursor ion of a detected target
on the basis of the ± 5 ppm criterion and 2.5% retention time deviation was selected for a further
MS/MS experiment. The reason for the exclusion is the intensity of these target ions, which
was lower than the most abundant ions resulting from co-eluting matrix compounds.

In this context it is important to discuss the limitations of hyphenating a chromatographic
separation with hybrid high resolution mass spectrometry. For quantitative analysis, usually 15

to 20 data points are required. For qualitative analysis, a lower number of data points over a chromatographic peak is also acceptable. To generate a sufficient number of data points, the cycle time needs to be very short and depends on the *m/z* range and the number of MS/MS experiments. One MS/MS experiment contains the selection of a specific precursor ion and its subsequent fragmentation. For example, 4 MS/MS experiments are equal to the fragmentation of the 4 most intensive ions that have been detected over a defined *m/z* range. A larger *m/z* detection range has only a negligible influence on the cycle time, whereas a higher number of MS/MS experiments with constant dwell time significantly increases the cycle time and reduces the number of data points. Furthermore, the decrease of the dwell time will usually decrease the signal-to-noise ratio, which is not recommended. The 1D-LC approach provides only a short period for the MS/MS experiments during the retention time window of a chromatographic peak. Because of the modulation in 2D-LC, the analyte signal will be cut into several fractions, which increases the possibility for an MS/MS experiment that contain the precursor ion of the target compound.

Generally, the number of MS/MS experiments should be increased with an increasing number of co-eluting signals in order to prevent the loss of MS/MS information. However, this strongly depends on the peak widths which are obtained in 1D-LC and 2D-LC. Table 3-1 summarizes the calculation of the number of data points over a chromatographic peak in dependence on the peak width and the cycle time.

Table 3-1:   Data points over a chromatographic peak for 1D-LC and 2D-LC in dependence on peak width and cycle time. Underlined numbers are calculated data points for the finally used MS parameters.

	Peak width / s		Cycle time / ms		Data points	
	1D-LC	2D-LC	1D-LC	2D-LC	1D-LC	2D-LC*
Scan + 2 MS/MS experiments	10	1	500	110	20	9
Scan + 4 MS/MS experiments	10	1	700	150	14	7
Scan + 8 MS/MS experiments	10	1	1110	710	9	1
Scan + 12 MS/MS experiments	10	1	1500	1110	7	1

*Number of calculated data points for only one fraction.

For the 1D-LC approach, the peak width (at 5% height) was about 10 seconds. Although it would have been possible to reduce the peak width to a few seconds with the available

instrumentation by increasing the steepness of the solvent gradient, a smaller peak width inevitably reduces the time for MS/MS experiments. Furthermore, the number of co-eluting peaks would also be higher because of a smaller elution period. This also means that for a suspected target screening, a highly efficient chromatographic separation will lead to a reduced time for obtaining additional MS/MS information that is useful for analyte identification. This limitation is frequently overlooked in the respective literature dealing with ultra-high performance separations for suspected target screening. According to Table 3-1 the chosen number of MS/MS experiments for both approaches (8 for 1D-LC and 4 for 2D-LC) is an acceptable compromise between the number of data points over a chromatographic peak and the extracted MS/MS information.

Although the number of possible MS/MS experiments per data point for 1D-LC is higher, the total number of MS/MS spectra is not necessarily lower for the 2D-LC approach, which is illustrated on the basis of Figure S 3-2. For the 1D-LC signal 10 data points could be observed, each containing 8 MS/MS spectra. In total it was therefore possible to generate 80 MS/MS spectra over the 1D-LC signal. For the 2D-LC signal in the second fraction, 6 data points could be observed, each containing 4 MS/MS spectra. In total it was possible to acquire 24 MS/MS spectra over the peak in a single fraction. However, the total number of MS/MS spectra consists of the sum of all spectra obtained in each fraction of the 2D-LC signal. This means that the total number of MS/MS spectra for 3 fractions is 72 and thus nearly equal to the 1D-LC approach.

On the basis of the chosen number of MS/MS experiments a ranking list for all target analytes fulfilling the 5 ppm and the 2.5% retention time criteria was created (see Table S 3-6). As can be seen, the priority for triggering an MS/MS experiment depends on the absolute intensity of the precursor ion. A closer look at the results of Table S 3-6 shows that only 23 of the possible 44 targeted precursor ions of the 1D-LC approach had a sufficient intensity for triggering an MS/MS experiment. An increase of the number of possible MS/MS experiments would not necessarily result in a significant increase of MS/MS information of the selected target compounds. In this case, a doubling of the MS/MS experiments to 16 would result in only one additional MS/MS-spectrum of targeted compounds. For the 2D-LC approach 38 of the possible 64 target compounds had a sufficient intensity for an MS/MS experiment. Further increasing the number of MS/MS experiments to eight in the 2D-LC approach would reduce the number of data points across a chromatographic peak to one and is therefore not acceptable. However,

not all MS/MS spectra of targeted compounds could confirm the analyte because of different product ion spectra in comparison to the reference standard. Therefore, the total number of identified targets shown in Figure 3-5 is smaller for both approaches in comparison to the number of available MS/MS spectra of the targeted compounds.

The main reason for the very small number of additional MS/MS-spectra of targeted compounds by doubling of the possible MS/MS experiments can be explained on the basis of the 1D-LC and 2D-LC TIC chromatogram of the wastewater sample presented in Figure 1-3.

In Figure 1-3 c the retention time of targets selected for MS/MS experiments is highlighted by green dashed lines for 1D-LC (panel b) and black dots for 2D-LC (panel d). Targets excluded from MS/MS experiments are highlighted by red solid lines for 1D-LC and red stars for 2D-LC. For the 1D-LC chromatogram it can be clearly noticed that at the retention time window of 14 to 17 min and at the maximum of the TIC intensity, a large number of precursor ions of targeted compounds were excluded from MS/MS experiments. At the retention time window of 12 to 14 min and 17 to 22 min where the TIC intensity is rising or falling, many of the precursor ions of targeted analytes were selected for MS/MS experiments. The same observation could be made for the 2D-LC plot. Most selected precursor ions from targets for MS/MS experiments are located around the maximum of the TIC cone, located between the 15th and 40th fraction in D1 and between 0.25 and 0.3 min in D2. Most of the excluded targets from MS/MS experiments could be found at the cone maximum.

The main reason for such an effect is the interfering matrix of the wastewater sample. Such a complex matrix can contain thousands of compounds. Their amount and concentration and/or intensity is often much higher in comparison to the targets of interest, especially at the TIC maxima. Therefore, the precursor ions of targeted analytes in this range often were not selected for an MS/MS experiment and thus excluded. Examples are given in Figures S-3 and S-4 of the chapter appendix, where the 1D TIC chromatogram, the MS spectrum at the retention time of the targeted compounds (bisoprolol and iopromide) and their MS/MS spectra for 1D-LC and 2D-LC approaches are shown. The MS spectra contain the selected precursor ions (8 for 1D-LC and 4 for 2D-LC) that were selected for MS/MS experiments on the basis of the absolute intensity. In general, it can be noticed that the MS spectra in both approaches contain a very high number of possible precursors which could be selected for MS/MS experiments.

Bisoprolol elutes at the local maximum inside the TIC chromatogram of both approaches (see Figure S 3-3). As discussed before, the matrix impact in this region is very high and the precursor ion for bisoprolol could not be selected for an MS/MS experiment due to the relatively low signal intensity for the 1D-LC approach. With the 2D-LC approach bisoprolol could be separated chromatographically from the interfering matrix. Therefore, bisoprolol could be selected as a precursor with the highest intensity for an MS/MS experiment.

At this point the 2D-LC system has an advantage compared to the 1D-LC system. In consequence of the much higher chromatographic resolution across the two dimensions, the co-eluting matrix compounds could be much better separated, which can increase the probability of selecting precursor ions from targeted analytes for an MS/MS experiment. Furthermore, by sampling the compounds in more than one fraction, the modulation provides a higher possibility that a relevant precursor ion will be selected for MS/MS experiments during several successive D2 chromatograms. This leads to a higher number of targets which can be additionally identified by their MS/MS spectra for the 2D-LC approach as summerized in Figure 3-5.

3.3.7 Comparison of detected targets for 1D-LC and 2D-LC approaches

To complete the comparison it is important to know how many of the detected targets could be identified with both approaches, only with 1D-LC and only with 2D-LC. The results are shown in Figure 3-6.
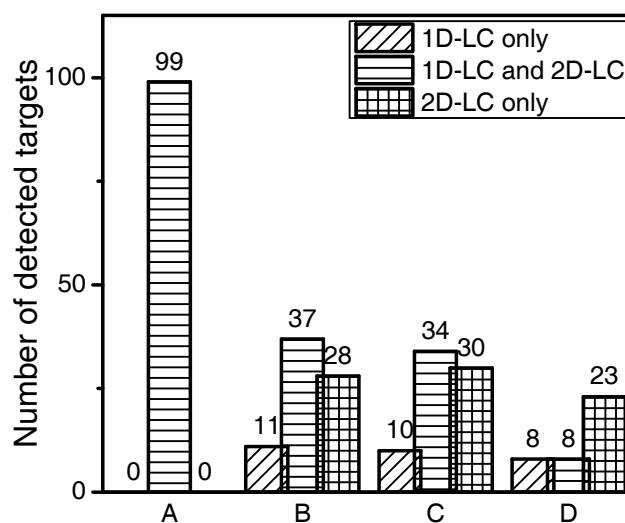
Figure 3-6:   Overview of detected targets with both approaches, only with 1D-LC and only with 2D-LC. (A) Detected targets in ref. standard by < 5 ppm; (B) Detected targets in wastewater sample by < 5 ppm; (C) Detected targets in wastewater sample by < 5 ppm and retention time < 2.5%; (D) Detected targets in wastewater sample by < 5 ppm, retention time < 2.5% and MS/MS hit.

Data evaluation shows that all 99 targets of the reference standard could be identified with both approaches. In the case of the wastewater sample, there are some compounds which will be either detected by the 1D-LC or by the 2D-LC approach. This is especially apparent when all three criteria which have been defined for analyte identification are applied. Here, only 8 targets could be identified with both approaches and the remaining 8 and 23 targets were only identified by either 1D-LC or 2D-LC, respectively. The comparison in Figure 3-5 and Figure 3-6 clearly reveals that the number of compounds which can be detected only with the 1D-LC approach is rather low.

If a too small mass accuracy value such as ± 1 ppm is used, the number of detected targets that fulfill all three criteria (mass accuracy of ± 1 ppm, retention time deviation of ± 2.5% and positive MS/MS spectra) is reduced to 4 for 1D-LC and 21 for 2D-LC. This means that for the selected conditions the higher mass accuracy has a significant negative influence on the absolute number of identified targets for both approaches. This finding underlines that for

reliable analyte identification a higher mass accuracy value like ± 5 ppm is more suitable in combination with additional criteria such as retention time and MS/MS information.

3.4 Conclusion and outlook

In this work a comparison of 1D-LC-MS and 2D-LC-MS approaches was performed on the basis of a multi component reference standard and a complex wastewater sample. For the comparison three different criteria for compound identification on the basis of mass accuracy of ± 5 ppm, retention time deviation of ± 2.5% and MS/MS information were chosen. At this point we would like to point out that the comparison was done under a "worst-case-scenario" for the 2D-LC set-up. The reason is that the inner diameter of the second dimension column is much smaller than that of the 1D-LC set-up. Therefore, only a much smaller sample volume could be injected onto the first dimension column. Consequently, peak concentrations are not directly comparable. However, the fact that the number of identified target peaks is always higher for the microscale LCxLC approach underlines the superior performance of the miniaturized comprehensive 2D-LC separation over a classical one-dimensional separation.

Furthermore, it could be shown that the accurate mass criterion of ± 5 ppm in combination with further criteria as, e. g., retention time deviation and MS/MS information leads to a higher reliability of identified compounds for both approaches. This does not imply that an identification of a compound should be always based on all selected criteria. Since there is currently no regulative guideline for environmental screening analyses, a point-by-point decision about the appropriate strategy [22] is placed in the hands of the operator.

The comparison also reveals the limitations of modern mass spectrometers in terms of compound identification. A reasonable way to increase the number of MS/MS experiments and therefore the possibility to obtain MS/MS information of all detected targets is the continuous increase in data acquisition rate of the mass spectrometer.

Finally, the results of the comparison could provide valuable information for further technical developments as well as data processing strategies.

3.5 References

1. Krauss M, Singer H, Hollender J. LC-high resolution MS in environmental analysis: from target screening to the identification of unknowns. Anal Bioanal Chem; 2010;397(3):943–51

2. Zedda M, Zwiener C. Is nontarget screening of emerging contaminants by LC-HRMS successful? A plea for compound libraries and computer tools. Anal Bioanal Chem; 2012;403(9):2493–502

3. Neue UD. Peak capacity in unidimensional chromatography. J Chromatogr A; 2008;1184(1–2):107–30

4. Di Palma S, Hennrich ML, Heck AJ, Mohammed S. Recent advances in peptide separation by multidimensional liquid chromatography for proteome analysis. J Proteomics; 2012;75(13):3791–813

5. Mondello L, C. Lewis A, D. Bartle K. Multidimensional Chromatography. Chichester, UK: John Wiley & Sons, Ltd; 2001.

6. Groskreutz SR, Swenson MM, Secor LB, Stoll DR. Selective comprehensive multi-dimensional separation for resolution enhancement in high performance liquid chromatography. Part I: Principles and instrumentation. J Chromatogr A; 2012;1228:31–40

7. Wang S, Qiao L, Shi X, Hu C, Kong H, Xu G. On-line stop-flow two-dimensional liquid chromatography-mass spectrometry method for the separation and identification of triterpenoid saponins from ginseng extract. Anal Bioanal Chem; 2015;407(1):331–41

8. Li D, Jakob C, Schmitz O. Practical considerations in comprehensive two-dimensional liquid chromatography systems (LCxLC) with reversed-phases in both dimensions. Anal Bioanal Chem; 2015;407(1):153–67

9. Li D, Schmitz OJ. Comprehensive two-dimensional liquid chromatography tandem diode array detector (DAD) and accurate mass QTOF-MS for the analysis of flavonoids and iridoid glycosides in Hedyotis diffusa. Anal Bioanal Chem; 2015;407(1):231–40

10. Schiesel S, Lämmerhofer M, Lindner W. Comprehensive impurity profiling of nutritional infusion solutions by multidimensional off-line reversed-phase liquid chromatography × hydrophilic interaction chromatography–ion trap mass-spectrometry

and charged aerosol detection with universal calibration. J Chromatogr A; 2012;1259:100–10

11. Dugo P, Cacciola F, Donato P, Mondello L. Comprehensive two-dimensional liquid chromatography applications. In: Mondello L (editor). Comprehensive chromatography in combination with mass spectrometry. Hoboken, NJ: Wiley; 2011, pp. 391–427.

12. Dugo P, Cacciola F, Donato P, Mondello L. Comprehensive two-dimensional liquid chromatography combined with mass spectrometry. In: Mondello L (editor). Comprehensive chromatography in combination with mass spectrometry. Hoboken, NJ: Wiley; 2011, pp. 331–390.

13. Stoll DR, Wang X, Carr PW. Comparison of the Practical Resolving Power of One- and Two-Dimensional High-Performance Liquid Chromatography Analysis of Metabolomic Samples. Anal Chem; 2007;80(1):268–78

14. Francois I, Sandra K, Sandra P. History, Evolution, And Optimization Aspects of Comprehensive Two-Dimensional Liquid Chromatography. In: Mondello L (editor). Comprehensive chromatography in combination with mass spectrometry. Hoboken, NJ: Wiley; 2011, pp. 281–330.

15. Haun J, Leonhardt J, Portner C, Hetzel T, Tuerk J, Teutenberg T, Schmidt TC. Online and Splitless NanoLC × CapillaryLC with Quadrupole/Time-of-Flight Mass Spectrometric Detection for Comprehensive Screening Analysis of Complex Samples. Anal Chem; 2013;85(21):10083–90

16. Leonhardt J, Hetzel T, Teutenberg T, Schmidt TC. Large Volume Injection of Aqueous Samples in Nano Liquid Chromatography Using Serially Coupled Columns. Chromatographia; 2015;78(1-2):31–8

17. Decaestecker TN, Clauwaert KM, Van Bocxlaer JF, Lambert WE, Van den Eeckhout EG, Van Peteghem CH, De Leenheer AP. Evaluation of automated single mass spectrometry to tandem mass spectrometry function switching for comprehensive drug profiling analysis using a quadrupole time-of-flight mass spectrometer. Rapid Commun Mass Sp; 2000;14(19):1787–92

18. Decaestecker TN, Vande Casteele SR, Wallemacq PE, Van Peteghem CH, Defore DL, Van Bocxlaer JF. Information-dependent acquisition-mediated LC-MS/MS screening procedure with semiquantitative potential. Anal Chem; 2004;76(21):6365–73

19. Keller BO, Sui J, Young AB, Whittal RM. Interferences and contaminants encountered in modern mass spectrometry. Anal Chim Acta; 2008;627(1):71–81

20. Moschet C, Piazzoli A, Singer H, Hollender J. Alleviating the reference standard dilemma using a systematic exact mass suspect screening approach with liquid chromatography-high resolution mass spectrometry. Anal Chem; 2013;85(21):10312–20

21. Kind T, Fiehn O. Metabolomic database annotations via query of elemental compositions: mass accuracy is insufficient even at less than 1 ppm. BMC Bioinformatics; 2006;7:234

22. Schymanski EL, Jeon J, Gulde R, Fenner K, Ruff M, Singer HP, Hollender J. Identifying small molecules via high resolution mass spectrometry: communicating confidence. Environ Sci Technol; 2014;48(4):2097–8

3.6 Chapter appendix

3.6.1 Wastewater sample preparation

To investigate the applicability of the comparison, a real wastewater sample (200 mL) was taken after the first sedimentation step of a municipal wastewater treatment plant. Prior to the analysis, the pH was adjusted to 3 by using hydrochloric acid (2.5% solution). Afterwards, the sample was extracted with a 200 mg Oasis HLB (6 mL) solid phase cartridge (Waters, Eschborn, Germany). The solid-phase extraction was based on the following steps: conditioning: 5 mL methanol (5 min residence time); equilibration: 5 mL water at pH 3; sample application; washing: 5 mL of a water – methanol mixture (95:5, v:v); drying for 5 min; elution: 3 x 3 mL methanol; evaporation of the eluent in a gentle nitrogen stream at 40 °C; dissolving in 2 mL acidified (0.1% FA) water – acetonitrile (95:5, v:v). The wastewater sample was not spiked with the reference compounds.

3.6.2 Column i.d. comparison

The main reason to use a 0.1 mm i.d. column for the 1st dimension is the maximum available injection volume. Theoretically, the maximum injection volume should be less than 10% of the column void volume. For example, the column void volume of a 50 mm long column with an i.d. of 0.1 mm is approximately 250 nL and the resulting maximum injection volume (10%) is 25 nL. If we reduce the i.d. of the same column to 0.05 mm (which is the smallest commercially available i.d.) the maximum injection volume is reduced to approximately 7 nL. The reduced injection volume has a negative effect on the limit of detection. In combination with the constant dilution by the modulation process, the signal intensity could be decreased dramatically.

Now the question arises, why we did not use an i.d. of 0.3 mm in the 1st dimension. It is also possible to use columns with larger i.d. on the 1st dimension, but the flowrate must be increased to avoid band broadening. A higher flowrate for example of 3 µL/min on the 1st dimension column drastically reduces the fill time of the 300 nL modulation loop. As a result of that, the cycle time of the 2nd dimension must be decreased dramatically to 0.1 minute. Otherwise, the effluent of the 1st dimension would be lost.

For this work we used a cycle time of 1 minute, which corresponds to the optimum of the developed 2D-LC system. Due to general technical limitations, it is not possible to reduce the cycle time to 0.1 minutes for LCxLC applications.

Therefore, the strategy to minimize problems in terms of decreased signal intensity is to use a slightly smaller column i.d. as of the 2nd dimension and the i.d. of 0.1 mm is a very good compromise between maximum injection volume and loop fill time (and the corresponding cycle time of the 2nd dimension).

Furthermore, the inner diameters of the miniaturized system of both dimensions could be compared to conventional online LCxLC setups by the following equation:

$$\Delta \, i.d. = \frac{d_{c,2} - d_{c,1}}{d_{c,2}}$$

$\Delta i.d.$ = relative difference of the column inner diameters of the two coupled LC dimensions
$d_{c,1}$ = i.d. of the 1st dimension
$d_{c,2}$ = i.d. of the 2nd dimension

For the 1st dimension of a non-miniaturized LCxLC typically inner diameters of 1.0 mm and 2.1 mm were used and for the 2nd dimension it is mainly 4.6 mm.

Table S 3-1:   Column i.d. comparison.

	D1 column i.d.	D2 column i.d.	Δ i.d.
Conventional setup 1	1.0	4.6	0.78
Conventional setup 2	2.1	4.6	0.54
Miniaturized setup	0.1	0.3	0.66

As shown in the Table, the $\Delta i.d.$ of the miniaturized set-up is comparable to the non-miniaturized approaches.

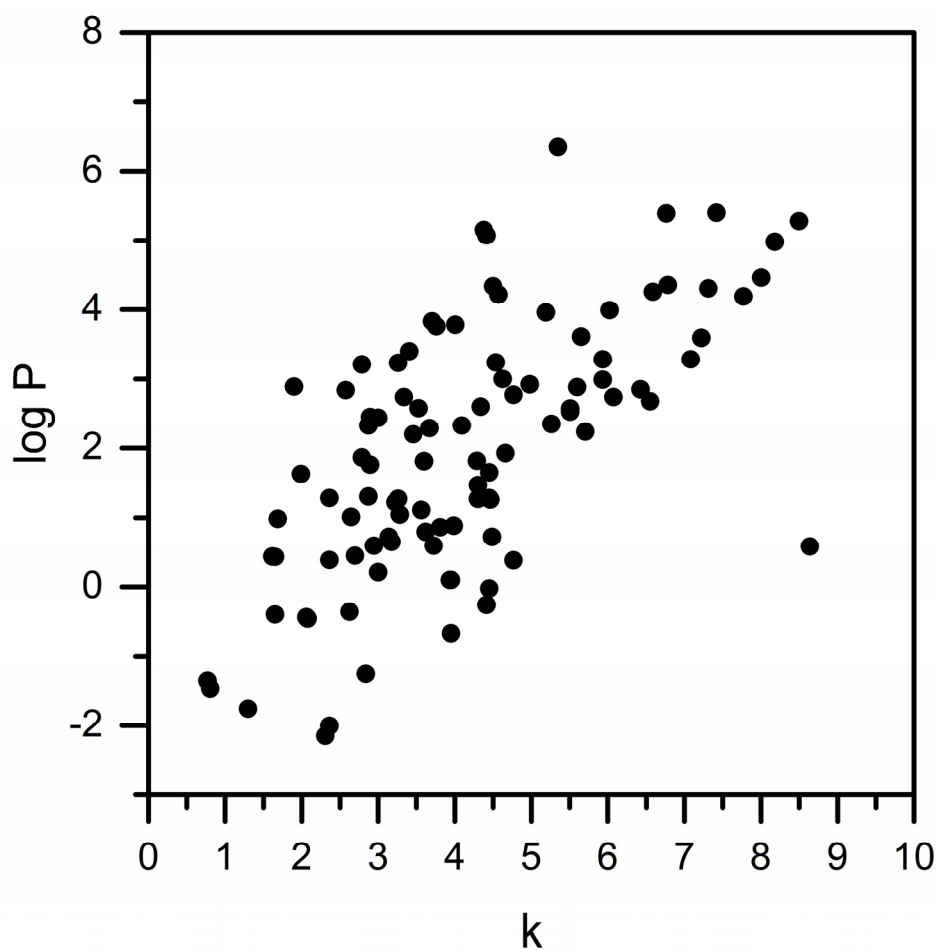## 3.6.3 Retention factor vs. octanol-water partition coefficient

Figure S 3-1: Correlation plot. The retention factor is plotted against the octanol-water partition coefficient.

It can be seen from the plot in Figure S 3-1 that there is no correlation when the retention factor is plotted against the log P and thus, the proposed criterion is neither applicable for a suspected-target nor non-target screening approach.

3.6.4 Comparison of 1D-LC and 2D-LC signal
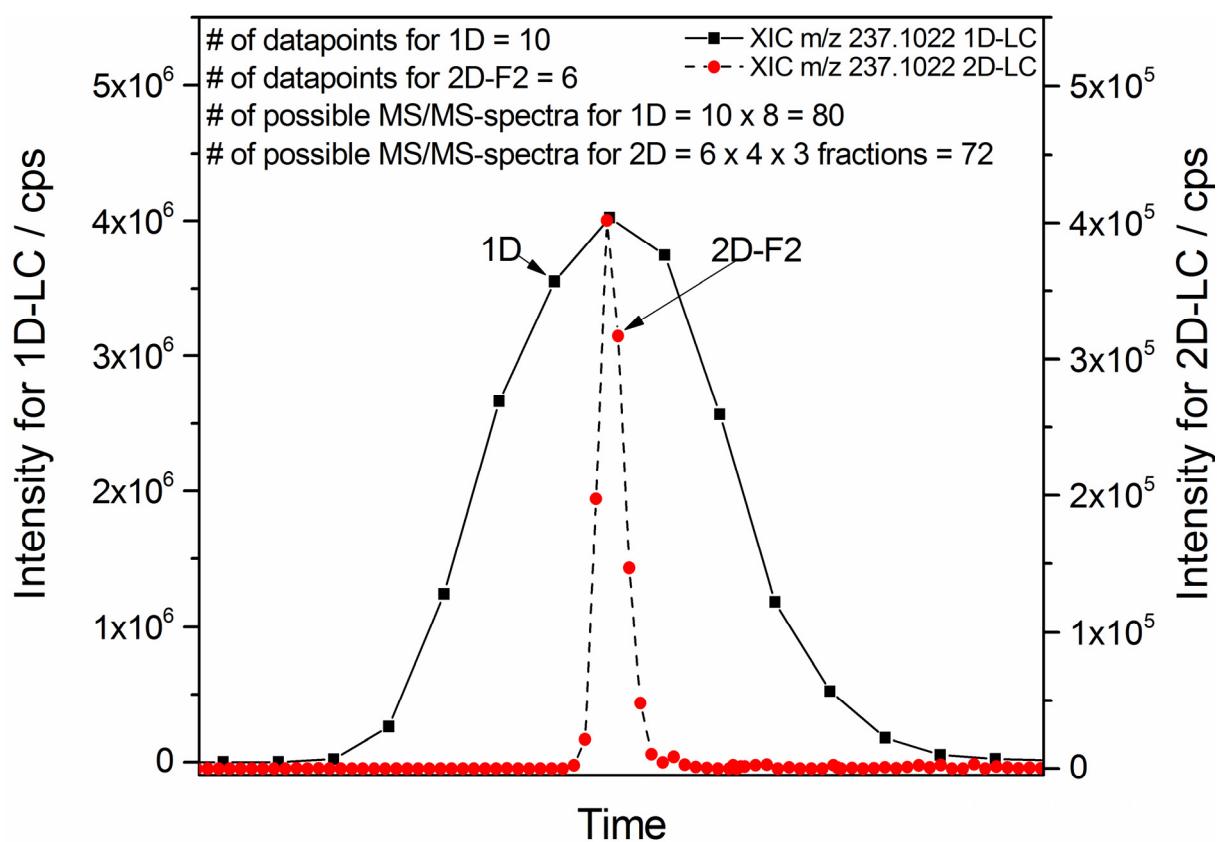
Figure S 3-2: Comparison of 1D-LC and 2D-LC signal of $[M+H]^+$ 237.1022 with a view to the number of data points and the possible number of MS/MS spectra.

For the 1D-LC signal 10 data points could be observed, each with 8 MS/MS spectra. In total it could be possible to get 80 MS/MS spectra over the 1D-LC signal. For the 2D-LC signal in the second fraction, 6 data points could be observed, each with 4 MS/MS spectra, giving up to 24 MS/MS spectra. However, the total number of possible MS/MS spectra consists of the sum of all spectra given in each fraction of the 2D-LC signal. For example the total number of MS/MS spectra for 3 fractions results in 72 and is nearly equal to the 1D-LC approach.

3.6.5 Comparison of 1D-LC and 2D-LC MS and MS/MS spectra of bisoprolol and iopromide

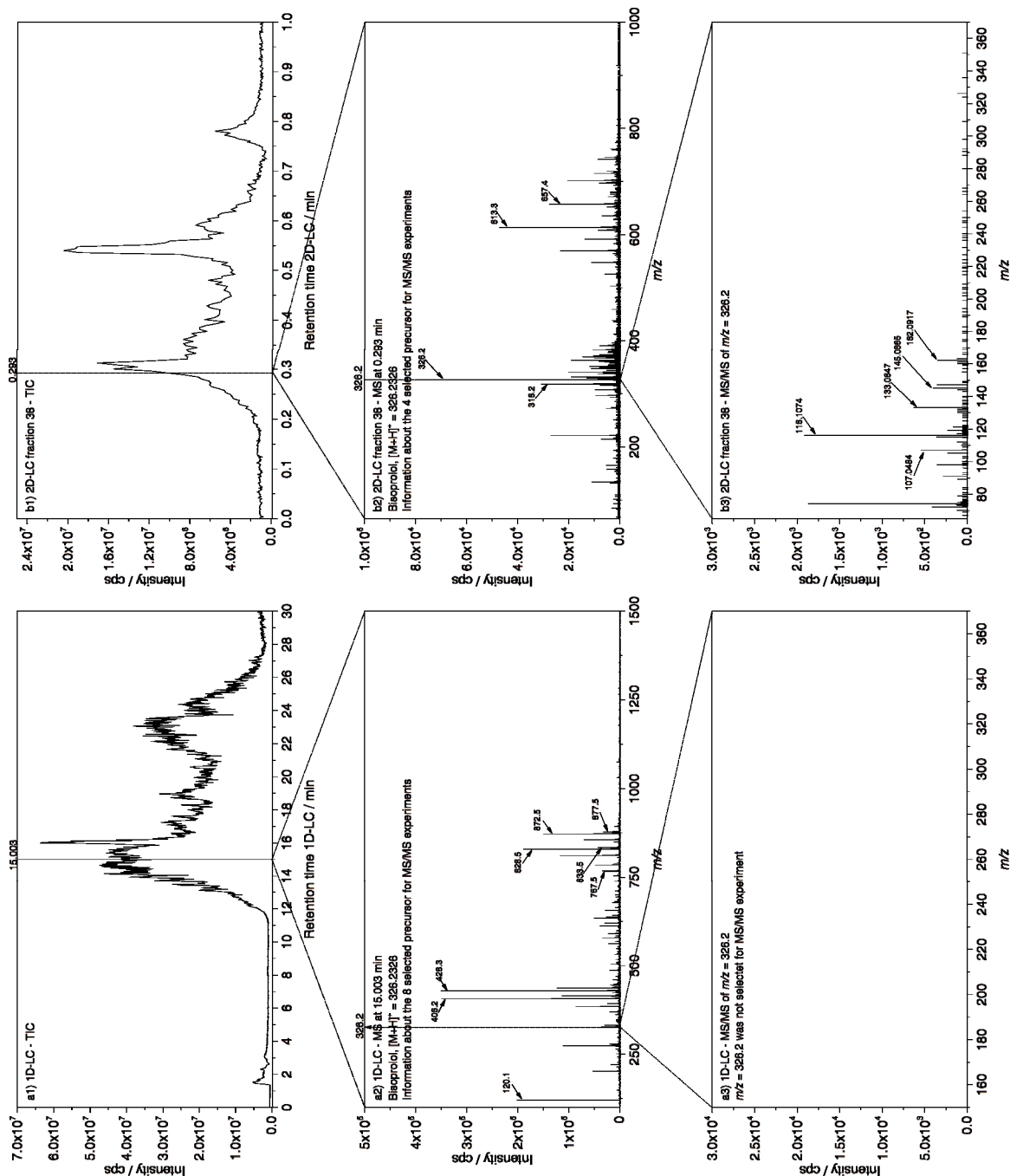Figure S 3-3: Comparison of (a) 1D-LC and (b) 2D-LC MS and MS/MS spectra of bisoprolol [M+H]+ 326.2326.
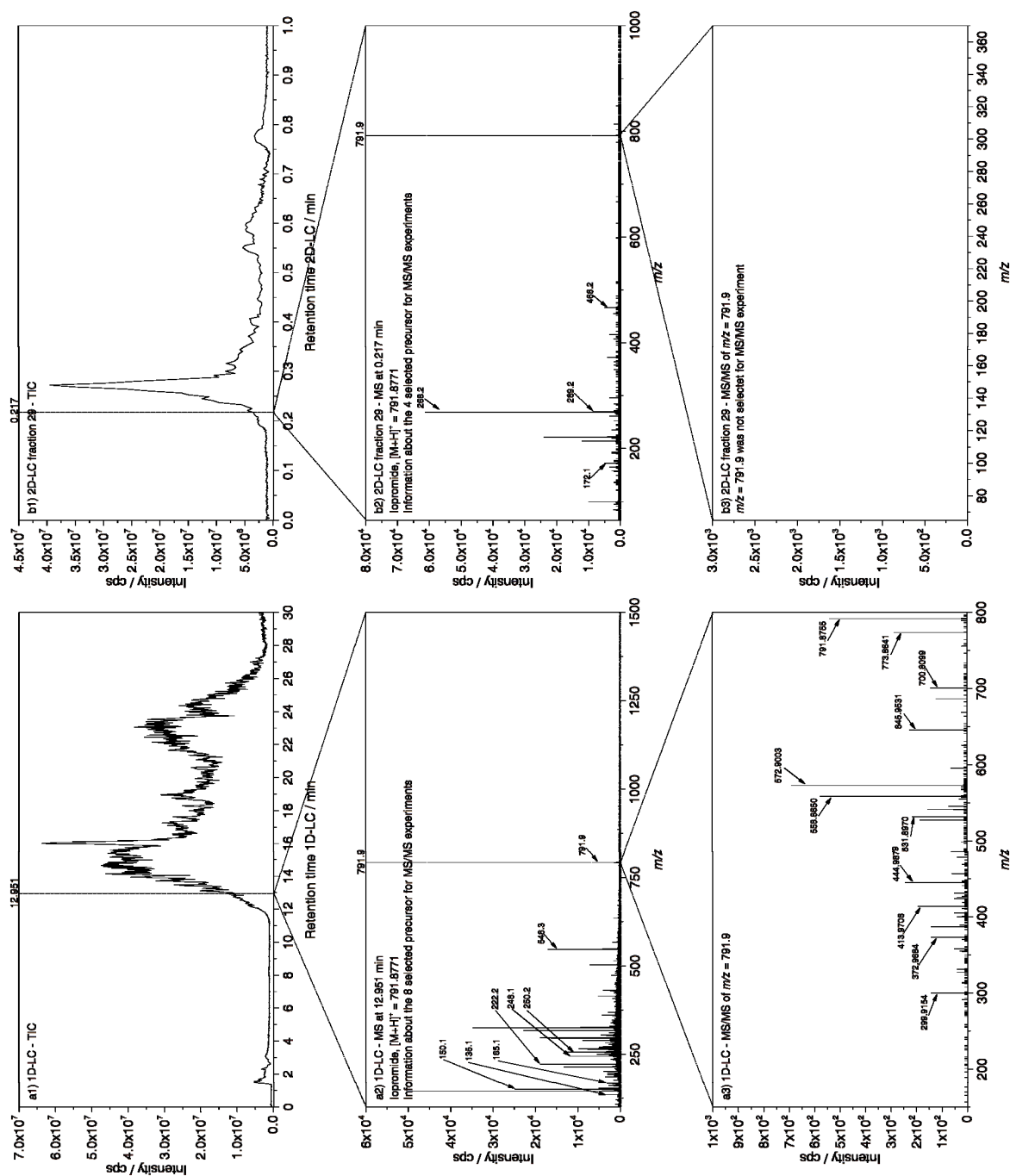
Figure S 3-4: Comparison of (a) 1D-LC and (b) 2D-LC MS and MS/MS spectra of iopromide [M+H]$^+$ 791.8771.

The retention time of bisoprolol is located at the local maximum inside the TIC chromatogram of both approaches (see Figure S 3-3). As discussed before it could be seen that the matrix

impact at this region is very high and the bisoprolol precursor ion could not be selected for an MS/MS experiment due to the relative low signal intensity for the 1D-LC approach. With the 2D-LC approach bisoprolol could be separated chromatographically from the interfering matrix. Therefore bisoprolol precursor could be selected as a precursor with the highest intensity for an MS/MS experiment.

The retention time of iopromide is located at the rising edge of the TIC chromatogram of both approaches (see Figure S 3-4). The matrix impact at this region is not as pronounced as for bisoprolol. The precursor intensity of iopromide for the 1D-LC approach is high enough for a selection for an MS/MS experiment. For the 2D-LC approach the absolute precursor intensity was not high enough, therefore iopromide was excluded from the MS/MS experiment.

3.6.6 Additional tables

Table S 3-2: Detailed list of the compounds used for the 99 component reference standard.

Analyte	purchased as	CAS No.	Purity*	Source	log P**
5,6-Dimethyl-1H-benzotriazole	5,6-Dimethyl-1H-benzotriazole monohydrate	4184-79-6	99%	Aldrich	2.33
5-Methyl-1H-benzotriazole	5-Methyl-1H-benzotriazole	136-85-6	≥ 98%	Fluka	1.81
Acetylsulfadiazine	N^4-Acetylsulfadiazine	127-74-2	99%	IUTA***	0.45
Acetylsulfadimidine	N^4-Acetylsulfamethazine	100-90-3	99%	IUTA***	0.72
Acetylsulfamerazine	N^4-Acetylsulfamerazine	127-73-1	99%	IUTA***	0.59
Acetylsulfamethoxazole	N^4-Acetylsulfamethoxazole	21312-10-7		LGC Standards	0.86
Allopurinol	Allopurinol	315-30-0		Sigma	-1.76
Ampicillin	Ampicillin	69-53-4		Sigma	-2.01
Atenolol	Atenolol	29122-68-7	≥ 98%	Sigma	0.43
Atorvastatin	Atorvastatin calcium salt	134523-03-8		Dr. Ehrenstorfer	5.39
Azithromycin	Azithromycin	83905-01-5	≥ 95%	Sigma	2.44
Benzotriazole	Benzotriazole	95-14-7	99%	Sigma-Aldrich	1.30
Bezafibrate	Bezafibrate	41859-67-0	≥ 98%	Sigma	3.99
Bisoprolol	Bisoprolol fumarate	104344-23-2		LGC Standards	2.20
Carbamazepine	Carbamazepine	298-46-4		Sigma	2.77
Carbetamide	Carbetamide	16118-49-3	Pestanal	Fluka	1.65
Cefalexin	Cephalexin hydrate	15686-71-2		Sigma	-2.15
Chloramphenicol	Chloramphenicol	56-75-7	≥ 98%	Sigma	0.88
Chlorbromuron	Chlorobromouron	13360-45-7	Pestanal	Fluka	2.85
Chloridazon	Chloridazon	1698-60-8	Pestanal	Fluka	1.11
Chlorprothixene	Chlorprothixene hydrochloride	6469-93-8		Sigma	5.07
Cilastatin	Cilastatin sodium salt	81129-83-1	≥ 98%	Sigma	-1.26
Citalopram	Citalopram hydrobromide	59729-32-7		Sigma	3.76
Clarithromycin	Clarithromycin	81103-11-9		LGC Standards	3.24
Clenbuterol	Clenbuterol hydrochloride	21898-19-1	≥ 95%	Sigma	2.33
Climbazole	Climbazole	38083-17-9	Pestanal	Fluka	4.34
Clindamycin	Clindamycin hydrochloride	21462-39-5		Sigma	1.04
Clozapine	Clozapine	5786-21-0		Sigma	3.40
Cyclophosphamide	Cyclophosphamide monohydrate	6055-19-2	≥ 97%	Sigma	0.10
Dapsone	Dapsone	80-08-0		Campro Scientific	1.27
Dehydrato-Erythromycin	Erythromycin	114-07-8		Sigma-Aldrich	2.60
Diacetoxyscirpenol	Diacetoxyscirpenol	2270-40-8		Sigma	0.38
Diatrizoate	Amidotrizoic acid dihydrate	50978-11-5		LGC Standards	2.89
Diclofenac	Diclofenac sodium salt	15307-79-6		Sigma	4.26
Dimpylate	Diazinon	333-41-5	Pestanal	Fluka	4.19
Diuron	Diuron	330-54-1	Pestanal	Fluka	2.53
Enalapril	Enalapril maleate	76095-16-4		Campro Scientific	0.59
Fenofibrate	Fenofibrate	49562-28-9	≥ 99%	Sigma	5.28
Fenofibric acid	Fenofibric acid	42017-89-0		Chemos	4.36
Fumonisin B1	Fuminosin B1	116355-83-0	95%	AppliChem	-0.67
Fumonisin B2	Fuminosin B2	116355-84-1		Iris Biotech	0.72
Gemcitabine	Gemcitabine hydrochloride	122111-03-9		LGC Standards	-1.47

Analyte	purchased as	CAS No.	Purity*	Source	log P**
Gliotoxin	Gliotoxin	67-99-2	≥ 98%	Fluka	-0.02
HT-2 Toxin	HT2 Toxin	26934-87-2	98%	AppliChem	0.58
Hydrocortisone	Hydrocortisone	50-23-7		Dr. Ehrenstorfer	1.28
Ifosfamide	Ifosfamide	3778-73-2		Sigma	0.10
Iopromide	Iopromide	73334-07-3	≥ 99%	LGC Standards	-0.44
Isoproturon	Isoproturon	34123-59-6	Pestanal	Fluka	2.57
Ketoprofen	Ketoprofen	22071-15-4	≥ 98%	Sigma	3.61
Lidocaine	Lidocaine	137-58-6		Sigma	2.84
Linuron	Linuron	330-55-2		Campro Scientific	2.68
Losartan	Losartan potassium salt	124750-99-8		Campro Scientific	3.96
Mefenamic acid	Mefenamic acid	61-68-7		Sigma	5.40
Megestrol	Megestrol acetate	595-33-5	Vetranal	Fluka	3.28
Melperone	Melperone hydrochloride	1622-79-3		Chemos	3.23
Metconazole	Metconazole	125116-23-6	Pestanal	Fluka	3.59
Metformin	1,1-Dimethylbiguanide hydrochloride	1115-70-4	97%	Aldrich	-1.36
Metobromuron	Metobromuron	3060-89-7	Pestanal	Fluka	2.24
Metoprolol	(±)-Metoprolol (+)-tartrate	56392-17-7	≥ 98%	Sigma	1.76
Metronidazole	Metronidazole	443-48-1		Sigma	-0.46
Mianserin	Mianserin hydrochloride	21535-47-7		Sigma	3.83
Mirtazapine	Mirtazapine	85650-52-8	≥ 98%	Sigma	3.21
Monuron	Monuron	150-68-5	Pestanal	Fluka	1.93
Nafcillin	Nafcillin sodium salt	985-16-0		Sigma	2.29
Naproxen	Naproxen	22204-53-1		Sigma-Aldrich	2.99
Oxazepam	Oxazepam	604-75-1		Sigma	2.92
Oxcarbazepine	Oxcarbazepine	28721-07-5	≥ 98%	Sigma	1.82
Paracetamol	Paracetamol	103-90-2		Fluka	1.63
Phenazone	Antipyrine	60-80-0		Fluka	1.22
Picoxystrobin	Picoxystrobin	117428-22-5		Campro Scientific	4.31
Pipamperone	Pipamperone dihydrochloride	2448-68-2	99%	Sigma	1.87
Piperacillin	Piperacillin sodium salt	59703-84-3		Sigma	-0.26
Prednisolone	Prednisolone	50-24-8	≥ 99%	Sigma	1.27
Propranolol	(±)-Propranolol hydrochloride	318-98-9	≥ 98%	Sigma	2.58
Propyphenazone	Propyphenazone	479-92-5		LGC Standards	2.35
Quinoxyfen	Quinoxyfen	124495-18-7	Pestanal	Fluka	4.98
Ramipril	Ramipril	87333-19-5		Campro Scientific	1.47
Ranitidine	Ranitidine hydrochloride	66357-59-3		Campro Scientific	0.98
Ritalinic acid	Ritalinic acid	19395-41-6	99%	Aldrich	-0.36
Roxithromycin	Roxithromycin	80214-83-1	≥ 90%	Sigma	3.00
Sertraline	Sertraline hydrochloride	79559-97-0		Campro Scientific	5.15
Simvastatin	Simvastatin	79902-63-9	≥ 97%	Sigma	4.46
Sotalol	Sotalol hydrochloride	959-24-0		Dr. Ehrenstorfer	-0.40
Stachybotrylactam	Stachybotrylactam	163391-76-2	≥ 95%	Bioaustralis	3.28
Sulfadiazine	Sulfadiazine	68-35-9	≥ 99%	Sigma	0.39
Sulfadimethoxine	Sulfadimethoxine	122-11-2	≥ 98.5%	Fluka	1.26
Sulfadimidine	Sulfamethazine	57-68-1	≥ 99%	Sigma	0.65
Sulfamethizole	Sulfamethizole	144-82-1	≥ 99%	Fluka	0.21
Sulfamethoxazole	Sulfamethoxazole	723-46-6		Fluka	0.79

Analyte	purchased as	CAS No.	Purity*	Source	log P**
Sulfapyridine	Sulfapyridine	144-83-2	≥ 99%	Fluka	1.01
Tamoxifen	Tamoxifen citrate	54965-24-1		Fluka	6.35
Terbutaline	Terbutaline hemisulfate	23031-32-5		Sigma	0.44
Terbutryn	Terbutryn	886-50-0	Pestanal	Fluka	2.88
Tramadol	Tramadol hydrochloride	36282-47-0	≥ 99%	Sigma	2.45
Trimethoprim	Trimethoprim	738-70-5	≥ 98%	Sigma	1.28
Venlafaxine	Venlafaxine hydrochloride	99300-78-4	≥ 98%	Sigma	2.74
Warfarin	Warfarin	81-81-2		Campro Scientific	2.74
Xylometazoline	Xylometazoline hydrochloride	1218-35-5		Sigma	3.78
Zuclopenthixol	Zuclopenthixol	53772-83-1		Chemos	4.22

Legend to Table S 3-2:

* Purity was at least pro analysi (p. a.) unless otherwise noted.

** log P values are predicted by ChemAxon – www.chemicalize.org

*** These standards have been prepared in-house according to the procedure described in the following article: Pfeifer T, Tuerk J, Bester K, Spiteller M (2002) Rapid Commun Mass Sp 16(7):663–669.

Manufacturer information:

Products from Aldrich, Fluka, Sigma and Supelco were purchased from Sigma-Aldrich, Schnelldorf, Germany.

AppliChem, Darmstadt, Germany.

Bioaustralis products via tebu-bio, Offenbach, Germany.

Campro Scientific, Berlin, Germany.

Chemos, Regenstauf, Germany.

Dr. Ehrenstorfer, Augsburg, Germany.

Iris Biotech, Marktredwitz, Germany.

LGC Standards, Wesel, Germany.

Table S 3-3:   MS Parameters for 1D-LC and 2D-LC approaches.

Parameter	1D-HPLC	2D-HPLC
m/z range	100 - 1500	65 - 1000
m/z range for IDA mode	150 - 1500	130 - 1000
# of MS/MS experiments / spectra	8	4
Dwell time fullscan / ms	250	20
Dwell time MS/MS experiment / ms	100	20
Period cycle time / ms	1101	150
MS/MS for ions greater than / Da	150	130
MS/MS mass tolerance / ppm	5	5
MS/MS exclusion after / occurrences	6	4
MS/MS exclusion time / s	30	6
Curtain gas / psi	35	10
Ion source gas 1 / psi	35	25
Ion source gas 2 / psi	45	25
IonSpray voltage floating / V	5500	5500
Temperature / °C	550	500
Collision energy / eV	10	10
Collision energy for MS/MS / eV	40	40
Declustering potential / V	60	80

Table S 3-4:   Detailed list of the 1D-LC separation of the 99 detected reference compounds with $\Delta\ m/z = \pm\ 5$ ppm.

Analyte	Molecular formula of [M]	Monoisotopic mass* of $[M+H]^+$	$\Delta\ m/z$ (ppm)	Retention time of 1 µg mL^{-1} ref. standard (min)	Average retention time of 0.45 ng mL^{-1} - 1 µg mL^{-1} ref. standard (min)
5,6-Dimethyl-1H-benzotriazole	$C_8H_9N_3$	148.0869	2.0	16.93	16.92
5-Methyl-1H-benzotriazole	$C_7H_7N_3$	134.0713	1.6	16.15	16.16
Acetylsulfadiazine	$C_{12}H_{12}N_4O_3S$	293.0703	0.6	14.66	14.67
Acetylsulfadimidine	$C_{14}H_{16}N_4O_3S$	321.1016	0.8	15.07	15.08
Acetylsulfamerazine	$C_{13}H_{14}N_4O_3S$	307.0859	0.6	14.90	14.91
Acetylsulfamethoxazole	$C_{12}H_{13}N_3O_4S$	296.0700	0.8	16.64	16.64
Allopurinol	$C_5H_4N_4O$	137.0458	-0.8	4.87	4.94
Ampicillin	$C_{16}H_{19}N_3O_4S$	350.1169	-0.4	13.44	13.46
Atenolol	$C_{14}H_{22}N_2O_3$	267.1703	0.3	12.02	12.04
Atorvastatin	$C_{33}H_{35}FN_2O_5$	559.2603	-2.7	20.66	20.65
Azithromycin	$C_{38}H_{72}N_2O_{12}$	749.5158	-0.6	13.97	14.01
Benzotriazole	$C_6H_5N_3$	120.0556	0.2	14.99	15.00
Bezafibrate	$C_{19}H_{20}ClNO_4$	362.1154	-1.0	19.63	19.62
Bisoprolol	$C_{18}H_{31}NO_4$	326.2326	0.7	14.64	14.67
Carbamazepine	$C_{15}H_{12}N_2O$	237.1022	0.7	17.80	17.79
Carbetamide	$C_{12}H_{16}N_2O_3$	237.1234	0.8	17.31	17.31
Cefalexin	$C_{16}H_{17}N_3O_4S$	348.1013	0.7	13.49	13.51
Chloramphenicol	$C_{11}H_{12}Cl_2N_2O_5$	323.0196	-1.0	16.81	16.81
Chlorbromuron	$C_9H_{10}BrClN_2O_2$	292.9687	0.4	21.15	21.15
Chloridazon	$C_{10}H_8ClN_3O$	222.0429	0.3	16.09	16.10
Chlorprothixene	$C_{18}H_{18}ClNS$	316.0921	0.8	16.14	16.17
Cilastatin	$C_{16}H_{26}N_2O_5S$	359.1635	1.1	14.32	14.33
Citalopram	$C_{20}H_{21}FN_2O$	325.1711	0.9	15.36	15.38
Clarithromycin	$C_{38}H_{69}NO_{13}$	748.4842	-1.8	15.82	15.84
Clenbuterol	$C_{12}H_{18}Cl_2N_2O$	277.0869	0.5	14.09	14.12
Climbazole	$C_{15}H_{17}ClN_2O_2$	293.1051	0.0	16.35	16.36
Clindamycin	$C_{18}H_{33}ClN_2O_5S$	425.1872	0.3	14.54	14.56
Clozapine	$C_{18}H_{19}ClN_4$	327.1371	0.9	14.56	14.59
Cyclophosphamide	$C_7H_{15}Cl_2N_2O_2P$	261.0321	0.7	16.51	16.52
Dapsone	$C_{12}H_{12}N_2O_2S$	249.0692	0.6	16.23	16.24
Dehydrato-Erythromycin	$C_{37}H_{65}NO_{12}$	716.4580	-2.6	15.61	15.21
Diacetoxyscirpenol	$C_{19}H_{26}O_7$	367.1751	-0.6	17.62	17.62
Diatrizoate	$C_{11}H_9I_3N_2O_4$	614.7769	-0.8	13.08	13.08
Diclofenac	$C_{14}H_{11}Cl_2NO_2$	296.0240	0.6	21.35	21.35
Dimpylate	$C_{12}H_{21}N_2O_3PS$	305.1083	0.7	23.37	23.37
Diuron	$C_9H_{10}Cl_2N_2O$	233.0243	-0.1	19.38	19.37
Enalapril	$C_{20}H_{28}N_2O_5$	377.2071	0.9	15.19	15.19
Fenofibrate	$C_{20}H_{21}O_4Cl$	361.1201	-1.8	24.92	24.92
Fenofibric acid	$C_{17}H_{15}ClO_4$	319.0732	0.8	21.44	21.43
Fumonisin B1	$C_{34}H_{59}NO_{15}$	722.3958	-2.4	15.49	15.51
Fumonisin B2	$C_{34}H_{59}NO_{14}$	706.4008	-2.7	16.19	16.18
Gemcitabine	$C_9H_{11}F_2N_3O_4$	264.0790	0.9	2.32	2.86

Analyte	Molecular formula of [M]	Monoisotopic mass* of $[M+H]^+$	$\Delta\,m/z$ (ppm)	Retention time of 1 µg mL^{-1} ref. standard (min)	Average retention time of 0.45 ng mL^{-1} - 1 µg mL^{-1} ref. standard (min)
Gliotoxin	$C_{13}H_{14}N_2O_4S_2$	327.0468	-0.7	17.40	17.39
HT-2 Toxin	$C_{22}H_{32}O_8$	425.2170	-0.5	17.93	17.93
Hydrocortisone	$C_{21}H_{30}O_5$	363.2166	0.9	16.91	16.91
Ifosfamide	$C_7H_{15}Cl_2N_2O_2P$	261.0321	0.7	16.36	16.37
Iopromide	$C_{18}H_{24}I_3N_3O_8$	791.8771	-0.8	12.98	13.02
Isoproturon	$C_{12}H_{18}N_2O$	207.1492	0.8	19.20	19.20
Ketoprofen	$C_{16}H_{14}O_3$	255.1016	0.3	19.54	19.54
Lidocaine	$C_{14}H_{22}N_2O$	235.1805	-0.9	13.56	13.61
Linuron	$C_9H_{10}Cl_2N_2O_2$	249.0192	0.2	20.92	20.92
Losartan	$C_{22}H_{23}ClN_6O$	423.1695	-1.0	18.23	18.23
Mefenamic acid	$C_{15}H_{15}NO_2$	242.1176	-0.2	22.47	22.47
Megestrol	$C_{24}H_{32}O_4$	385.2373	-0.4	22.42	22.42
Melperone	$C_{16}H_{22}FNO$	264.1758	0.9	14.67	14.72
Metconazole	$C_{17}H_{22}ClN_3O$	320.1524	-0.1	21.85	21.85
Metformin	$C_4H_{11}N_5$	130.1087	1.0	1.74	1.77
Metobromuron	$C_9H_{11}BrN_2O_2$	259.0077	-0.5	19.81	19.81
Metoprolol	$C_{15}H_{25}NO_3$	268.1907	0.2	14.04	14.07
Metronidazole	$C_6H_9N_3O_3$	172.0717	0.3	12.68	12.73
Mianserin	$C_{18}H_{20}N_2$	265.1699	0.4	15.26	15.29
Mirtazapine	$C_{17}H_{19}N_3$	266.1652	0.4	13.75	13.79
Monuron	$C_9H_{11}ClN_2O$	199.0633	0.8	17.87	17.87
Nafcillin	$C_{21}H_{22}N_2O_5S$	415.1322	-0.7	15.81	15.80
Naproxen	$C_{14}H_{14}O_3$	231.1016	-1.0	19.65	19.65
Oxazepam	$C_{15}H_{11}ClN_2O_2$	287.0582	0.3	18.11	18.11
Oxcarbazepine	$C_{15}H_{12}N_2O_2$	253.0972	0.7	16.98	16.98
Paracetamol	$C_8H_9NO_2$	152.0706	-2.7	12.97	13.03
Phenazone	$C_{11}H_{12}N_2O$	189.1022	-0.5	15.11	15.12
Picoxystrobin	$C_{18}H_{16}F_3NO_4$	368.1104	-0.7	22.65	22.64
Pipamperone	$C_{21}H_{30}FN_3O_2$	376.2395	0.9	13.05	13.13
Piperacillin	$C_{23}H_{27}N_5O_7S$	518.1704	-2.3	17.28	17.27
Prednisolone	$C_{21}H_{28}O_5$	361.2010	-0.7	16.79	16.79
Propranolol	$C_{16}H_{21}NO_2$	260.1645	-0.1	15.00	15.03
Propyphenazone	$C_{14}H_{18}N_2O$	231.1492	0.0	18.56	18.56
Quinoxyfen	$C_{15}H_8Cl_2FNO$	308.0040	-0.3	24.28	24.28
Ramipril	$C_{23}H_{32}N_2O_5$	417.2384	0.1	15.73	15.74
Ranitidine	$C_{13}H_{22}N_4O_3S$	315.1485	1.2	12.17	12.22
Ritalinic acid	$C_{13}H_{17}NO_2$	220.1332	-0.6	13.92	13.93
Roxithromycin	$C_{41}H_{76}N_2O_{15}$	837.5319	-1.9	15.90	15.92
Sertraline	$C_{17}H_{17}Cl_2N$	306.0811	1.0	16.05	16.08
Simvastatin	$C_{25}H_{38}O_5$	419.2792	-2.1	24.24	24.26
Sotalol	$C_{12}H_{20}N_2O_3S$	273.1267	-0.4	10.35	10.66
Stachybotrylactam	$C_{23}H_{31}NO_4$	386.2326	-1.2	19.56	19.56
Sulfadiazine	$C_{10}H_{10}N_4O_2S$	251.0597	0.1	13.98	14.00
Sulfadimethoxine	$C_{12}H_{14}N_4O_4S$	311.0809	0.9	17.40	17.39
Sulfadimidine	$C_{12}H_{14}N_4O_2S$	279.0910	0.9	15.29	15.30
Sulfamethizole	$C_9H_{10}N_4O_2S_2$	271.0318	0.7	15.41	15.41
Sulfamethoxazole	$C_{10}H_{11}N_3O_3S$	254.0594	0.2	16.67	16.68

Analyte	Molecular formula of [M]	Monoisotopic mass* of $[M+H]^+$	Δ m/z (ppm)	Retention time of 1 µg mL^{-1} ref. standard (min)	Average retention time of 0.45 ng mL^{-1} - 1 µg mL^{-1} ref. standard (min)
Sulfapyridine	$C_{11}H_{11}N_3O_2S$	250.0645	0.9	14.47	14.47
Tamoxifen	$C_{26}H_{29}NO$	372.2322	-0.4	17.39	17.40
Terbutaline	$C_{12}H_{19}NO_3$	226.1438	-0.5	9.41	9.75
Terbutryn	$C_{10}H_{19}N_5S$	242.1434	-0.7	18.13	18.12
Tramadol	$C_{16}H_{25}NO_2$	264.1958	0.3	14.06	14.09
Trimethoprim	$C_{14}H_{18}N_4O_3$	291.1452	1.2	13.39	13.42
Venlafaxine	$C_{17}H_{27}NO_2$	278.2115	0.4	14.63	14.66
Warfarin	$C_{19}H_{16}O_4$	309.1121	0.1	20.45	20.44
Xylometazoline	$C_{16}H_{24}N_2$	245.2012	0.6	15.52	15.55
Zuclopenthixol	$C_{22}H_{25}ClN_2OS$	401.1449	0.5	15.77	15.81

* The monoisotopic mass was calculated by using the integrated calculator of the PeakView software (Sciex).

Table S 3-5: Detailed list of the detected targets with 1D-LC and 2D-LC approach in the wastewater sample on the basis of the three criteria (Δ *m/z* = $\pm$ 5 ppm, Δ t_R = $\pm$ 2.5% and MS/MS database hit). "v" = criteria are fulfiled; "-" = criteria are not fulfilled.

Analyte	$\pm$ 5 ppm		$\pm$ 5 ppm + 2.5 %		$\pm$ 5 ppm + 2.5% + MS/MS	
	1D	2D	1D	2D	1D	2D
5,6-Dimethyl-1H-benzotriazole	v	v	v	v	-	v
5-Methyl-1H-benzotriazole	v	v	v	v	-	v
Acetylsulfadiazine	v	-	v	-	-	-
Acetylsulfamerazine	-	v	-	v	-	-
Acetylsulfamethoxazole	v	v	v	v	v	-
Atenolol	v	v	v	v	v	v
Atorvastatin	v	-	v	-	-	-
Benzotriazole	v	v	v	v	-	-
Bezafibrate	v	v	v	v	v	-
Bisoprolol	v	v	v	v	-	v
Carbamazepine	v	v	v	v	v	v
Carbetamide	-	v	-	v	-	-
Chlorbromuron	-	v	-	v	-	-
Chloridazon	-	v	-	v	-	-
Cilastatin	v	-	v	-	v	-
Citalopram	-	v	-	v	-	-
Clarithromycin	v	v	v	v	-	v
Clenbuterol	-	-	-	-	-	-
Climbazole	v	v	v	v	-	-
Clindamycin	-	v	-	v	-	-
Clozapine	-	v	-	v	-	-
Cyclophosphamide	-	v	-	v	-	v
Dehydrato-Erythromycin	-	v	-	v	-	-
Diatrizoate	v	-	v	-	-	-
Diclofenac	v	v	v	v	v	v
Diuron	v	v	v	v	-	-
Enalapril	v	v	v	v	-	-
Fenofibrate	-	v	-	v	-	-
Fenofibric acid	v	v	v	v	v	-
Gemcitabine	-	v	-	-	-	-
Hydrocortisone	v	-	v	-	-	-
Ifosfamide	-	v	-	v	-	-
Iopromide	v	v	v	v	v	-
Isoproturon	-	v	-	v	-	v
Ketoprofen	v	v	v	v	-	-
Lidocaine	v	v	v	v	-	-
Linuron	-	v	-	v	-	-
Losartan	v	v	v	v	v	v
Mefenamic acid	-	v	-	v	-	v
Megestrol	-	v	-	v	-	v
Melperone	-	v	-	v	-	v
Metconazole	-	v	-	v	-	-

Analyte	± 5 ppm		± 5 ppm + 2.5 %		± 5 ppm + 2.5% + MS/MS	
	1D	2D	1D	2D	1D	2D
Metformin	v	v	v	v	-	v
Metobromuron	-	v	-	v	-	-
Metoprolol	v	v	v	v	v	v
Metronidazole	-	v	-	v	-	v
Monuron	-	v	-	v	-	v
Nafcillin	v	-	v	-	-	-
Naproxen	v	-	v	-	v	-
Oxazepam	v	v	v	v	v	v
Oxcarbazepine	v	-	v	-	-	-
Paracetamol	v	v	v	v	v	v
Phenazone	-	v	-	v	-	-
Piperacillin	v	-	v	-	-	-
Prednisolone	v	v	v	v	-	-
Propranolol	v	v	v	v	-	v
Propyphenazone	-	v	-	v	-	-
Quinoxyfen	v	v	v	v	-	-
Ramipril	v	v	-	v	-	v
Ranitidine	v	v	v	v	-	v
Ritalinic acid	v	v	v	v	v	-
Roxithromycin	v	v	v	v	-	-
Sertraline	-	v	-	v	-	-
Simvastatin	v	-	-	-	-	-
Sotalol	v	v	-	v	-	v
Sulfadimethoxine	-	v	-	v	-	v
Sulfamethoxazole	v	v	v	v	-	-
Sulfapyridine	v	-	v	-	-	-
Tamoxifen	-	v	-	v	-	v
Terbutaline	-	v	-	v	-	v
Terbutryn	v	v	v	v	-	v
Tramadol	v	v	v	v	v	-
Trimethoprim	v	v	v	v	v	v
Venlafaxine	v	v	v	v	-	v
Warfarin	v	v	v	v	-	v
Xylometazoline	v	v	-	v	-	v
Zuclopenthixol	-	v	-	v	-	-

Table S 3-6:   Detailed list of the detected targets with (a) 1D-LC and (b) 2D-LC approach in the wastewater sample on the basis of the two criteria Δ m/z = $\pm$ 5 ppm and Δ t_R = $\pm$ 2.5%. The ranking position shows the priority, based on the signal intensity at the given retention time, for a selection for an IDA experiment. For 1D-LC all targets with the priority between 1 to 8 are selected for an IDA experiment. For 2D-LC all targets with the priority between 1 to 4 are selected for an IDA experiment.

a) Analyte 1D-LC	Ranking position 1D-LC	MS/MS found at (min)	b) Analyte 2D-LC	Ranking position 2D-LC	MS/MS found in D1 fraction #	MS/MS found in D2 at (min)
5,6-Dimethyl-1H-benzotriazole	8	16.63	5,6-Dimethyl-1H-benzotriazole	3	46	0.330
5-Methyl-1H-benzotriazole	2	16.15	5-Methyl-1H-benzotriazole	4	37	0.303
Acetylsulfadiazine	57	14.72	Acetylsulfamerazine	36	30	0.345
Acetylsulfamethoxazole	1	16.65	Acetylsulfamethoxazole	46	44	0.317
Atenolol	1	12.09	Atenolol	3	26	0.189
Atorvastatin	156	20.65	Benzotriazole	22	31	0.262
Benzotriazole	3	15.00	Bezafibrate	139	65	0.439
Bezafibrate	1	19.64	Bisoprolol	2	28	0.294
Bisoprolol	31	15.00	Carbamazepine	4	33	0.364
Carbamazepine	1	17.80	Carbetamide	23	35	0.350
Cilastatin	8	14.33	Chlorbromuron	76	69	0.464
Clarithromycin	380	16.08	Chloridazon	4	43	0.302
Climbazole	23	16.67	Citalopram	73	36	0.322
Diatrizoate	150	13.14	Clarithromycin	1	54	0.370
Diclofenac	8	21.35	Climbazole	6	37	0.354
Diuron	675	19.38	Clindamycin	24	28	0.281
Enalapril	91	15.43	Clozapine	41	31	0.288
Fenofibric acid	2	21.43	Cyclophosphamide	4	28	0.324
Hydrocortisone	95	16.89	Dehydrato-Erythromycin	41	50	0.345
Iopromide	3	12.95	Diclofenac	4	63	0.485
Ketoprofen	173	19.56	Diuron	19	68	0.416
Lidocaine	4	13.61	Enalapril	2	33	0.309
Losartan	7	18.25	Fenofibrate	13	63	0.593
Metformin	5	1.76	Fenofibric acid	1	56	0.488
Metoprolol	4	14.07	Ifosfamide	11	26	0.323
Nafcillin	6	15.84	Iopromide	8	29	0.217
Naproxen	7	19.65	Isoproturon	2	36	0.410
Oxazepam	3	18.13	Ketoprofen	14	38	0.413
Oxcarbazepine	56	16.98	Lidocaine	10	25	0.246
Paracetamol	2	13.02	Linuron	24	59	0.468
Piperacillin	637	17.29	Losartan	4	41	0.394
Prednisolone	8	17.10	Mefenamic acid	4	54	0.516
Propranolol	172	14.83	Megestrol	2	46	0.501
Quinoxyfen	572	24.34	Melperone	1	42	0.287
Ranitidine	30	12.24	Metconazole	3	58	0.507

a) Analyte 1D-LC	Ranking position 1D-LC	MS/MS found at (min)	b) Analyte 2D-LC	Ranking position 2D-LC	MS/MS found in D1 fraction #	MS/MS found in D2 at (min)
Ritalinic acid	7	13.92	Metformin	1	12	0.135
Roxithromycin	650	16.14	Metobromuron	27	44	0.421
Sulfamethoxazole	9	16.68	Metoprolol	4	30	0.262
Sulfapyridine	20	14.46	Metronidazole	3	29	0.213
Terbutryn	41	17.84	Monuron	1	43	0.362
Tramadol	3	13.81	Oxazepam	2	33	0.385
Trimethoprim	8	13.43	Paracetamol	1	31	0.209
Venlafaxine	66	14.66	Phenazone	2	26	0.279
Warfarin	631	20.47	Prednisolone	2	28	0.345
			Propranolol	1	51	0.299
			Propyphenazone	1	27	0.395
			Quinoxyfen	112	71	0.557
			Ramipril	2	36	0.341
			Ranitidine	1	30	0.194
			Ritalinic acid	11	22	0.247
			Roxithromycin	38	42	0.359
			Sertraline	74	41	0.349
			Sotalol	1	25	0.191
			Sulfadimethoxine	4	56	0.352
			Sulfamethoxazole	53	34	0.306
			Tamoxifen	2	39	0.405
			Terbutaline	1	21	0.185
			Terbutryn	3	42	0.415
			Tramadol	16	28	0.265
			Trimethoprim	2	39	0.229
			Venlafaxine	4	26	0.295
			Warfarin	4	41	0.446
			Xylometazoline	3	33	0.325
			Zuclopenthixol	36	63	0.364

Chapter 4   Large volume injection of aqueous samples in nano liquid chromatography using serially coupled columns

One of the biggest challenges in the field of water analysis is the determination of trace concentrations of emerging contaminants. These contaminants must therefore be enriched, typically by either off-line or online solid phase extraction. An alternative method is the direct large volume injection onto the separation column. In liquid chromatography, the limitation of the injection volume depends on the column dimensions, the analyte hydrophobicity, the injection solvent and the nature of the stationary phase. Exceeding of the maximum injection volume is indicated by a deterioration of peak shapes and a loss in signal intensity. By serial coupling of two stationary phases with different hydrophobicities, the focusing can be improved and the maximum injection volume can be increased. A suitable combination could be the hyphenation of a carbon-based phase like Hypercarb and a C18 phase. This paper describes how to implement this concept based on nano-LC and UV detection. To cover a wide range of polarity, a polar, semi-polar and non-polar compound were used as model analytes. The recommended injection volume of 25 nL for a nanobore column could be successfully increased to 3,000 nL, without deterioration of peak shapes.

4.1 Introduction

Global water pollution by organic chemicals is a topic of high relevance and the list of priority hazardous substances is getting longer [1–7]. Furthermore, polar substances and metabolites are coming more and more into the focus of research and regulation. Therefore, a continuous multi-residue monitoring of such compounds is implemented in many routine laboratories. Gas chromatography-mass spectrometry (GC-MS) is a widely used technique, although many polar compounds are not directly amenable to GC analysis without derivatization [8, 9]. Therefore, liquid chromatography–mass spectrometry (LC-MS) is emerging as the method of choice because of low detection limits and a broad range of detectable substances [10, 11].

The polarity range of trace organic pollutants is very wide and their concentrations can be in the low ng L^{-1} range. Usually solid phase extraction (SPE), either offline or online, is used to enrich the analytes prior to LC separation.

An alternative enrichment technique is the direct injection of large sample volumes that is defined as an injection volume > 10 % of the column void volume [12]. Little and Fallick [13] used a liquid chromatography (LC) system with an additional external pump for a successful online enrichment of non-polar analytes on a C18 column. Others used single column large volume injection (SC-LVI) for the analysis of alkylbenzene sulfonates or different drugs [14–17]. Hagendoorn et al. [18, 19] worked on a further improvement of this technology. They used LVI of several hundred microliters (μL) on a pre-column for the enrichment and simple pre-separation of analytes and matrix. The relevant analyte fraction was trapped and re-injected on the main column for further separation, through a valve, which was located between the pre- and main column. Such an injection technique is known as coupled column large volume injection (CC-LVI) and is used successfully until today as online SPE [20–22].

In contrast, a direct LVI on an LC-MS system often results in a substantial introduction of matrix into the very sensitive MS system. The resulting matrix effects can lead to ion suppression and thus to a collapse of the signal intensity or sensitivity of the mass spectrometer [23, 24]. These effects can be minimized by reducing the flow rates and column i.d. of the LC system. In 1996, Rezai [25] reported about the reduction of the flow rates and column i.d. in the field of micro liquid chromatography (μLC) and the positive effect of reduced flow rates on MS detection. Further downscaling to nano liquid chromatography (nano-LC) can enhance the

positive impact, because the flow rate is adjusted between 50 and 2,000 nL min^{-1}. A significant problem of nano-LC is the extra column volume, as a result of high dead volume connections between valves, pre- and separation columns or in-line filters. To minimize the dead volume, special coupling techniques must be used.

The online enrichment of non-polar components on a silica-based C18 stationary phase is simple and based on strong interactions with the non-polar C18 moieties. As a result of strong interactions with the mobile phase, polar components cannot be retarded on these columns. However, polar analytes, metabolites and transformation products nowadays play a predominant role in water analysis, so that their enrichment is mandatory. Because of missing focusing of polar analytes on a C18 phase, there is no possibility to enrich this analyte group either by SPE or a direct LVI.

Although the use of hydrophilic interaction liquid chromatography (HILIC) columns has proven to be a successful approach for the analysis of polar compounds, HILIC is not compatible with the direct injection of large sample volumes when the injection solvent is water as has been demonstrated by Ruta et al. [26].

The aim of this work is therefore to introduce a concept that allows an online enrichment of polar compounds on a nano bore porous graphitic carbon (PGC) pre-column. The retention mechanism is regarded as a combination of dispersive hydrophobic interactions between the analyte-mobile phase and analyte-graphitic surface and charge-induced interactions of polar analytes with the polarizable surface of the graphite [27, 28]. Furthermore, different column coupling concepts will be evaluated, because the low dead volume connection is technically demanding. Based on the best technology the maximum injection volume will be investigated by monitoring the loss of signal intensity and peak deterioration.

4.2 Materials and methods

4.2.1 HPLC systemSolvents and additives

For collecting of chromatographic data, an Eksigent NanoLC - Ultra 2D system (AB Sciex, Dublin, CA) with the standard nano-flow module (50 - 500 nL min^{-1}) was used. The pneumatic

pump can mix binary-gradients at backpressure up to 10 kpsi with a gradient delay volume lower than 1 µL. It is recommended to operate the pump channels at 1% of mobile phase A and B at the start and end of the solvent gradient. Otherwise, mobile phase from pump channel A might enter the pump channel B and vice versa, which leads to irregularities in gradient elution. Furthermore, an HTS PAL autosampler (CTC Analytics, Zwingen, Switzerland) with a Hamilton syringe (Bonaduz, Switzerland) and an external UV/Vis-Detector SpectraFlow 501 (SunChrom, Friedrichsdorf, Germany) were used. All connection capillaries including the injection loop (calculated volume of 4 µL) were 360 µm (before main column) or 280 µm (after the main column) outer diameter (o.d.) fused-silica purchased from Postnova Analytics (Landsberg, Germany) and cut to size by a Shortix GC (SGT, Middelburg, The Netherlands) diamond cutter. The reduction of the o.d. is necessary for coupling the column to the built-in capillary of the UV-detector. All capillary/column i.d., o.d., lengths and calculated volumes used for the LVI concept are listed in Supporting information Table S 4-1 and shown schematically in Figure S 4-1.

Data processing was performed using the Eksigent software package (version 3.10, Build 110228) and Excel 2010 (Microsoft, Redmont, WA). For visualization OriginPro 9 (OriginLab, Northampton, MA) was used.

4.2.2 Material used for column coupling

For coupling of the pre- and main-column several connection types were tested. A one piece fused silica adapter with a 360 µm i.d. (VICI VALCO, Schenkon, Switzerland) and a ProteCol-Union (SGE Analytical Science, Ringwood Victoria, Australia) with a double side ferrule were employed.

4.2.3 Gradient programming

For experiments without pre-column a water + 0.1% FA (eluent A) - acetonitrile + 0.1% FA (eluent B) gradient at a flow rate of 500 nL min^{-1} was applied according to the following

program: 4 min hold at 1% B, 1-99% B in 10 min, 16 min hold at 99% B, 99-1% B in 0.5 min, 9.5 min re-equilibration (~19 column volumes).

For experiments with pre-column also a water + 0.1% FA (eluent A) - acetonitrile + 0.1% FA (eluent B) gradient at a flow rate of 500 nL min^{-1} was applied according to the following program: 8 min hold at 1% B, 1−99% B in 10 min, 16 min hold at 99% B, 99-1% B in 0.5 min, 9.5 min re-equilibration (~19 column volumes).

During the initial 4 or 8 min of isocratic elution, the sample loop was switched for a defined time into the flow to inject the analyte solution.

4.2.4 Columns
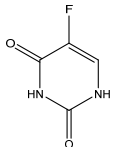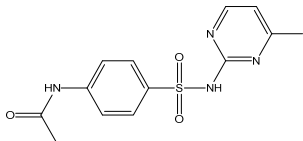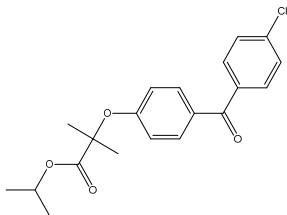
A core-shell stationary phase was used as the main analytical column (Kinetex C18, 2.6 μm by Phenomenex, Aschaffenburg, Germany). The material was packed by Grace (Grace Davison Discovery Sciences - Alltech Grom, Worms, Germany) into a nanobore column with 5 cm length and 100 μm i.d.

For the on-line pre-column enrichment concept a nanobore pre-column filled with Hypercarb 5 μm particles (Thermo Fisher Scientific, Dreieich, Germany) was used. This pre-column is commercially available as Hypercarb IntegraFrit capillary column with 1.2 cm length and 75 μm i.d. It consists of a capillary column with an integrated frit at one end.

4.2.5 Chemicals

Acetonitrile and water were purchased from Th. Geyer - Chemsolute (Renningen, Germany) and of LC-MS grade. As a solvent additive, formic acid (p. a. grade) purchased from Sigma-Aldrich (Seelze, Germany) was used. The probe compound mixture is shown in Table 4-1 and represents a broad range of polarity. It consists of 5-fluorouracil (5-FU), acetyl-sulfamerazine (AC-S) (in house synthesized according to [29]) and fenofibrate (FEN) (Sigma-Aldrich, Seelze, Germany).

Table 4-1:   Properties of model compounds.

Name	Formula	MW (g mol^{-1})	log P	pKa (acid)	CAS-No.	References
1) 5-fluorouracil		130.07	-0.66	7.8	51-21-8	[30]
2) Acetyl-sulfamerazine		306.34	0.59	6.9	127-73-1	[31]
3) Fenofibrate		360.83	5.28	-	49562-28-9	[32]

For the preparation of stock solutions, 10 mg of each component were dissolved in 10 mL water/acetonitrile + 0.1% FA (50/50, v/v) resulting in a concentration of 1 mg mL^{-1}. For the analyte mix, 0.25 mL of each standard mix and 0.25 mL of a dilution solvent (50/50, water/acetonitrile) were mixed. This solution was diluted with water to the final concentration of 2 µg mL^{-1} containing 0.4% residual organic solvent.

This solution was used for all further dilutions with water up to a concentration of 0.025 µg mL^{-1} with a residual organic fraction of 0.007% for the 3000 nL injection. The injected mass was always 0.1 ng for each component regardless of the injection volume in order to compare peak shapes and to avoid mass overloading.

For further peak shape experiments, a separate 5-FU solution with a resulting concentration of 2 µg mL^{-1} was prepared by the same procedure using only water as dilution solvent.

4.3 Results and discussion

4.3.1 Effect of large volume injection on single column (RP C18)

To demonstrate the effect of the LVI on the peak shape without pre-column, 50, 500 and 1000 nL of the analyte mixture were injected on the Kinetex C18 column with a theoretical maximal injection volume of 25 nL [12] (column void volume: 250 nL). Figure 4-1 shows an overlay of the resulting chromatograms. For the semi-polar AC-S and the non-polar FEN there are no adverse effects on peak shape and signal intensity for all injection volumes. For 5-FU, an injection volume of 50 nL results in a good peak shape. Increasing the injection volume to 500 nL and 1000 nL reduces the peak height by a factor of 2.5 and 7, respectively, as shown in

Table 4-2 a. The peak width increases rapidly by a factor of 2.5 for an injection volume of 500 nL and by a factor of 4.7 for an injection volume of 1000 nL. This clearly demonstrates that the injection of large volumes will lead to a severe loss in signal intensity for very polar compounds such as 5-FU.

Table 4-2:   Comparison of different parameters characterizing peak shape in dependence on injection volume for 5-FU with and without pre-column (n=3).

	Injection volume (nL)	Peak area (mAU s)	Area RSD (%)	Peak width (s)	Width RSD (%)	Peak Height (mAU)	Height RSD (%)	Asymmetry
a) without pre-column	50	1196	3.4	40	8.3	54	4.5	2.49
	500	1238	2.6	82	1.8	22	2.4	0.80
	1000	859	13.6	135	0.9	8	9.2	2.37
b) with pre-column	50	1245	0.6	49	0.4	44	0.7	0.95
	250	1279	1.4	55	0.5	41	1.7	0.63
	2000	1337	0.7	46	0.5	51	0.2	1.18
	3000	1274	1.2	49	0.7	48	1.8	1.28
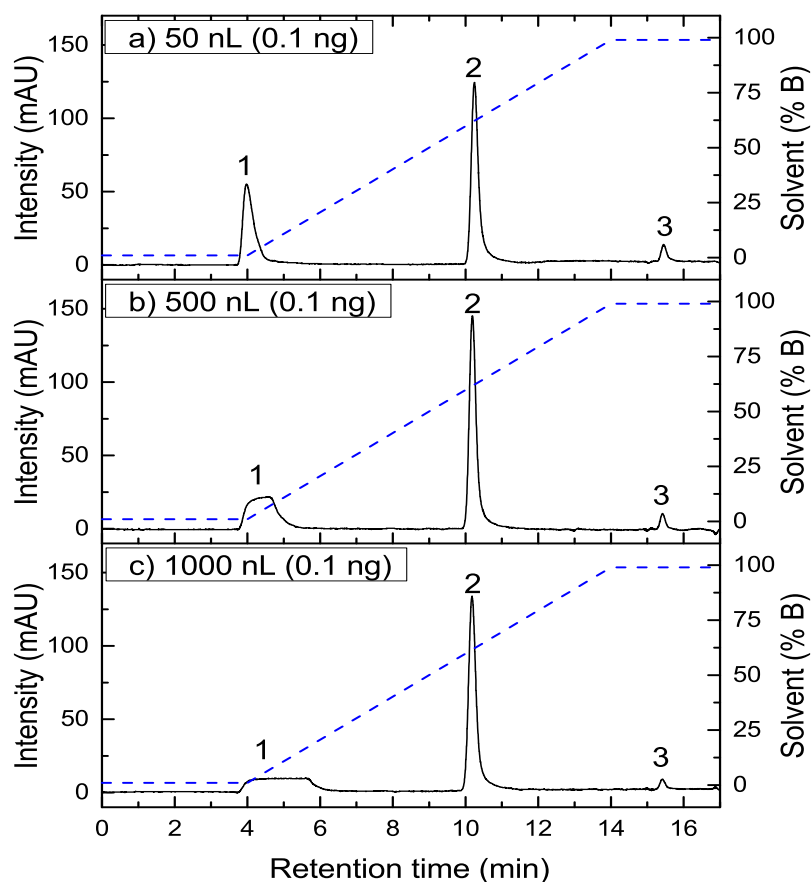
Figure 4-1:   Injection of 50, 500 and 1000 nL of the analyte mixture and the influence of LVI on peak shapes of 5-FU (1), AC-S (2) and FEN (3). Chromatographic conditions: stationary phase: Kinetex C18 (50 x 0.1 mm; 2.6 μm); mobile phase: gradient, A) water + 0.1% formic acid (FA), B) acetonitrile + 0.1% FA; flow rate: 500 nL min^{-1}; injection volume: 50, 500, 1000 nL with 0.1 ng of each compound; temperature: isothermal at 30 °C; detection: UV at 254 nm.

4.3.2 Evaluation of coupling concepts

The pre-column concept for the on-line enrichment is based on a direct hyphenation of a 1.2 cm long Thermo Scientific Hypercarb pre-column and a 5 cm nanobore Phenomenex Kinetex C18 main column.

The Hypercarb IntegraFrit consists of a 360 µm o.d. and a 75 µm i.d. fused-silica (FS) capillary and a thermally immobilized frit. During the immobilization process of the frit, the FS capillary loses its protective polyimide coating, which results in irregular o.d. at the end of the pre-column and increases the risk of fracture. A direct coupling at the main column head with a polyether ether ketone (PEEK) sleeve and a stainless steel ferrule often ends in a destroyed frit and clogged main column. Therefore, other coupling concepts had to be evaluated.

At first a direct coupling with a one piece FS adapter was tested unsuccessfully. It was not possible to achieve a leak-free connection without damaging the pre-column frit. The second coupling concept is based on a connection to a short FS transfer capillary with an identical o.d. and protective polyimide coating, which is regularly connected with the main column. One possibility to connect the IntegraFrit pre-column with the transfer capillary is the use of a very tight Teflon (polytetrafluoroethylene) sleeve delivered with the pre-column. However, because of the high resulting pressure above 100 bar, the capillaries will be pushed out of the sleeve rendering a leak- and dead volume free connection impossible. The other possibility is the use of a short glass tubing to fix the capillaries under thermal sealing. However, during the thermal process the protective polyimide coating is destroyed and a soot layer is formed between the glass tubing and capillaries, which prevents the sealing. The usage of glue was excluded because its ingredients could enter the chromatographic system.

Another coupling concept is based on the ProteCol-Union with a double side ferrule to connect with the FS transfer capillary. By placing the capillaries absolutely planar and in the center of the double side ferrule, the connection is outside the fragile area of the pre-column. This results in a successful connection of the IntegraFrit pre-column and was used in all further investigations

4.3.3 Effect of large volume injection on coupled columns and influence of residual organic solvent

For the evaluation of the described pre-column concept 1500, 2000 and 3000 nL of the analyte mixture were injected. As can be seen from the resulting chromatograms presented in Figure 4-2, no significant changes in terms of peak shape and signal intensity are observed for AC-S and FEN when the injection volume is increased to 3000 nL. The data given in Table S 4-2 and Table S 4-3 reveals that peak width slightly increases for AC-S and FEN. A concomitant small loss is observed for the peak height. These effects might be attributed to the introduction of an additional extra-column volume when the columns are connected via a short capillary. Also, FEN elutes after some minutes at the end of the solvent gradient. Therefore, the additional broadening of the chromatographic band can be explained when compared to the elution on the C18 stationary phase.
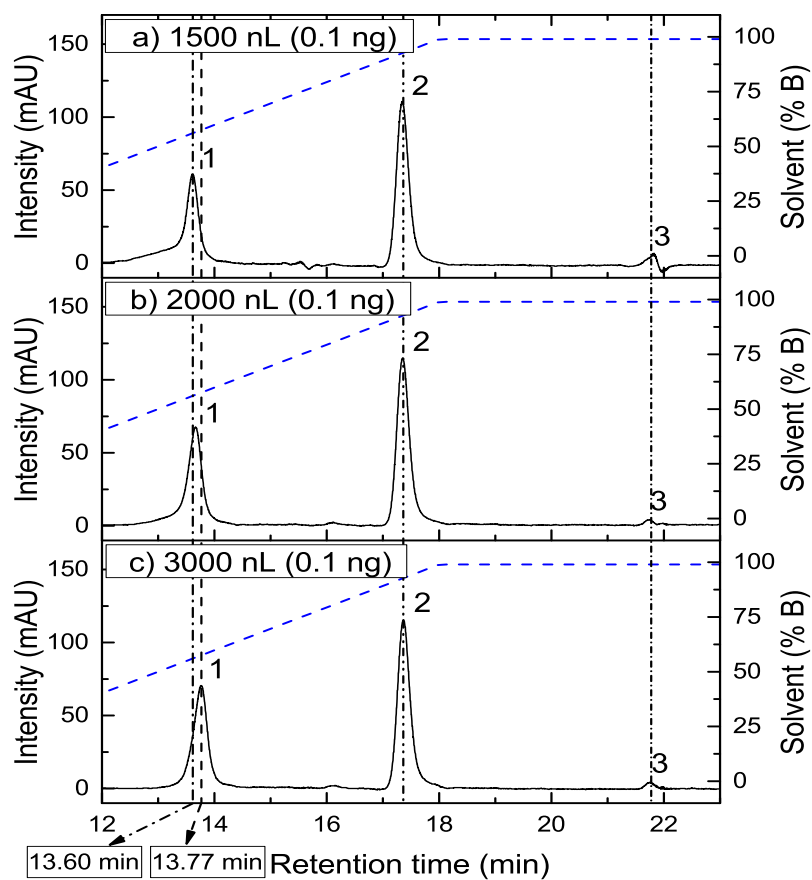
Figure 4-2: Injections between 1500 and 3000 nL of the analyte mixture 5-FU (1), AC-S (2) and FEN (3). Chromatographic conditions: stationary phase: Hypercarb IntegraFrit pre-column (12 x 0.075 mm, 5 μm) coupled with Kinetex C18 (50 x 0.1 mm; 2.6 μm); mobile phase: gradient, A) water + 0.1% FA, B) acetonitrile + 0.1% FA; flow rate: 500 nL min^{-1}; injection volume: 1500 – 3000 nL with 0.1 ng of each compound; temperature: isothermal at 30 °C; detection: UV at 254 nm.

However, the peak profile of 5-FU at an injection volume of 1500 nL as shown in Figure 4-2 is not ideal. There is a strong fronting, which decreases with an increase of the injection volume to 3000 nL. At first sight, this is unexpected because one would assume that the peak profile will be disturbed by a larger rather than a lower injection volume. An explanation for this effect could be the residual organic fraction in the injection mixture. For dissolving of the non-polar components, acetonitrile as organic modifier is necessary. During the dilution process of the stock solution with water, the organic fraction can be reduced to 0.4% for an injection volume of 50 nL. A further dilution for the injection solutions for 1500 nL and 3000 nL decreases the content of acetonitrile to 0.013% and 0.007%. These residual organic fractions are very small and can be usually neglected, but here a negative effect on the chromatographic performance is observed. This is also supported by the small retention time shift of 5-FU. The reduction of the organic fraction increases the interaction between 5-FU and the stationary phase, which results in higher retention times. The RSD of the retention time of the system was determined by AC-S and is 0.07%. The RSD of the retention time of 5-FU shows a significantly higher deviation with 0.5%, which was not caused by the LC system. Furthermore, the asymmetry factors shown in Table 4-3 increase from 0.35 to 0.8 with decreasing of the organic fraction.

Table 4-3:   Comparison of different parameters characterizing peak shape and retention time shift of 5-FU in dependence on organic solvent fraction.

Injection volume (nL)	Percentage of residual organic fraction (%)	Retention time (min)	Peak area (mAU s)	Peak width (s)	Peak Height (mAU)	Asymmetry
1500	0.013	13.6	1397	59.3	61	0.35
2000	0.010	13.7	1433	42.1	67	0.64
3000	0.007	13.8	1407	36.4	70	0.80

In order to confirm the hypothesis that very low fractions of the organic solvent in the injection solution were responsible for these effects, only 5-FU was dissolved and diluted with water + 0.1% FA for injection of 50, 250, 2000 and 3000 nL as verification experiment.

On the basis of the data given in

Table 4-2 b it can be seen that the RSDs of the peak area, width and height are acceptable with a maximum RSD of 1.8%. The peak profiles vary only slightly in intensity and peak width. The peak area of 1297 mAU s ± 4% is nearly constant and the small variance can be attributed to the dilution steps.

The strong fronting which was observed before (see Figure 4-2) is not evident any longer, which supports our hypothesis. In contrast, a small tailing is observed for an injection of 3000 nL. This result has severe implications for quantitation in trace analysis. For the direct injection of water samples it can be assumed that there are no organic solvents in the samples. For the quantification of these samples by an external calibration, however, organic modifiers such as acetonitrile or methanol are often used to improve the solubility, especially if the method covers a broad range of polarity. Furthermore, organic modifiers are used to avoid the adsorption of analytes onto hydrophilic materials [33]. In this context, however, the usage of organic modifier must be minimized to avoid a loss in signal intensity.

4.3.4 Comparison to other studies of 5-FU

The results of this work show that it is possible to overfill the column void volume by 1200% for 5-FU during the injection without a deterioration of the peak shape. In order to underline the importance of our findings, we have made a comparison of the retention factor of 5-fluorouracil obtained on the PGC pre-column to the retention factor obtained in other studies. As can be seen from the data compiled in

Table 4-4, the highest retention factor was obtained on the Atlantis dC18 stationary phase [34]. In these studies, the mobile phase contains a very low concentration of the organic modifier (3.3%). Thus, a significantly higher retention will not be possible on this type of column. Interestingly, the retention factor in HILIC mode is even lower than in reversed phase mode. Although it is often assumed that HILIC stationary phases will lead to a higher retention for polar compounds than reversed phase materials, this cannot be supported by the data given in

Table 4-4. Remaud [35] and Tsume [36] both used a PGC column for the analysis of 5-FU. However, a pronounced difference in the retention factor is observed. This can be attributed to the higher portion of the organic modifier at the beginning of the gradient. Tsume et al. used

20% organic modifier for the mobile phase and injected 10 µL (4.5% of the column void volume) of a sample with a residual organic solvent of 36%. Remaud et al. used a gradient start point of 12% organic modifier and injected 40 µL (12% of the column void volume) of an aqueous sample without organic modifier. This fact also supports our findings that very small differences in the concentration of the residual organic solvent which is either used in the injection solution or in the initial start concentration of the solvent gradient can have a pronounced effect on the retention and peak shape.

Table 4-4:   Comparison of different studies of 5-FU.

Study	Stationary phase	Pre-column dim. (mm)	Column dim. (mm)	Retention factor k [+]
This work	PGC:Hypercarb, RP: Kinetex C18	12 x 0.075	50 x 0.1	146*
Büchel [34]	RP: Atlantis dC18	1 x 2.1	150 x 2.1	2.52
Chen [37]	RP: Venusil RP-C18		250 x 4.6	0.71
de Mattos [38]	RP: Xterra C18		250 x 4.6	0.39
Deenen [39]	HILIC: Luna HILIC		150 x 2.1	0.72
Kosovec [40]	HILIC: Asahipak NH2P-50 2D		150 x 2.0	1.74
Kovalova [41]	HILIC: ZIC-HILIC from SeQuant	20 x 2.1	150 x 2.1	2.32
Maring [42]	RP: Atlantis dC18	4 x 3.0	250 x 4.6	2.23
Pisano [43]	HILIC: Asahipak NH250D		150 x 4.6	1.29
Remaud [35]	RP: XTerra MSC18		100 x 2.1	0.72
Remaud [35]	PGC: Hypercarb		150 x 2.1	5.37
Tsume [36]	PGC: Hypercarb		100 x 2.1	1.87
Van Kuilenburg [44]	RP: Phenomenex Aqua	4 x 3.0	250 x 4.6	1.53
Woo [45]	RP: Zorbax C18	18 x 2.1	100 x 2.1	0.27
Zhu [46]	RP: Nova-pack C18		150 x 3.9	0.66

* Calculated retention factor for the Hypercarb pre-column only. + The dead volume for the calculation of the retention factor was calculated by ChromSword Auto on the basis of the given column dimensions.

In this respect we would like to stress why we used two serially connected columns with a small PGC pre-column instead of a long PGC column. At first the PGC material is very hydrophobic, which results in very strong interactions with non-polar analytes. This can lead to very broad elution profiles which can also be observed in Figure 4-1 and Figure 4-2. While 5-FU and AC-S elute during the solvent gradient, FEN is eluted during the isocratic plateau. Therefore, a band compression is not possible. When a longer column is used, this effect will be even more pronounced. However, short columns have a significant disadvantage in terms of peak capacity

and this is the reason to use a longer C18 phase as a second column. Another advantage of the combination of a PGC and a C18 stationary phase is the resulting selectivity. In that regard, this strategy resembles the concept of phase optimized liquid chromatography, where stationary phases with different selectivities are coupled to achieve a higher critical peak pair resolution [46]. Furthermore, the pre-column acts as a guard column and protects the main-column from non-polar sample matrix and thereby increases the lifetime of the analytical column.

4.4 Concluding remarks

The presented pre-column large volume injection concept based on nano-LC demonstrates the feasibility of simultaneous analysis of a wide range of polar to non-polar components in aqueous matrices with symmetrical peak shapes. It could be shown that extremely small amounts of residual organic solvents in the injection solutions exhibit a negative effect on the peak shape and retention time of polar analytes. Therefore, the injection of large volumes of organic extracts obtained after solid phase extraction will result in highly deteriorated peaks, unless a solvent-exchange or a high dilution with water is carried out before separation. According to this fact the introduced concept can only be used for direct large volume injections of aqueous samples. Although environmental analysis is not the typical area for nano-LC because sample volumes are usually not limited, a positive effect can result to counteract ion suppression caused by the matrix components. In an on-going study we will therefore investigate to what degree the sensitivity can be enhanced if nano-LC-MS hyphenation is compared to normal bore LC-MS methods.

4.5 References

1. Gómez-Canela C, Cortés-Francisco N, Ventura F, Caixach J, Lacorte S. Liquid chromatography coupled to tandem mass spectrometry and high resolution mass spectrometry as analytical tools to characterize multi-class cytostatic compounds. J Chromatogr A; 2013;1276:78–94

2. Martín J, Camacho-Muñoz D, Santos JL, Aparicio I, Alonso E. Simultaneous determination of a selected group of cytostatic drugs in water using high-performance liquid chromatography-triple-quadrupole mass spectrometry. J Sep Sci; 2011;34(22):3166–77

3. Kowal S, Balsaa P, Werres F, Schmidt TC. Reduction of matrix effects and improvement of sensitivity during determination of two chloridazon degradation products in aqueous matrices by using UPLC-ESI-MS/MS. Anal Bioanal Chem; 2012;403(6):1707–17

4. Otaka H, Shimono H, Hashimoto S. Optimization of solid-phase extraction procedure for determination of polychlorinated dibenzo- p-dioxins, polychlorinated dibenzofurans, and coplanar polychlorinated biphenyls in humic acid containing water. Anal Bioanal Chem; 2004;378(7):1854–60

5. Quiroz R, Arellano L, Grimalt JO, Fernández P. Analysis of polybrominated diphenyl ethers in atmospheric deposition and snow samples by solid-phase disk extraction. J Chromatogr A; 2008;1192(1):147–51

6. Ozcan S, Aydin ME. Organochlorine Pesticides in Urban Air: Concentrations, Sources, Seasonal Trends and Correlation with Meteorological Parameters. Clean-Soil Air Water; 2009;37(4-5):343–8

7. Algarra M, Lamotte M, Fornier De Violet, P., Hernandez M, Garrigues P. Solid phase enhanced direct spectrofluoro-metric determination of polychlorinated biphenyls (PCB's) in natural waters. Polycycl Aromat Comp; 2000;19(1-4):241–51

8. Erger C, Balsaa P, Werres F, Schmidt TC. Multi-component trace analysis of organic xenobiotics in surface water containing suspended particular matter by solid phase extraction/gas chromatography–mass spectrometry. J Chromatogr A; 2012;1249(0):181–9

9. Kosjek T, Perko S, Žigon D, Heath E. Fluorouracil in the environment: Analysis, occurrence, degradation and transformation. J Chromatogr A; 2013;1290(0):62–72

10. de Almeida Azevedo D, Lacorte S, Vinhas T, Viana P, Barceló D. Monitoring of priority pesticides and other organic pollutants in river water from portugal by gas chromatography-mass spectrometry and liquid chromatography-atmospheric pressure chemical ionization mass spectrometry. J Chromatogr A; 2000;879(1):13–26

11. Richardson SD. The role of GC-MS and LC-MS in the discovery of drinking water disinfection by-products. J Environ Monit; 2002;4(1):1–9

12. Busetti F, Backe WJ, Bendixen N, Maier U, Place B, Giger W, Field JA. Trace analysis of environmental matrices by large-volume injection and liquid chromatography-mass spectrometry. Anal Bioanal Chem; 2012;402(1):175–186

13. Little JN, Fallick GJ. New considerations in detector-application relationships. J Chromatogr; 1975;112:389–397

14. Gloor R, Johnson E. PRACTICAL ASPECTS OF REVERSE PHASE ION PAIR CHROMATOGRAPHY. J Chromatogr Sci; 1977;15(9):413–423

15. D'Orazio G, Fanali S. Combination of two different stationary phases for on-line pre-concentration and separation of basic drugs by using nano-liquid chromatography. J Chromatogr A; 2013;1285(0):118–23

16. D'Orazio G, Fanali S. Enantiomeric separation by using nano-liquid chromatography with on-column focusing. J Sep Sci; 2008;31(14):2567–71

17. D'Orazio G, Rocco A, Fanali S. Fast-liquid chromatography using columns of different internal diameters packed with sub-2 μm silica particles. J Chromatogr A; 2012;1228(0):213–20

18. Hogendoorn EA, Jong APJM de, van Zoonen P, Brinkman JAT. Reversed-phase liquid chromatographic column switching for the trace-level determination of polar compounds. Application to chloroallyl alcohol in ground water. J Chromatogr A; 1990;511(0):243–256

19. Hogendoorn EA, Verschraagen C, Brinkman UAT, van Zoonen P. Coupled column liquid chromatography for the trace determination of polar pesticides in water using direct large-volume injection: method development strategy applied to methyl isothiocyanate. Anal Chim Acta; 1992;268(2):205–215

20. D'Orazio G, Cifuentes A, Fanali S. Chiral nano-liquid chromatography–mass spectrometry applied to amino acids analysis for orange juice profiling. Food Chem; 2008;108(3):1114–21

21. Buszewski B, Szultka M. Past, Present, and Future of Solid Phase Extraction: A Review. Crit Rev Anal Chem; 2012;42(3):198–213

22. Vázquez PP, Vidal JM, Fernández JM. A restricted access medium column for the trace determination of triadimefon and tetraconazole in water with large-volume injection coupled-column RPLC with UV detection. Analyst; 2000;125(9):1549–53

23. Gosetti F, Mazzucco E, Zampieri D, Gennaro M. Signal suppression/enhancement in high-performance liquid chromatography tandem mass spectrometry. J Chromatogr A; 2010;1217(25):3929–37

24. van Eeckhaut A, Lanckmans K, Sarre S, Smolders I, Michotte Y. Validation of bioanalytical LC-MS/MS assays: evaluation of matrix effects. J Chromatogr B; 2009;877(23):2198–207

25. Rezai MA, Famiglini G, Cappiello A. Enhanced detection sensitivity by large volume injection in reversed-phase micro-high-performance liquid chromatography. J Chromatogr A; 1996;742(1–2):69–78

26. Ruta J, Rudaz S, McCalley DV, Veuthey J-L, Guillarme D. A systematic investigation of the effect of sample diluent on peak shape in hydrophilic interaction liquid chromatography. J Chromatogr A; 2010;1217(52):8230–40

27. West C, Elfakir C, Lafosse M. Porous graphitic carbon: A versatile stationary phase for liquid chromatography. J Chromatogr A; 2010;1217(19):3201–16

28. Pereira L. HILIC–MS Sensitivity without Silica. LC GC N Am; 2011;29(3):262–9

29. Pfeifer T, Tuerk J, Bester K, Spiteller M. Determination of selected sulfonamide antibiotics and trimethoprim in manure by electrospray and atmospheric pressure chemical ionization tandem mass spectrometry. Rapid Commun Mass Sp; 2002;16(7):663–9

30. Chemicalize.org   Properties   viewer.   5-fluorouracil. http://www.chemicalize.org/structure/#!mol=5-fluorouracil. Accessed 16 January 2014

31. Chemicalize.org   Properties   viewer.   Acetylsulfamerazine. http://www.chemicalize.org/structure/#!mol=N-{4-[(4-methylpyrimidin-2-yl)sulfamoyl]phenyl}acetamide. Accessed 16 January 2014

32. Chemicalize.org   Properties   viewer.   Fenofibrate. http://www.chemicalize.org/structure/#!mol=fenofibrate. Accessed 16 January 2014

33. Su Y-H, Zhu Y-G, Sheng G, Chiou CT. Linear Adsorption of Nonionic Organic Compounds from Water onto Hydrophilic Minerals: Silica and Alumina. Environ Sci Technol; 2006;40(22):6949–54

34. Büchel B, Rhyn P, Schürch S, Bühr C, Amstutz U, R. Largiadèr C. LC-MS/MS method for simultaneous analysis of uracil, 5,6-dihydrouracil, 5-fluorouracil and 5-fluoro-5,6-dihydrouracil in human plasma for therapeutic drug monitoring and toxicity prediction in cancer patients. Biomed Chromatogr; 2013;27(1):7–16

35. Remaud G, Boisdron-Celle M, Morel A, Gamelin A. Sensitive MS/MS–liquid chromatography assay for simultaneous determination of tegafur, 5-fluorouracil and 5-fluorodihydrouracil in plasma. J Chromatogr B; 2005;824(1–2):153–60

36. Tsume Y, Provoda CJ, Amidon GL. The achievement of mass balance by simultaneous quantification of floxuridine prodrug, floxuridine, 5-fluorouracil, 5-dihydrouracil, α-fluoro-β-ureidopropionate, α-fluoro-β-alanine using LC–MS. J Chromatogr B; 2011;879(13–14):915–20

37. Chen W, Shen Y, Rong H, Lei L, Guo S. Development and application of a validated gradient elution HPLC method for simultaneous determination of 5-fluorouracil and paclitaxel in dissolution samples of 5-fluorouracil/paclitaxel-co-eluting stents. J Pharmaceut Biomed; 2012;59(0):179–83

38. de Mattos, Ana Cristina, Khalil NM, Mainardes RM. Development and validation of an HPLC method for the determination of fluorouracil in polymeric nanoparticles. Braz J Pharm Sci; 2013;49(1):117–26

39. Deenen MJ, Rosing H, Hillebrand MJ, Schellens, Jan H. M., Beijnen JH. Quantitative determination of capecitabine and its six metabolites in human plasma using liquid chromatography coupled to electrospray tandem mass spectrometry. J Chromatogr B; 2013;913–914(0):30–40

40. Kosovec JE, Egorin MJ, Gjurich S, Beumer JH. Quantitation of 5-fluorouracil (5-FU) in human plasma by liquid chromatography/electrospray ionization tandem mass spectrometry. Rapid Commun Mass Sp; 2008;22(2):224–30

41. Kovalova L, McArdell CS, Hollender J. Challenge of high polarity and low concentrations in analysis of cytostatics and metabolites in wastewater by hydrophilic interaction chromatography/tandem mass spectrometry. J Chromatogr A; 2009;1216(7):1100–8

42. Maring JG, Schouten L, Greijdanus B, Vries EG de, Uges, Maring JG, Schouten L, Greijdanus B, de Vries Elisabeth G E, Uges Donald R A. A simple and sensitive fully validated HPLC-UV method for the determination of 5-fluorouracil and its metabolite 5,6-dihydrofluorouracil in plasma. Ther Drug Monit; 2005;27(1):25–30

43. Pisano R, Breda M, Grassi S, James CA. Hydrophilic interaction liquid chromatography–APCI–mass spectrometry determination of 5-fluorouracil in plasma and tissues. J Pharmaceut Biomed; 2005;38(4):738–45

44. van Kuilenburg AB, van Lenthe H, Maring JG, van Gennip AH. Determination of 5-fluorouracil in plasma with HPLC-tandem mass spectrometry. Nucleos Nucleot Nucl; 2006;25(9-11):1257–60

45. Woo Y-A, Kim G-H, Jeong EJ, Kim C-Y. Simultaneous determination of doxifluridine and 5-fluorouracil in monkey serum by high performance liquid chromatography with tandem mass spectrometry. J Chromatogr B; 2008;875(2):487–92

46. Zhu L, Shen G-J, Ding S-Q, Hua X. Determination of 5-Fluorouracil in 5-Fluorouracil Injection and Human Serum by HPLC. J Food Drug Anal; 2012;20(4):947–50

4.6 Chapter appendix

4.6.1 Schematic view of the LVI concept
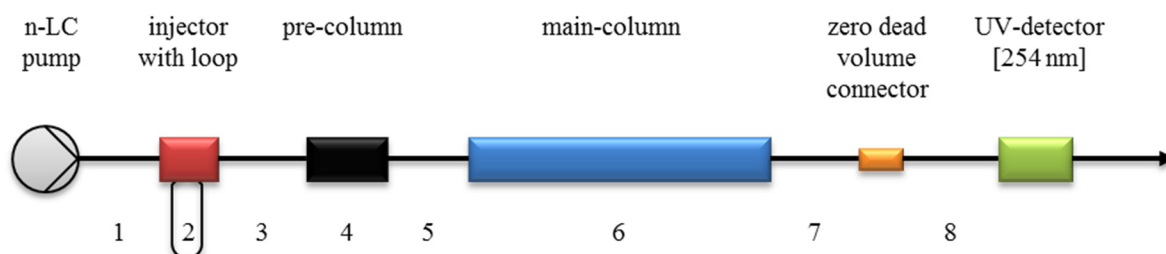
Figure S 4-1:   Schematic view of the LVI concept on the basis of nano-LC. The numbers 1 to 8 are indices for the capillary/column i.d., o.d., lengths, porosity and calculated volumes listed in Table S 4-1.

Table S 4-1:   List of used capillary/column i.d., o.d., lengths, porosity factors and calculated capillary volumes or void volumes of the columns.

Number	i.d. (µm)	o.d. (µm)	Length (cm)	Calculated (void*) volume (nL)
1	50	360	15.5	304
2	100	360	51.0	4006
3	75	360	10.5	464
4	75	360	1.2	34*
5	75	360	4.5	199
6	100	360	5	250*
7	75	280	9	398
8	75	280	14.5	641
		calculated system volume (nL):		2290

* Column void volume was calculated as (Vm (nL)= 0.5 x col. length (mm) x col. i.d. (mm)2 x 1000). The factor 1000 contains the metric conversions of cm to mm and mL to nL. [Snyder, L.R., Dolan, J.W., High-Performance Gradient Elution: The Practical Application of the Linear-Solvent-Strength Model, John Wiley & Sons, Inc, Hoboken, NJ, 2006]

4.6.2 Comparison of chromatographic parameters

Table S 4-2:   Comparison of different parameters characterizing peak shape and retention time
of 5-FU, AC-S and FEN without pre-column.

Analyte	Injection volume (nL)	Retention time (min)	Peak area (mAU s)	Peak width (s)	Peak Height (mAU)	Asymmetry
5-FU	50	4.0	1150	37.7	55	2.33
	500	4.6	1276	83.7	23	--- +
	1000	4.4	794	134.6	8	--- +
AC-S	50	10.2	1898	28.2	124	1.75
	500	10.2	2145	26.6	143	1.55
	1000	10.2	2123	28.1	133	1.50
FEN	50	15.5	128	20.7	12	1.48
	500	15.4	108	16.4	11	1.85
	1000	15.4	68	16.4	7	1.28

* Cannot be determined

Table S 4-3:   Comparison of different parameters characterizing peak shape and retention time
of 5-FU, AC-S and FEN with pre-column.

Analyte	Injection volume (nL)	Retention time (min)	Peak area (mAU s)	Peak width (s)	Peak Height (mAU)	Asymmetry
5-FU	1500	13.6	1397	59.3	61	0.35
	2000	13.7	1433	42.1	67	0.64
	3000	13.8	1407	36.4	70	0.80
AC-S	1500	17.4	1927	30.4	112	1.32
	2000	17.3	1956	30.3	115	1.33
	3000	17.4	1975	30.1	116	1.31
FEN	1500	21.7	44	17.8	4	0.61
	2000	21.7	37	18.0	4	0.76
	3000	21.8	58	19.4	5	0.88

Chapter 5   Large volume injection of organic extracts in micro liquid chromatography using serially coupled columns

5.1 Introduction

The number of water contaminant substances is growing from year to year and the contaminants are coming more and more into the focus of research and regulation. Therefore, we should not be surprised, that the list of priority hazardous substances is getting longer [1–8]. A number of the listed substances has a very low effect concentration in the range of pg L^{-1} and should be continuously monitored.

The majority of the substances has a semi- or non-polar character, therefore, reversed phase liquid chromatography mass spectrometry is the technique of choice for an advanced monitoring. However, the requirements on the analytics are enormously if contaminants in pg L^{-1} range needs to be detected.

Even with the latest instrument technology it is very difficult to detect such low concentrations in real samples. Therefore, samples need to be prepared and enriched prior the analysis. One of the most common and well established methods is the offline solid phase extraction (SPE) on reversed phase materials. At this sample preparation the contaminants of interest should reversibly sorb on the SPE phase while possible interfering matrix compounds should be eliminated. Unfortunately, only a part but not the complete matrix could be eliminated, since these also could interact with the stationary phase of the SPE. In addition to the cartridge capacity this is the reason why not an infinite amount of sample can or should be enriched at once. However, finally the enriched contaminants and definitely a part of the matrix were eluted with a small volume of a strong and mostly organic solvent from the SPE phase for the analysis.

In some cases, the preparation and enrichment steps are not sufficient to achieve the predetermined limits of detection. Finally, a direct injection of large sample volume that is defined as an injection volume > 10% of the column void volume, is the last possibility to increase the sensitivity and therefore decrease the limit of detection. However, the large volume injection of organic extracts is not trivial, since the complete column volume could be overfilled several times, whereby the injected solution acts/behaves as a mobile phase with a high elution

strength. A high injection volume of organic extracts in the reversed phase C_{18} chromatography can usually be indicated by a fronting, a shift to shorter retention time, peak broadening or even peak splitting [9–13]. With regard to micro-LC, where the large volume injection is often inevitable, the mentioned negative effect is much more pronounced.

Therefore, the organic extracts could be diluted with water prior the injection to reduce the organic content of the injection solution, which unfortunately counteracts the previous enrichment.

Alternatively, a solvent exchange could be applied, wherein the organic content of the sample is evaporated and replaced by an aqueous solution. While the organic extracts are evaporated to dryness, non-polar contaminants could precipitate due to their low solubility in water. Therefore, a solvent exchange is not a real alternative, since important contaminants could be lost. Ideally the complete/total volume of the organic extract needs to be injected at once to achieve the highest possible sensitivity and the lowest limit of detection, which is unfortunately not possible due to the high organic content of the extract (as mentioned before).

The aim of this work is therefore to introduce a pre-column concept that allows the large volume injection of organic solvents on reversed phase micro liquid chromatography. To that end, a normal phase pre-column and the reversed phase main column were serially coupled.
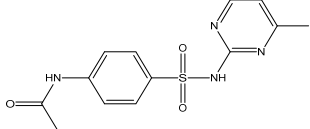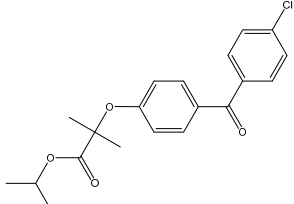
5.2 Experimental Section

5.2.1 Chemicals

Acetonitrile, methanol and water (Chemsolute, LC/MS grade) were purchased from Th. Geyer (Renningen, Germany). The eluents were acidified by 0.1% formic acid by volume (puriss. p. a., ~ 98%, Sigma-Aldrich, Schnelldorf, Germany).

Acetyl-sulfamerazine (AC-S) and fenofibrate (FEN) were used as reference compounds. Acetyl-sulfamerazine, a semi-polar compound was synthesized in house [14] and fenofibrate represents a non-polar compound as can be seen on log P values in Table 5-1 (purchased from Sigma-Aldrich, Schnelldorf, Germany).

Table 5-1:   Properties of model compounds.

Name	Formula	MW (g mol^{-1})	log P	pKa (acid)	CAS-No.	References
1) Acetyl-sulfamerazine		306.34	0.59	6.9	127-73-1	[15]
2) Fenofibrate		360.83	5.28	-	49562-28-9	[16]

For the preparation of stock solutions, 10 mg of each component were dissolved in 10 mL methanol + 0.1% FA resulting in a concentration of 1 mg mL^{-1}. For the analyte mix, 0.1 mL of each standard solution and 0.8 mL of methanol were mixed. This resulting solution of 100 µg mL^{-1} for each compound was used for the smallest injection of 50 nL. The mass injected on column for each compound of this solution is equal to 5 ng. For larger injection volumes, the analyte mix solution was diluted by methanol (99.9% methanol + 0.1% FA) and the absolute mass injected was kept constant at 5 ng. At the largest injection volume of 1750 nL the solution had a concentration of 2.86 µg mL^{-1}. All injection solutions consisted of 99.9% methanol + 0.1% FA.

5.2.2 Columns

For the on-line pre-column dilution concept a microbore pre-column (50 mm x 0.3 mm) filled with Grom-Sil 5 µm particles from Grace Davison (Worms, Germany) was used. The column void volume of this column and therefore the dilution volume is 2.25 µL.

For the separation a superficially porous 2.6 µm SunShell C18 particle (ChromaNik Technologies, Osaka, Japan) packed by Grace Davison (Worms, Germany) into a 50 mm x 0.3 mm i.d. hardware was used.

5.2.3 Pre-column concept description

Figure 5-1 shows the pre-column concept. The main function of the pre-column is not the additional separation or pre concentration, the column is only a reservoir for the dilution solution. Additionally the normal phase acts as a mixer without any interactions to contaminants. This is only possible because water is the strongest eluent in normal phase chromatography.

Prior to each analysis both columns were filled with the re-equilibration solution of the reversed phase gradient (99% water and 1% acetonitrile), then the large volume injection was applied. The organic extract reaches at first the normal phase pre-column, where it is diluted and mixed with the aqueous mobile phase. At the next step, the diluted solution with the lower organic content reached the main-column for the separation and following detection.
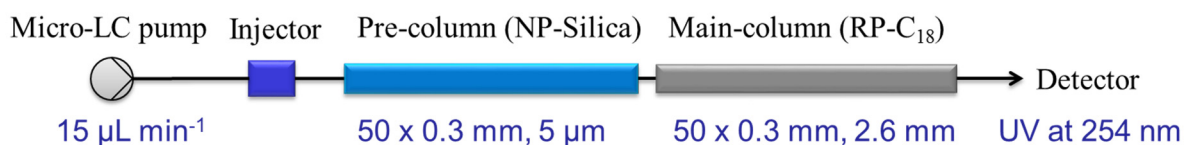
Figure 5-1:   Schematic presentation of the concept.

5.2.4 HPLC Instrument

The separations were performed on the Eksigent ExpressLC-Ultra system (SCIEX, Darmstadt, Germany) with a standard micro-flow module (5-50 µL min^{-1}). This HPLC system contained a column oven, an integrated six port two-position valve and a binary-gradient pneumatic pump, which is able to generate a maximum backpressure of 680 bar (10 kpsi). The system was controlled by the Eksigent Control Software version 3.12.1.

Furthermore, an HTS PAL autosampler (CTC Analytics, Zwingen, Switzerland) with a Hamilton syringe (Bonaduz, Switzerland) and an external UV/Vis-Detector SpectraFlow 501 (SunChrom, Friedrichsdorf, Germany) at 254 nm were used. All connection capillaries including the injection loop (calculated volume of 6 µL) were 360 µm (before main column) or

280 μm (after the main column) outer diameter (o.d.) fused silica purchased from Postnova Analytics (Landsberg, Germany) and cut to size by a Shortix GC (SGT, Middelburg, The Netherlands) diamond cutter. The reduction of the o.d. is necessary for coupling the column to the built-in capillary of the UV-detector.

The flow rate was adjusted to 15 μL min^{-1} and the oven temperature was set to 30 °C. The mobile phase consisted of acidified (0.1% FA) water (% A) and acetonitrile (% B). A solvent gradient was applied according to the following program: start at 1% B, in 1.2 min 1-99% B, 0.6 min hold at 99% B, in 0.3 min 99-1% B, re-equilibration for 0.9 min (~ 6 column void volumes). The re-equilibration solution of the gradient was used as dilution solution for the online dilution of the next run and separation. The partial loop injection volume between 0.05 and 5 μL was chosen.

Data processing was performed by Eksigent software package and Excel 2010 (Microsoft, Redmont, WA, USA). For visualization OriginLab Pro 9 (OriginLab, Northampton, MA, USA) was used.

5.3 Results and discussion

5.3.1 Retention on Normal Phase

At first it must be shown that the normal phase works only as a mixing chamber and does not interact with the model compounds. In normal phase chromatography, water is the eluent with the strongest elution power. Due to the fact that the normal phase was used under reversed phase conditions starting at 99% water, the interactions should be minimized as far as possible. For the evaluation, two experiments were performed in which only the dilution pre-column and two different dilution media (acetonitrile and water) were used. The resulting chromatograms are shown in Figure 5-2.
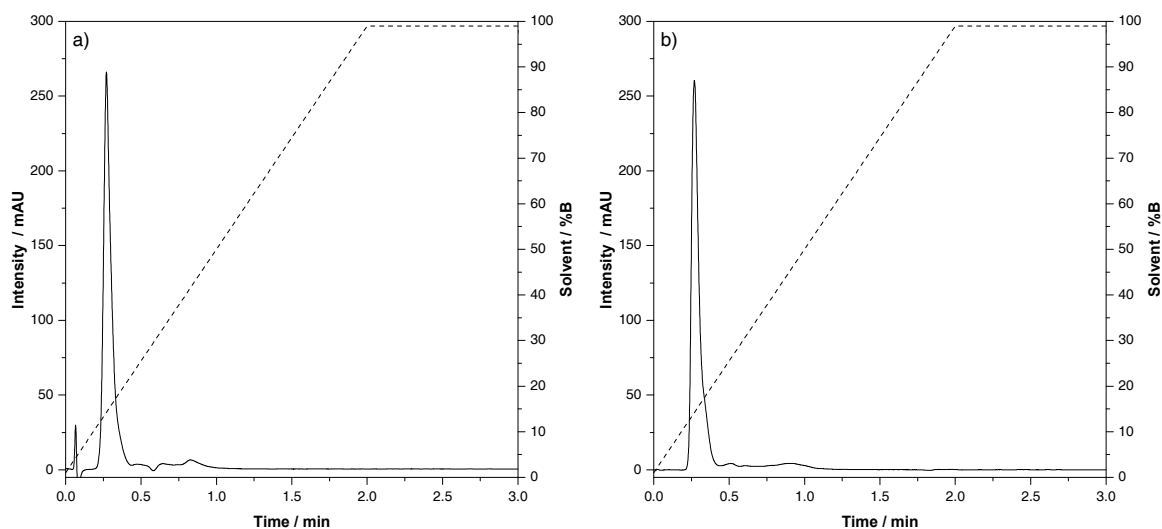
Figure 5-2:   Elution of acetyl-sulfamerazine on NP dilution pre-column. Prior to the analysis the column was filled with the dilution solution a) acetonitrile + 0.1% FA and b) water + 0.1% FA. Chromatographic conditions: pre-column stationary phase: Grom-Sil 100 Si NP-1 (50 x 0.3 mm; 5 μm); mobile phase: gradient, (A) water + 0.1% FA, (B) acetonitrile + 0.1% FA; flow rate: 15 μL min^{-1}; injection volume: 300 nL with 5 ng of compound; temperature: isothermal at 30 °C; detection: UV at 254 nm.

The signals of acetyl-sulfamerazine show a retention time of 0.27 minutes, which corresponds to the calculated void volume of 0.3 minutes. The peak width at 10% peak height corresponds to 7.1 seconds for acetonitrile and 7.4 seconds for water as dilution media. The results confirmed the hypothesis that the NP phase works only as a mixing chamber.

5.3.2 Effect of large volume injection on RP-C18 column and on the NP-RP-C18 column combination

For the evaluation of the described online dilution pre-column concept, injections between 150 and 500 nL for acetyl-sulfamerazine and 150 to 1750 nL for fenofibrate were performed on a single RP-C18 column and on the NP-RP-C18 column combination. Figure 5-3 shows an overlay of the resulting peak profiles and Table 5-2 the chromatographic parameters for the data evaluation.
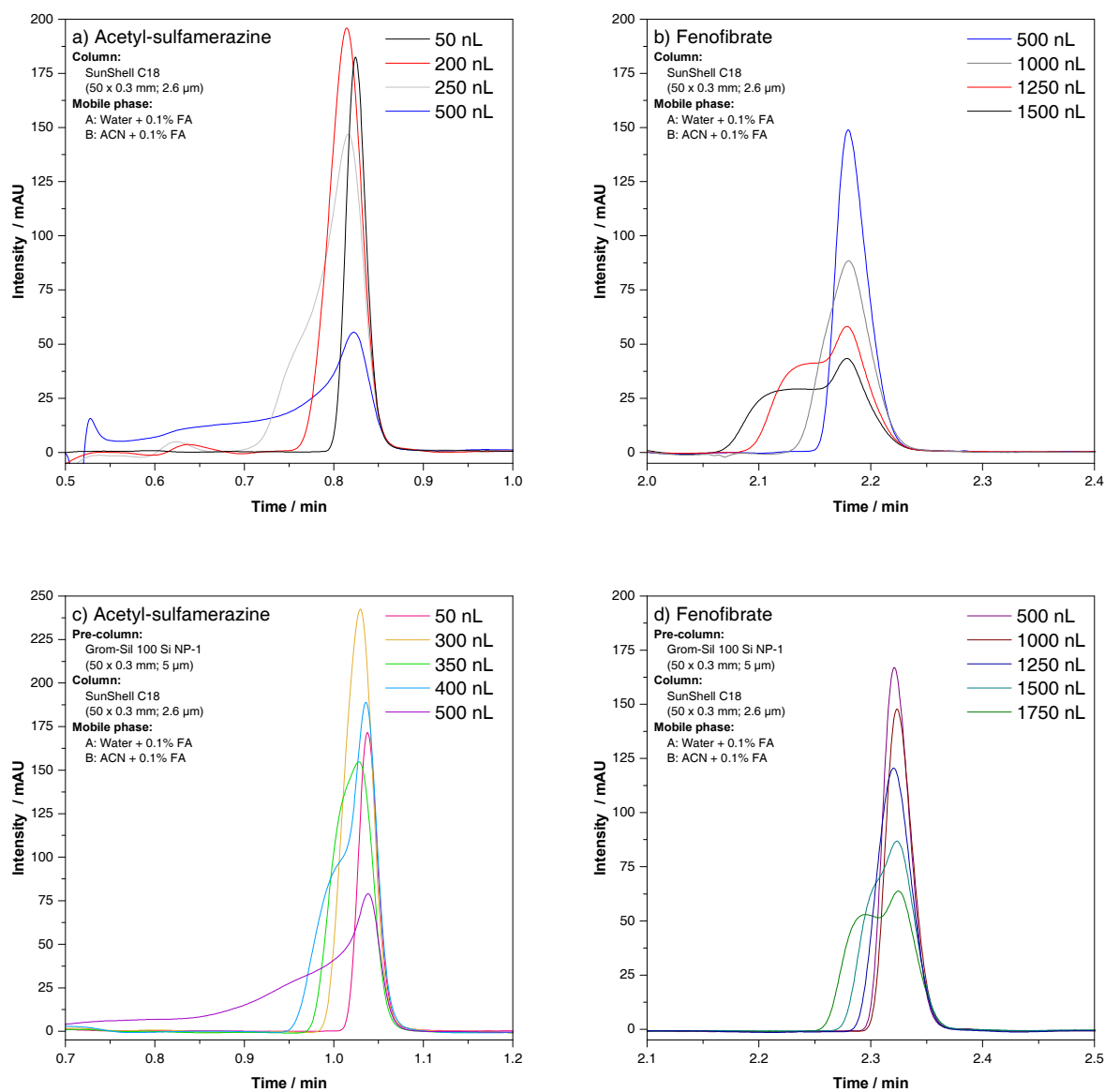
Figure 5-3:   Injections between 150 and 500 nL of a) acetyl-sulfamerazine and 150 to 1750 nL for b) fenofibrate on RP-C18 phase and on serially coupled NP-RP-C18 phases c) and d) and the influence of the large volume injection.

Table 5-2: Comparison of different parameters characterizing peak shape in dependence on injection volume for acetyl-sulfamerazine and fenofibrate on RP-C18 phase and serially coupled NP-RP-C18 phases (n=3). Numbers highlighted in bold font show the peak profile of the highest injection volume with acceptable chromatographic parameters.

Injection volume / nL	Acetyl-sulfamerazine								Fenofibrate							
	RP-C18				NP-RP-C18				RP-C18				NP-RP-C18			
	$A_{S,0.1}$	RSD / %	$w_{0.1}$ / s	RSD / %	$A_{S,0.1}$	RSD / %	$w_{0.1}$ / s	RSD / %	$A_{S,0.1}$	RSD / %	$w_{0.1}$ / s	RSD / %	$A_{S,0.1}$	RSD / %	$w_{0.1}$ / s	RSD / %
150	1.1	4.5	3.5	1.6	1.2	2.1	2.7	1.2	1.5	1.8	3.2	0.4	1.6	6.9	3.1	2.6
200	**0.9**	**4.0**	**4.4**	**5.4**	1.2	2.7	2.8	2.2	1.5	2.7	3.3	1.3	1.5	3.0	3.0	1.9
250	0.5	21.5	6.7	10.9	1.1	6.7	3.3	4.9	1.6	3.0	3.3	0.9	1.5	2.6	3.0	1.2
300	0.4	31.4	10.0	1.6	**0.8**	**6.0**	**3.9**	**1.2**	1.6	2.0	3.4	1.9	1.5	2.1	3.0	1.0
350	0.2	10.0	13.5	6.1	0.6	15.9	5.1	6.5	1.6	1.2	3.4	0.9	1.5	2.7	3.0	1.1
400	0.2	0.0	15.0	1.0	0.6	56.8	7.0	21.3	1.7	2.2	3.4	1.0	1.6	1.0	3.0	0.9
450	0.2	9.4	15.3	2.4	0.2	13.5	9.4	12.3	1.7	1.8	3.4	1.3	1.5	1.2	3.0	1.4
500	0.2	3.3	14.0	2.5	0.2	0.0	12.7	2.8	1.7	0.9	3.5	0.3	1.5	2.2	2.9	0.1
750									1.4	2.5	4.3	2.6	1.5	0.7	2.9	0.7
1000									**1.2**	**15.6**	**4.7**	**10.0**	1.5	2.3	2.9	1.6
1250									0.6	12.8	7.2	8.3	1.4	18.4	3.5	5.3
1500									0.8	7.6	8.4	7.6	**0.9**	**15.9**	**4.4**	**8.1**
1750									0.3	6.3	10.8	4.9	0.6	10.0	5.5	5.3

$A_{S,0.1}$: Peak asymmetry factor at 10% height

$w_{0.1}$: Peak width at 10% height

For data evaluation peak symmetry and peak width are chosen. Acceptable values for good peak asymmetry are between 0.8 and 1.2. Figure 5-3 as well as Table 5-2, show that the increased injection volume leads to a stronger fronting and higher peak width. Therefore, the maximum injection volume is defined by a peak profile with an asymmetry value ≥ 0.8 and in addition a maximum peak width twice that of the peak of the smallest injection volume.

For acetyl-sulfamerazine a maximum possible injection volume of 200 nL on RP-C18 column could be observed and for fenofibrate of 1000 nL. Using the dilution-column concept the injection volumes could be increased by a factor of 1.5 for both compounds.

A direct comparison of peak widths for identical injection volumes (listed in Table 5-2) reveals equal or smaller peak widths for the pre-column concept. Theoretically, the peak width for the pre-column concept should be larger, as a result of the additional volume and the turbulent flow inside the dilution column. This effect could not be observed, because of the better band focusing of the RP column, favored by the dilution and smaller organic solvent amount.

The chromatographic parameters listed in Table 5-2 show that the standard deviation of the asymmetry and peak width increased significantly, if the maximum possible injection volume was exceeded. Additionally, higher injection volumes lead to a strong broadening of the signals with a pronounced fronting. The reason for this is the organic solvent of the injection solution, which inhibits the interactions of the compound with the stationary RP-C18 phase and therefore the band focusing. The increasing of the injection volume, is equal to increasing of the organic solvent amount on the separation column, which behaves as a mobile phase, if it is present in excess. The additional pre-column dilutes the organic injection solution with water and increased the interaction between the compounds and the stationary phase. However, the beneficial effect has a limitation, as a result of a constant dilution volume of 2250 nL. A larger dilution volume could increase the maximum injection volume, but also increase the gradient delay volume and therefore the analysis time.

5.4 Conclusion and Outlook

In this work a dilution pre-column concept was introduced, which increases the maximal injection volume of organic solvent samples by a factor of 1.5 for semi- and non-polar

compounds. The applicability was demonstrated successfully for serially coupled micro-bore columns. An upscale of the demonstrated method to conventional HPLC columns is possible and should be investigated.

The demonstrated concept could be used for organic solvent samples or organic SPE extract solutions, which were typically diluted prior to the injection on RP systems.

Additionally, this concept could be used in the field of online or offline two-dimensional liquid chromatography. Using a full gradient in the first dimension, for normal, HILIC or RP phases, transfer volumes could contain up to 100% organic solvent, which could decrease the separation performance of the second dimension resulting in asymmetrical and broad peak profiles. The introduced pre-column dilution concept in the second dimension could minimize such effects and increase the performance. For comprehensive two-dimensional LC, where the gradient delay volume of the second dimension should be very small and the separation very fast, the additional column results in larger cycle time and reduces therefore the total 2D-LC system performance in terms of analysis time of both dimensions, M-S-F criterion, transfer volume and the performance of the first dimension. The last one is the result of the adaptation of the system parameters like flow rate to the larger cycle time on the second dimension.

5.5 References

1. Gómez-Canela C, Cortés-Francisco N, Ventura F, Caixach J, Lacorte S. Liquid chromatography coupled to tandem mass spectrometry and high resolution mass spectrometry as analytical tools to characterize multi-class cytostatic compounds. J Chromatogr A; 2013;1276:78–94

2. Martín J, Camacho-Muñoz D, Santos JL, Aparicio I, Alonso E. Simultaneous determination of a selected group of cytostatic drugs in water using high-performance liquid chromatography-triple-quadrupole mass spectrometry. J Sep Sci; 2011;34(22):3166–77

3. Kowal S, Balsaa P, Werres F, Schmidt TC. Reduction of matrix effects and improvement of sensitivity during determination of two chloridazon degradation products in aqueous matrices by using UPLC-ESI-MS/MS. Anal Bioanal Chem; 2012;403(6):1707–17

4. Otaka H, Shimono H, Hashimoto S. Optimization of solid-phase extraction procedure for determination of polychlorinated dibenzo- p-dioxins, polychlorinated dibenzofurans, and coplanar polychlorinated biphenyls in humic acid containing water. Anal Bioanal Chem; 2004;378(7):1854–60

5. Quiroz R, Arellano L, Grimalt JO, Fernández P. Analysis of polybrominated diphenyl ethers in atmospheric deposition and snow samples by solid-phase disk extraction. J Chromatogr A; 2008;1192(1):147–51

6. Ozcan S, Aydin ME. Organochlorine Pesticides in Urban Air: Concentrations, Sources, Seasonal Trends and Correlation with Meteorological Parameters. Clean-Soil Air Water; 2009;37(4-5):343–8

7. Algarra M, Lamotte M, Fornier De Violet, P., Hernandez M, Garrigues P. Solid phase enhanced direct spectrofluoro-metric determination of polychlorinated biphenyls (PCB's) in natural waters. Polycycl Aromat Comp; 2000;19(1-4):241–51

8. European Commission; 2015. Commission Implementing Decision (EU) 2015/495 of 20 March 2015 establishing a watch list of substances for Union-wide monitoring in the field of water policy pursuant to Directive 2008/105/EC of the European Parliament and of the Council. Off J Eur Union(78):40–2. Accessed 13 June 2016

9. Udrescu S, Sora ID, Albu F, David V, Medvedovici A. Large volume injection of 1-octanol as sample diluent in reversed phase liquid chromatography: Application in bioanalysis for assaying of indapamide in whole blood. J Pharm Biomed Anal; 2011;54(5):1163–72

10. Snyder LR, Kirkland JJ, Glajch JL. Practical HPLC method development. 2. ed. New York: Wiley; 1997.

11. Snyder LR, Kirkland JJ, Dolan JW. Introduction to modern liquid chromatography. 3. ed. Hoboken, N.J: Wiley; 2010.

12. Layne J, Farcas T, Rustamov I, Ahmed F. Volume-load capacity in fast-gradient liquid chromatography Effect of sample solvent composition and injection volume on chromatographic performance. J Chromatogr A; 2001;913(1):233–42

13. Lovin I, Albu F, Tache F, David V, Medvedovici A. Solvent and salting effects on sample preparation for the determination of fenofibric acid in human plasma by HPLC-DAD. Microchem J; 2003;75(3):179–87

14. Pfeifer T, Tuerk J, Bester K, Spiteller M. Determination of selected sulfonamide antibiotics and trimethoprim in manure by electrospray and atmospheric pressure chemical ionization tandem mass spectrometry. Rapid Commun Mass Sp; 2002;16(7):663–9

15. Chemicalize.org   -   Properties   Viewer.   Acetylsulfamerazine. http://www.chemicalize.org/structure/#!mol=N-{4-[(4-methylpyrimidin-2-yl)sulfamoyl]phenyl}acetamide. Accessed 16 January 2014

16. Chemicalize.org   -   Properties   Viewer.   Fenofibrate. http://www.chemicalize.org/structure/#!mol=fenofibrate. Accessed 16 January 2014

Chapter 6   A new method for the determination of peak distribution across a two-dimensional separation space.

For the identification of the optimal column combinations, a comparative orthogonality study of single columns and columns coupled in series for the first dimension of a microscale two-dimensional liquid chromatographic approach was performed. In total eight columns or column combinations were chosen. For the assessment of the optimal column combination, the orthogonality value as well as the peak distribution across the first and second dimension was used.

In total, three different methods of orthogonality calculation, namely the *Convex Hull*, *Bin Counting* and *Asterisk* method, were compared. Unfortunately, the first two methods do not provide any information of peak distribution. The third method provides this important information, but is not optimal when only a limited number of components is used for method development. Therefore, a new concept for peak distribution assessment across the separation space of two-dimensional chromatographic systems and clustering detection was developed.

It could be shown that the *Bin Counting* method in combination with additionally calculated histograms for the respective dimensions is well suited for the evaluation of orthogonality and peak clustering. The newly-developed method could be used generally in the assessment of 2D separations.

6.1 Introduction

The technological progress to more sensitive detection techniques such as mass spectrometry reveals the complexity of environmental samples including wastewater samples from communal wastewater treatment plants [1, 2]. Such samples might contain several thousands of different compounds [3, 4]. Analytical methods based on one-dimensional liquid chromatography (1D-LC) have limitations in terms of peak capacity [5]. Therefore, alternative separation techniques with higher peak capacity are deemed necessary to resolve as many compounds as possible.

One very promising approach is online two-dimensional liquid chromatography (2D-LC) due to the possibility to re-analyze the effluent from the first dimension (D1) on a second dimension (D2) column with a different selectivity. 2D-LC systems are well established in several analytical fields including proteomic [6, 7] and genomic [8] research and may also be a powerful tool for the analysis of complex food [9] and environmental [2, 10] samples.

Two-dimensional liquid chromatographic systems can be operated in different modes as e.g. "heart-cut-mode" (LC-LC) [11] or "selective-mode" (sLCxLC) [12, 13], where only one or a few selected fractions from the first dimension effluent are re-analyzed on the second dimension. A more complex approach is the "comprehensive-mode" (LCxLC), where the whole effluent of D1 is transferred to the second dimension in small fractions [11, 14, 15]. The hardware configuration of online comprehensive LCxLC systems is very complex and has some disadvantages, one of which is the dilution introduced by the modulation between the first and second dimension, resulting in lower sensitivity. A further disadvantage is the very fast cycle time needed on the second dimension separation. Cycle times of less than one minute are preferred to fulfil the Murphy-Schure-Foley (M-S-F) criterion, which implies that every D1 signal must be sampled at about three to four times to conserve the D1 separation [16, 17]. To achieve cycle times of less than one minute, very high flow rates up to 5 mL min^{-1} are necessary when columns with an inner diameter (i.d.) of 2.1 mm are used [18–20]. Unfortunately, this is not the optimal flow rate for electrospray ionization (ESI) mass spectrometry. To minimize the solvent load introduced into the ESI source, flow splitters are frequently used [21] with drawbacks in terms of reproducibility and loss in sensitivity.

For a splitless coupling to mass spectrometry, a microscale online LCxLC system was developed in a previous work [1]. The system is based on nano-LC for the first and micro-LC for the second dimension with a maximum flow rate of 50 µL min^{-1}. To counteract the previously mentioned dilution effect caused by the modulation and to increase the sensitivity, large volume injection of about 1.6 µL was applied on the first dimension nano-LC column with an i.d. of 0.1 mm and a length of 50 mm. The optimal injection volume (smaller than 10% of the column void volume) of columns with this dimension is < 25 nL. To achieve such an extraordinarily large volume injection without significant peak broadening and loss of signal intensity, a stationary phase material based on porous graphitic carbon (PGC) was used. The high retentivity even for polar compounds allows focusing on the head of the column [22]. Unfortunately, non-polar compounds may be adsorbed permanently or eluted as very broad bands when the plateau of the gradient is reached [22]. In this respect, the length of the column significantly contributes to the retention of non-polar compounds. In a recent study [23], we used a short PGC column of 10 mm length to overcome the problem of band broadening at the end of the gradient while maximizing the injection volume for polar compounds. Li et al. [24] recently demonstrated that a serial column coupling of two stationary phases for the first dimension has a pronounced influence on the overall selectivity of the two-dimensional system, which resembles the concept of phase optimized liquid chromatography. Therefore, the aim of this study was to further increase the selectivity of the two-dimensional system. A column screening was performed using stationary phases on the basis of pentafluorophenyl (PFP), cyano (CN), hydrophilic interaction chromatography (HILIC) and porous graphitic carbon. All columns were used as single stationary phases and also serially coupled to a short PGC pre-column. For the evaluation of the optimal column combination, the orthogonality value was used and calculated on the basis of three well established concepts. In addition, the peak distribution across the respective dimensions was evaluated. As a result, a new concept for peak distribution assessment across the separation space of two-dimensional chromatographic systems and clustering detection was developed.

6.2 Experimental section

6.2.1 Solvents and additives

Acetonitrile, methanol and water were all of LC-MS grade and purchased from Th. Geyer (Chemsolute, Th. Geyer, Renningen, Germany). The eluents were acidified by adding 0.1% formic acid (FA) by volume (puriss. p. a. 98%, Sigma-Aldrich, Schnelldorf, Germany).

6.2.2 Multi-component reference standard solution

In order to obtain valid information about the orthogonality of the column combinations, a multi-component reference standard solution with a total of 42 different compounds was prepared. The selected compounds represent a subset of so-called emerging contaminants in the field of water analysis. A detailed compound list is provided in chapter appendix Table S 6-1. The resulting multi-component reference standard contained $10 \ \mu g \ mL^{-1}$ of each compound. Based on the log D value, the polarity of the compounds could be estimated. They cover a very broad log D range between -3.16 and 5.46 (predicted by ChemAxon, chemicalize.org). For the detailed discussion, the compounds were classified into three groups, polar (log D: -3.16 to 0.29), semi-polar (log D: 0.30 to 2.59) and non-polar (log D: 2.60 to 5.46) compounds.

6.2.3 2D-HPLC instrument

For column screening the Eksigent NanoLC 425 system (SCIEX, Darmstadt, Germany) with a fully integrated autosampler was used. This system contained two binary-gradient pneumatic pumps, which can be operated separately at flow rates between 0.1 and $50 \ \mu L \ min^{-1}$ at a maximum backpressure of ~ 690 bar (10 kpsi). The integrated autosampler contained a two-position six-port valve, used for the injection of the sample onto the first dimension and an additional two-position ten-port valve used for the modulation of the first dimension effluent. For the modulation, the two-loop-technique with symmetrical flow paths (see Figure S 6-1) was applied. For the first dimension, an external column oven μOV HTG200-17 (AμMass, Leverkusen, Germany) was used and adjusted to 30 °C. The integrated column oven of the

NanoLC 425 was used for temperature control of the second dimension column and adjusted to 50 °C. The 2D-LC system was controlled by the Eksigent Control Software (version 4.1, build 130717-1043).

In order to operate the NanoLC 425 system in comprehensive mode, some further system modifications are required. Since the modulation valve is a part of the autosampler and not the pump module, the modulation steps need to be programmed into the autosampler methods. A detailed description of the programmed autosampler methods is given in Table S 6-2 and Table S 6-3.

Furthermore, the gradient delay volume had to be reduced in order to speed up the cycle time of the second dimension and the total analysis time of a single 2D-LC run. In order to achieve very low gradient delay volumes, the gradient mixers of the pumps were positioned closer (~ 20 cm) to the modulation and injection valve. For the complete flow path of the first dimension fused silica capillaries with an i.d. of 25 μm were used. For the second dimension and the modulation loops capillaries with an i.d. of 50 μm were installed.

For the separation on the first dimension, following stationary phases are used: Hypersil GOLD PFP (PFP, 5 μm), Bio Basic CN (Cyano, 5 μm), Hypercarb (PGC, 5 μm) all purchased from Thermo Fisher Scientific (Dreieich, Germany) and SeQuant ZIC-HILIC (HILIC, 3.5 μm Merck, Darmstadt, Germany).For the selectivity study in the first dimension, different columns and column combinations listed in Table 6-1 were used.

Table 6-1:   Detailed list of columns and column combinations for the selectivity study.

1st dimension pre-column		1st dimension main-column	
None		PGC	50 x 0.100 mm
None		PFP	10 x 0.075 mm
None		Cyano	100 x 0.075 mm
None		HILIC	100 x 0.100 mm
PGC	10 x 0.13 mm	None	
PGC	10 x 0.13 mm	PFP	150 x 0.075 mm
PGC	10 x 0.13 mm	Cyano	100 x 0.075 mm
PGC	10 x 0.13 mm	HILIC	100 x 0.100 mm

Acidified (0.1% FA) water (solvent A) and methanol (solvent B) were chosen for the mobile phases of the first dimension and the flow rate was adjusted to 300 nL min^{-1}. The injection volume was always 450 nL. A solvent gradient was applied according to the following programs: i) used for PGC, PFP and Cyano columns; gradient start at 3% B, in 18 min 3-97% B, 16 min hold at 97% B, in 0.5 min 97-3% B, re-equilibration for 16.5 min. ii) used for HILIC column; isocratic at 99% B, hold at 99% B for 51 min.

For the separation on the second dimension superficially porous 2.6 µm SunShell RP-AQUA C28 particles (ChromaNik Technologies, Osaka, Japan) packed into 0.3 mm x 50 mm i.d. hardware were used. The flow rate was adjusted to 35 µL min^{-1}. Acidified (0.1% FA) water (solvent A) and acetonitrile (solvent B) were chosen for the second dimension mobile phases. A solvent gradient was applied according to the following program: gradient start at 3% B, in 0.5 min 3-97% B, 0.08 min hold at 97% B, in 0.04 min 97-3% B, re-equilibration for 0.13 min. The total gradient cycle time of 0.75 minutes was repeated until the end of the gradient of the first dimension. In total 68 D2 cycles were performed. The transfer volume onto the second dimension column was 225 nL. For transfer loops, fused silica capillaries with an i.d. of 50 µm and a length of 15.6 cm were used.

6.2.4 MS instrument

For the mass spectrometric detection a 3200 QTRAP MS/MS system with a Turbo V ion source and a TurboIonSpray probe for electrospray ionization was used (SCIEX, Darmstadt, Germany). To avoid band broadening, an emitter tip optimized for micro-LC flow rates and an i.d. of 50 µm replaced the standard emitter tip with an i.d. of 130 µm. The mass spectrometer was controlled by SCIEX Analyst 1.6.2 software, which was also used for data evaluation. The mass spectrometer was operated in multiple reaction monitoring (MRM) mode to detect two transitions of each target during the complete 2D-LC run. The detailed MS conditions are listed in chapter appendix Table S 6-4 and Table S 6-5.

6.3 Theory and calculation

The orthogonality value is a well suited parameter for the evaluation of the different column combinations. It describes the distribution of the targets over the two-dimensional chromatographic separation area. In general, a homogeneous distribution of all target compounds should be achieved to fully utilize the separation space and to minimize the number of co-eluting analytes. The distribution of target analytes across the separation space depends on the overall selectivity of the first and second dimension and is not related to efficiency or peak capacity.

In order to achieve the best peak distribution, the respective separation mechanisms need to be independent. Such configuration is called orthogonal and represents a theoretical optimum for a two-dimensional separation system. In practice, this cannot be achieved, because each separation mechanism is a combination of several interactions. Therefore, the same interactions will occur on both dimensions.

Examples of a low and a high orthogonal system are shown in chapter appendix Figure S 6-2. The dots represent the peak maxima of each compound and do not provide information about peak area, width or height. If the separation mechanisms of the first and the second dimension are identical, the distribution is lowest and the targets are located around the bisecting line.

Three different methods are mainly used for the calculation of orthogonality. One of these methods describes the effective area by using a vector cross product calculation [25–27]. In this method, the orthogonality determination is based on the location of the outer analytes, defining the convex hull area. The compound eluting first from the first and second dimension is defined as the origin corner point. For calculating orthogonality the convex hull area is divided into triangles defined by vectors between the origin corner point and the outermost analytes (see Figure S 6-3).

Unfortunately, cluster detection is not possible when applying this method. Moreover, the unused separation area within the hull is not considered. Also, compounds which are located in one of the corner points will significantly affect the orthogonality value although the majority of compounds might elute in a very small fraction of the separation space inside the convex hull.

Another approach was introduced by Camenzuli and Schoenmakers [28] and is termed *Asterisk* method. This method describes the orthogonality by calculation of spread (S_{Z_-}, S_{Z_+}, S_{Z_1} and S_{Z_2}) and standard deviation (σ) of peaks to four lines (Z_-, Z_+, Z_1 and Z_2) crossing the separation space. Z_-, Z_+ are affected by both dimensions, with Z_1 being related to the spread of components in the first dimension whilst the spread around the Z_2 line is only related to the second dimension (see Figure S 6-4).

The authors noted that this approach is more suited to samples that contain more than 50 components. If less than 50 compounds are used for method development, the orthogonality value dropped considerably and the standard deviation increased significantly for different simulation scenarios (up to 14%). In terms of method development it would be beneficial if the orthogonality value could also be calculated with a lower standard deviation when fewer compounds are used. The reason is that the availability of reference standards is often related to high costs. Moreover, using fewer reference compounds for method development would also decrease the overall complexity of method development and concomitant data analysis.

The third method is the *Bin Counting* method introduced by Gilar et al. in 2005 [29]. This method defines the effective area by dividing the separation space into rectangular bins of a defined size, which depends on the total number of compounds. By definition, the maximum distribution of 63% could be achieved if a Poisson distribution is assumed. Therefore, 100% orthogonality is equal to 63% coverage of the separation space. In a non-orthogonal system, the compounds are located across the bisecting line of the normalized separation space. Therefore, 0% orthogonality corresponds to the number of bins covering the bisector line.

At first, the size of the bins (BS) is calculated according to Equation 6-1, where NC_{total} is the total number of compounds.

Equation 6-1: $$BS = rounded\ integer \left(\sqrt{NC_{total}} \right)$$

In total, 42 compounds were used for method development in our study. The calculated bin size value is 6.48 and not an integer. Therefore, it was rounded down to 6 for a practicable calculation of the orthogonality.

Next, the normalized 2D plots were divided into 6x6 bins, which represent the maximum bin number B_{max}. For the calculation of the orthogonality value O, the bins filled with at least one compound need to be summed (see Figure S 6-5) and the calculation is performed according to Equation 6-2.

Equation 6-2: $$O = \frac{\sum bins - \sqrt{B_{max}}}{0.63 \times B_{max}}$$

In order to be able to compare the column combinations with all methods described above, the fraction numbers of the first dimension and the retention times of the second dimension were normalized by Equation 6-3.

Equation 6-3: $$RT_{i(norm)} = \frac{RT_i - RT_{min}}{RT_{max} - RT_{min}}$$

RT_{min} and RT_{max} represent the fraction numbers or the retention times of the least and the most retained compound, respectively. The normalized values $RT_{i(norm)}$ ranged between 0 and 1. The normalization allows a comparison of different chromatographic data in a uniform two-dimensional distribution space.

Since the *Convex Hull* and the *Bin Counting* methods do not provide any information of peak distribution across the respective dimensions, additional histograms for the first and second dimension are proposed in this study. For the calculation, the elution window of each dimension is divided into equally broad segments S_X as shown in Figure 6-1. The width of each segment is calculated according to Equation 6-1 and therefore equal to the bin size of the *Bin Counting* method.
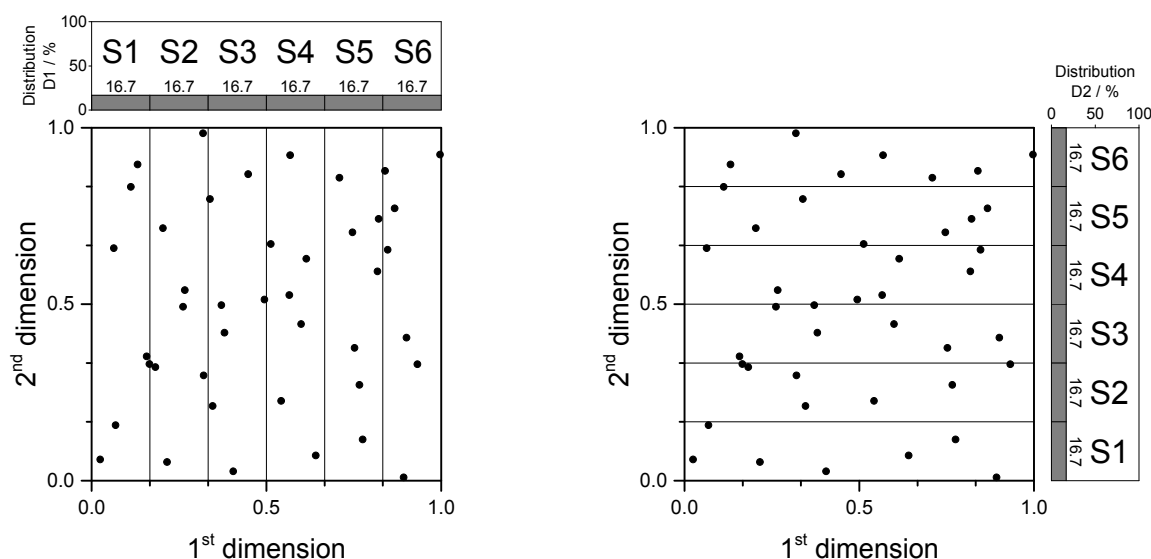
Figure 6-1: Normalized simulated dot-plot with 42 orthogonally distributed compounds and the additional histograms of the first dimension (left) and second dimension (right).

The percentage distribution (D_x) of segment x is calculated according to Equation 6-4, where NC_{total} is the total number of compounds and $NC_{area,x}$ the number of compounds eluting inside the respective segment of the chosen dimension.

Equation 6-4: $$D_x = \frac{NC_{area,x}}{NC_{total}} \times 100$$

Equation 6-5: $$D_{x\,(orthogonal)} = \frac{1}{BS} \times 100$$

A fully orthogonal system would provide the same D_x values, which are equal to $D_{x\,(orthogonal)}$ for all respective segments of the first and second dimension as shown in Figure 6-1. A D_x value significantly higher than $D_{x\,(orthogonal)}$ indicates a clustering inside the respective segment, whereas a D_x value significantly lower than $D_{x\,(orthogonal)}$ indicates a void space.

In general, the square root of the sum of the squares of the differences between the respective D_x values and $D_{x\,(orthogonal)}$ can reveal the clustering or anti-clustering across the first (SD_{first}) and second (SD_{second}) dimensions as well as the coverage of the effective separation space (SD_{total}), according to Equation 6-6. For the calculation of (SD_{total}), D_x values for both dimensions should be used.

Equation 6-6: $$SD = \sqrt{\sum_{1}^{x}\left(D_x - D_{x\,(orthogonal)}\right)^2}$$

Assuming a homogeneous distribution of all compounds across the respective two-dimensional separation space, an SD value of 0 should be calculated. With a higher clustering, the SD value will increase. Therefore, a column combination with the lowest possible value should be chosen. However, it must be noted that this concept should be used in combination with the orthogonality value. The reason is that an even distribution is not necessarily equivalent to a high orthogonality. This has been demonstrated for simulated examples of peak spreading and is included in the chapter appendix (see Figure S 6-6a-k and Figure S 6-7a-i, and Table S 6-7 and Table S 6-8).

6.4 Results and discussion

6.4.1 Overview of the normalized dot-plots and histogram distributions

For the comparative orthogonality study of single columns and columns coupled in series for the first dimension, a multi-component reference mix was analysed using the microscale online comprehensive miniaturized 2D-LC system. The normalized dot-plots are shown in Figure 6-2.
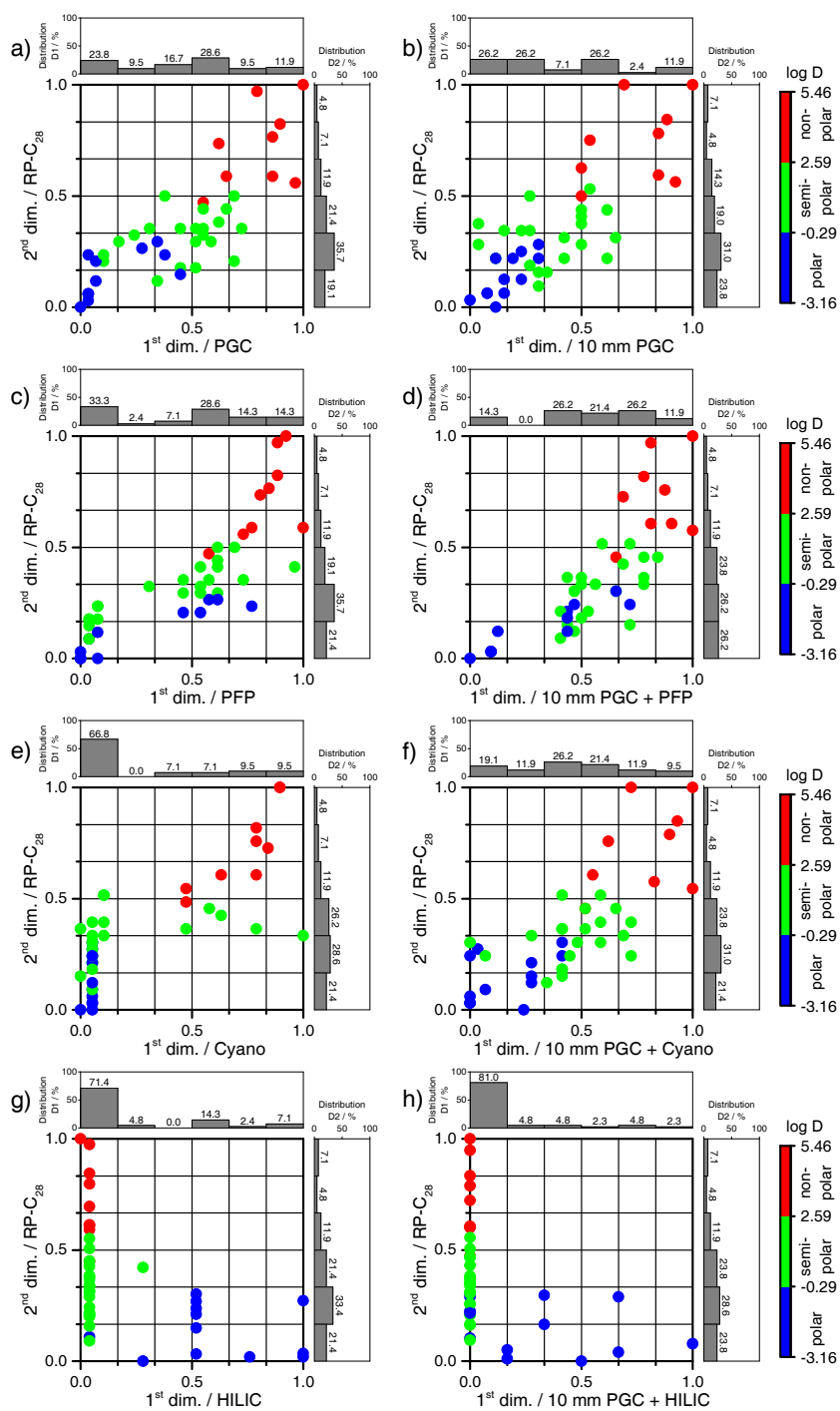
Figure 6-2: Normalized dot-plots for single columns and serial column combinations used in the first dimension and the RP-C28 column in the second dimension. Stationary phases for the first dimension: a) PGC phase, b) 10 mm PGC pre-column, c) PFP phase, d) 10 mm PGC pre-column coupled to PFP phase, e) Cyano phase, f) 10 mm PGC pre-column coupled to Cyano phase, g) HILIC phase, h) 10 mm PGC pre-column coupled to HILIC phase.

The histograms shown in Figure 6-2 show the compound distribution across the respective dimensions. Since the column used for the second dimension remained unchanged, the small differences in D_x values are a result of slight retention time shifts. The polarity distribution is also given by the colour of dots. As expected, the polar compounds elute at the beginning of the gradient on the RP-C_{28} phase used for the second dimension, followed by the semi-polar and non-polar compound groups. However, a retention time prediction based only on the specific log D value is not possible as some of the semi-polar compounds elute before some of the polar compounds and some of the non-polar compounds elute before some of the semi-polar compounds. In fact, this holds true for both dimensions.

For further evaluation, the orthogonality values have been calculated and all three methods are used and compared.

6.4.2 Orthogonality comparison calculated by *Convex Hull* method

The advantage of the *Convex Hull* method is the low dependence on the number of analytes [26, 27]. The orthogonality values calculated according to the *Convex Hull* method are summarized in Figure 6-3a).
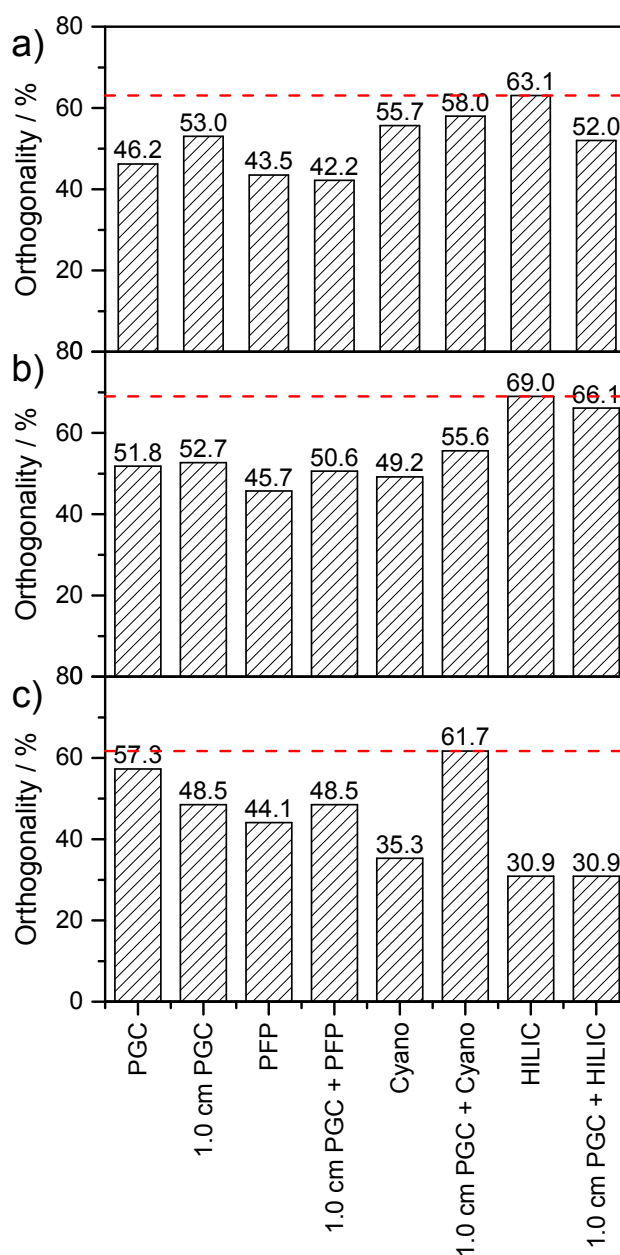
Figure 6-3: Comparison of the calculated orthogonality values for single columns and serial column combinations used in the first dimension and the RP-C$_{28}$ column in the second dimension. The values are calculated according to a) *Convex Hull*, b) *Asterisk* and c) *Bin Counting* method.

The 50 mm PGC column yields an orthogonality value of 46.2%. However, the disadvantages that were mentioned earlier exclude the further use of this column dimension. Compared to the 50 mm PGC column and based solely on the orthogonality values it can be concluded that the

HILIC phase in the first and RP-C$_{28}$ phase in the second dimension is the best column combination for the separation of the reference mixture.

A detailed view on the distribution histograms shown in Figure 6-4 clearly demonstrates that 71.4% of all compounds elute in a single fraction on the HILIC phase in the first dimension. Therefore, despite the high orthogonality value it appears that this column combination is not appropriate for the separations of the target analytes of this study.
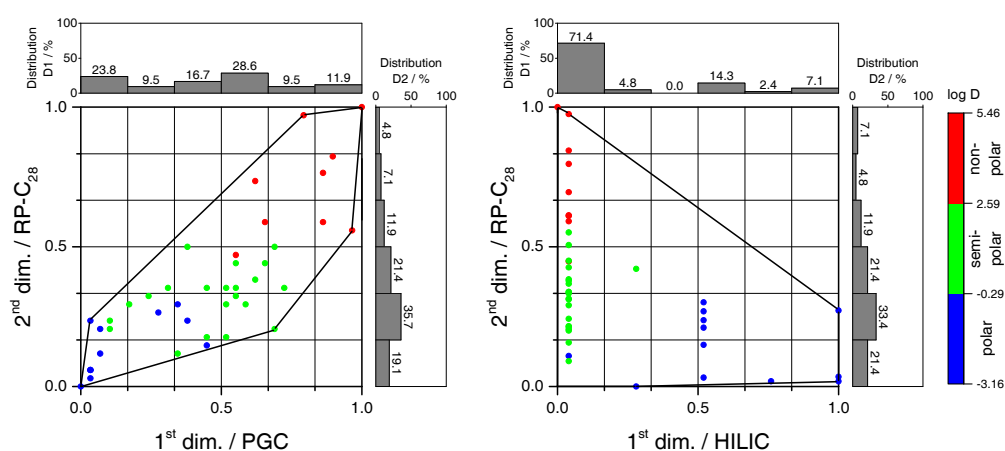
Figure 6-4:   Comparison of peak distribution across the normalized separation space obtained with a 50 mm PGC phase (left) and HILIC phase (right) for the first dimension.

The reason is that the calculated orthogonality value does not correlate with the distribution of the compounds inside the hull and only a few outlier compounds significantly increase the orthogonality value as can be seen in Figure 6-4. The elimination of only one point (D1:D2, 1.0:0.3) reduces the orthogonality value from 63.1 to 51.0% for the HILIC x RP-C$_{28}$ combination. This effect has also been demonstrated for other 2D scenarios [30]. Therefore, this method is not suitable for the orthogonality study of this work, despite the fact that the missing information concerning clusters and compound distribution within the hull can be shown by the additionally calculated histograms.

6.4.3 Orthogonality comparison calculated by *Asterisk* method

The biggest advantage of the *Asterisk* method is the cluster detection based on Z_x parameters. The orthogonality values calculated according to the *Asterisk* method are given in Figure 6-3b). The 50 mm PGC column yields an orthogonality value of 51.8%. The single HILIC phase and the combination of the 10 mm PGC pre-column with the HILIC phase for the first dimension leads to high orthogonality values of 69% and 66.1%. It appears that both approaches could be an alternative to the use of the 50 mm long PGC phase for the first dimension. However, as already mentioned and shown in Figure 6-4, this column or column combination is not suitable for the separation of the chosen reference compounds as demonstrated by the Z_x parameters listed in Table 6-2. The higher the Z_x parameter value, the better the distribution around the Z_x line. Therefore, a fully orthogonal system would provide the value of 100% for all four parameters. The smaller the Z_x parameter value, the higher the clustering around the Z_x line.

Table 6-2:   Detailed list of Z_x parameters calculated by the *Asterisk* method.

D1 Column	Z_-	Z_+	Z_1	Z_2
PGC	43%	74%	98%	86%
1.0 cm PGC	43%	78%	94%	89%
PFP	46%	61%	83%	89%
1.0 cm PGC + PFP	40%	80%	91%	89%
Cyano	53%	63%	83%	88%
1.0 cm PGC + Cyano	47%	76%	100%	87%
HILIC	82%	70%	95%	88%
1.0 cm PGC + HILIC	99%	64%	79%	87%

Since the column used for the second dimension remained unchanged, the mean Z_2 value is indicative of the retention time stability for the second dimension separation. The mean Z_2 value of 88% and the standard deviation of only 1.3% show the very low clustering for the second dimension and therefore a good distribution is obtained. A comparison of the Z_1 value for the 50 mm PGC column of 98% and the HILIC column of 95% indicates that only negligible clustering and an equally good separation is obtained. However, as discussed before, 71.4% (see Figure 6-4) of all compounds elute in the first fraction when using the HILIC phase. Based on the given Z_x values for the HILIC phase it is not possible to detect this clustering. This could

be a result of a low number of compounds used for the reference mix as has been noted by Camenzuli et al., which underlines that the *Asterisk* method is not applicable for the orthogonality study of this work.

6.4.4 Orthogonality comparison calculated by *Bin Counting* method

In comparison to the *Convex Hull* method, the *Bin Counting* method considers the separation space that is not filled with peaks. Single outer-most compounds have only a negligible influence on the orthogonality value, which is the main advantage of this method. The orthogonality values of the normalized 2D plots are shown in Figure 6-3c which demonstrates that the HILIC phase and 10 mm PGC / HILIC combination have a much lower orthogonality value of only 30.9%, when compared to the *Convex Hull* and *Asterisk* methods. The *Bin Counting* method confirms that the expected low orthogonality value of the HILIC phase is caused by the clustering in the first segment, although it is not possible to locate the cluster. Therefore, this concept seems to be suitable for method development and the missing information about clusters is obtained by the additional calculation of the histograms. The calculated SD_{first}, SD_{second} and the SD_{total} values are listed in Table 6-3.

Table 6-3:   Detailed list of SD_{first}, SD_{second} and SD_{total} values.

		Distribution		
	O / %	SD_{first}	SD_{second}	SD_{total}
PGC	57.3	18	25	31
1.0 cm PGC	48.5	24	22	33
PFP	44.1	27	25	37
1.0 cm PGC + PFP	48.5	23	22	32
Cyano	35.3	55	23	60
1.0 cm PGC + Cyano	61.7	15	23	27
HILIC	30.9	61	24	66
1.0 cm PGC + HILIC	30.9	70	22	74

As can be seen, the use of the single 10 mm PGC pre-column results also in a moderate orthogonality value of 48.5% with an acceptable SD_{first} value of 24. This result demonstrates that the short pre-column could be used in the first dimension without an additional main-column. However, as the data reveals, an even higher orthogonality value and therefore better selectivity is obtained if the PGC pre-column is coupled to a Cyano phase.

The orthogonality values obtained with single PFP, Cyano and HILIC columns for the first dimension are significantly lower than the value reached by the 50 mm PGC and RP-C$_{28}$ column combination. Therefore, the single columns are not suitable as an alternative for the first dimension. However, it could be shown that the 10 mm PGC pre-column concept increases the system orthogonality, if used in combination with PFP or Cyano main-columns for the first dimension. In particular, the combination of 10 mm PGC pre- and Cyano main-column resulted in a higher orthogonality of 61.7% with the lowest SD_{first} value of 15 and therefore the best distribution across the first dimension. A detailed view on the histograms for the first dimension given in Figure S 6-8 shows a slight clustering on the 50 mm PGC phase located within the first and fourth segments. The peak distribution when using the 10 mm PGC / Cyano phase for the first dimension was equal and only a negligible clustering could be observed within segments three and four. The peak distribution for the second dimension was almost constant and varied only slightly due to minor variations in the second dimension retention times. The histograms for the second dimension show a moderate clustering in the second and third segment.

For the analysis of complex samples on the basis of a suspected- or non-target screening approach, the retention time is a very important identification criterion that should not be ignored. Especially for a suspected target screening, the accurate mass in combination with the retention time can be used for compound identification. A high variation in retention time could lead to false positive or false negative results. Therefore, the intraday retention time stability was evaluated on the basis of the standard reference mixture, analysed on three consecutive days using the optimal column combination. The detailed list containing the elution fraction numbers for the first and the retention times for the second dimension is given in Table S 6-6.

The data evaluation provides a mean standard deviation for the elution fraction number of 2.1% and for the retention time for the second dimension of 1.5%. The results fulfil the maximum acceptable standard deviation of 2.5% and demonstrate the stability of the miniaturized 2D-LC system.

6.5 Conclusion

Existing procedures for determining the orthogonality and therefore the separation performance of two-dimensional systems have drawbacks, since they provide no or only partial information about the peak distribution of the compounds across the separation space. However, this information is important, because it is indicative of whether the separation space is equally filled. These disadvantages have been successfully overcome with the introduction of the additional histogram information presented in this work. The advantage of this concept is that the retention times of the selected target analytes have to be measured only once on each column. The optimal column combination can then be deduced according to the respective SD_{first} and SD_{second} values.

Independent of the method used for the determination of the orthogonality, the concept described for the identification of clusters reveals the possibility of getting information for the optimal column combination for both the first and second dimensions through the use of one single investigation of each column in any desirable combination. In this respect, the approach might be not only applicable for LCxLC, but also for other 2D separation methods such as GCxGC.

6.6 References

1. Haun J, Leonhardt J, Portner C, Hetzel T, Tuerk J, Teutenberg T, Schmidt TC. Online and Splitless NanoLC × CapillaryLC with Quadrupole/Time-of-Flight Mass Spectrometric Detection for Comprehensive Screening Analysis of Complex Samples. Anal Chem; 2013;85(21):10083–90

2. Leonhardt J, Teutenberg T, Tuerk J, Schlüsener MP, Ternes TA, Schmidt TC. A comparison of one-dimensional and microscale two-dimensional liquid chromatographic approaches coupled to high resolution mass spectrometry for the analysis of complex samples. Anal Methods; 2015;7(18):7697–706

3. Krauss M, Singer H, Hollender J. LC-high resolution MS in environmental analysis: from target screening to the identification of unknowns. Anal Bioanal Chem; 2010;397(3):943–51

4. Zedda M, Zwiener C. Is nontarget screening of emerging contaminants by LC-HRMS successful? A plea for compound libraries and computer tools. Anal Bioanal Chem; 2012;403(9):2493–502

5. Neue UD. Peak capacity in unidimensional chromatography. J Chromatogr A; 2008;1184(1–2):107–30

6. Ralston-Hooper KJ, Turner ME, Soderblom EJ, Villeneuve D, Ankley GT, Moseley MA, Hoke RA, Ferguson PL. Application of a label-free, gel-free quantitative proteomics method for ecotoxicological studies of small fish species. Environ Sci Technol; 2013;47(2):1091–100

7. Nägele E, Vollmer M, Hörth P. Improved 2D nano-LC/MS for proteomics applications. A comparative analysis using yeast proteome. J Biomol Tech; 2004;15(2):134–43

8. Zhao L, Liu L, Leng W, Wei C, Jin Q. A proteogenomic analysis of Shigella flexneri using 2D LC-MALDI TOF/ TOF. BMC Genomics; 2011;12:528

9. Willemse CM, Stander MA, Vestner J, Tredoux AG, de Villiers A. Comprehensive Two-Dimensional Hydrophilic Interaction Chromatography (HILIC) × Reversed-Phase Liquid Chromatography Coupled to High- Resolution Mass Spectrometry (RP-LC-UV-MS) Analysis of Anthocyanins and Derived Pigments in Red Wine. Anal Chem; 2015;87(24):12006–15

10. Ouyang X, Leonards PEG, Tousova Z, Slobodnik J, de Boer J, Lamoree MH. Rapid Screening of Acetylcholinesterase Inhibitors by Effect-Directed Analysis Using LC × LC Fractionation, a High Throughput in Vitro Assay, and Parallel Identification by Time of Flight Mass Spectrometry. Anal Chem; 2016;88(4):2353–60

11. Mondello L, Lewis AC, Bartle KD. Multidimensional Chromatography. Chichester: Wiley; 2001.

12. Wang S, Qiao L, Shi X, Hu C, Kong H, Xu G. On-line stop-flow two-dimensional liquid chromatography-mass spectrometry method for the separation and identification of triterpenoid saponins from ginseng extract. Anal Bioanal Chem; 2015;407(1):331–41

13. Groskreutz SR, Swenson MM, Secor LB, Stoll DR. Selective comprehensive multi-dimensional separation for resolution enhancement in high performance liquid chromatography. Part I: Principles and instrumentation. J Chromatogr A; 2012;1228:31–40

14. Li D, Schmitz OJ. Comprehensive two-dimensional liquid chromatography tandem diode array detector (DAD) and accurate mass QTOF-MS for the analysis of flavonoids and iridoid glycosides in Hedyotis diffusa. Anal Bioanal Chem; 2015;407(1):231–40

15. Li D, Jakob C, Schmitz O. Practical considerations in comprehensive two-dimensional liquid chromatography systems (LCxLC) with reversed-phases in both dimensions. Anal Bioanal Chem; 2015;407(1):153–67

16. Stoll DR, Cohen JD, Carr PW. Fast, comprehensive online two-dimensional high performance liquid chromatography through the use of high temperature ultra-fast gradient elution reversed-phase liquid chromatography. J Chromatogr A; 2006;1122(1):123–37

17. Murphy RE, Schure MR, Foley JP. Effect of Sampling Rate on Resolution in Comprehensive Two-Dimensional Liquid Chromatography. Anal Chem; 1998;70(8):1585–94

18. Dugo P, Cacciola F, Donato P, Mondello L. Comprehensive two-dimensional liquid chromatography applications. In: Mondello L (editor). Comprehensive chromatography in combination with mass spectrometry. Hoboken, NJ: Wiley; 2011, pp. 391–427.

19. Dugo P, Cacciola F, Donato P, Mondello L. Comprehensive two-dimensional liquid chromatography combined with mass spectrometry. In: Mondello L (editor). Comprehensive chromatography in combination with mass spectrometry. Hoboken, NJ: Wiley; 2011, pp. 331–390.

20. Stoll DR, Wang X, Carr PW. Comparison of the Practical Resolving Power of One- and Two-Dimensional High-Performance Liquid Chromatography Analysis of Metabolomic Samples. Anal Chem; 2007;80(1):268–78

21. Francois I, Sandra K, Sandra P. History, evolution, and optimization aspects of comprehensive two-dimensional liquid chromatography. In: Mondello L (editor). Comprehensive chromatography in combination with mass spectrometry. Hoboken, NJ: Wiley; 2011, pp. 281–330.

22. West C, Elfakir C, Lafosse M. Porous graphitic carbon: A versatile stationary phase for liquid chromatography. J Chromatogr A; 2010;1217(19):3201–16

23. Leonhardt J, Hetzel T, Teutenberg T, Schmidt TC. Large Volume Injection of Aqueous Samples in Nano Liquid Chromatography Using Serially Coupled Columns. Chromatographia; 2015;78(1-2):31–8

24. Li D, Dück R, Schmitz OJ. The advantage of mixed-mode separation in the first dimension of comprehensive two-dimensional liquid-chromatography. J Chromatogr A; 2014:128–35

25. Semard G, Peulon-Agasse V, Bruchet A, Bouillon J-P, Cardinaël P. Convex hull: A new method to determine the separation space used and to optimize operating conditions for comprehensive two-dimensional gas chromatography. J Chromatogr A; 2010;1217(33):5449–54

26. Dück R, Sonderfeld H, Schmitz OJ. A simple method for the determination of peak distribution in comprehensive two-dimensional liquid chromatography. J Chromatogr A; 2012:69–75

27. Rutan SC, Davis JM, Carr PW. Fractional coverage metrics based on ecological home range for calculation of the effective peak capacity in comprehensive two-dimensional separations. J Chromatogr A; 2012;1255:267–76

28. Camenzuli M, Schoenmakers PJ. A new measure of orthogonality for multi-dimensional chromatography. Anal Chim Acta; 2014;838:93–101

29. Gilar M, Olivova P, Daly AE, Gebler JC. Orthogonality of separation in two-dimensional liquid chromatography. Anal Chem; 2005;77(19):6426–34

30. Gilar M, Fridrich J, Schure MR, Jaworski A. Comparison of orthogonality estimation methods for the two-dimensional separations of peptides. Anal Chem; 2012;84(20):8722–32

6.7 Chapter appendix

6.7.1 Schematic illustration of the system flow paths

For a better overview of the system flow paths, a schematic illustration is given in Figure S 6-1.
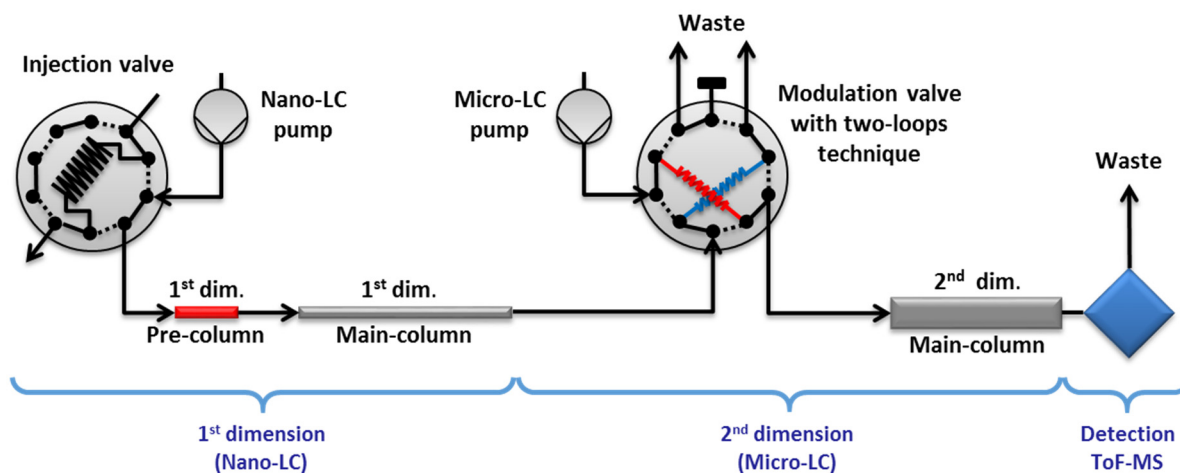
Figure S 6-1: Schematic overview over flow paths (symmetric) of the used 2D-LC system with the two-loops modulation technique.

6.7.2 An exapmle for a low and a high orthogonal system
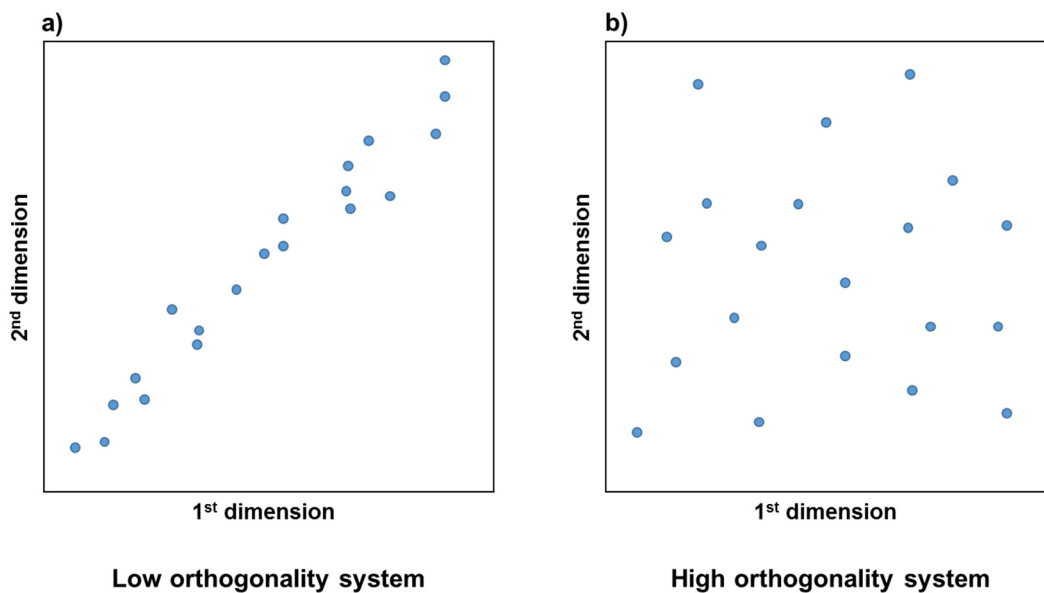
Figure S 6-2: An example for a) low and b) high orthogonal system. The dots represents the peak maximum of each compound.

6.7.3 An example for the orthogonality calculation according to the *Convex Hull* method
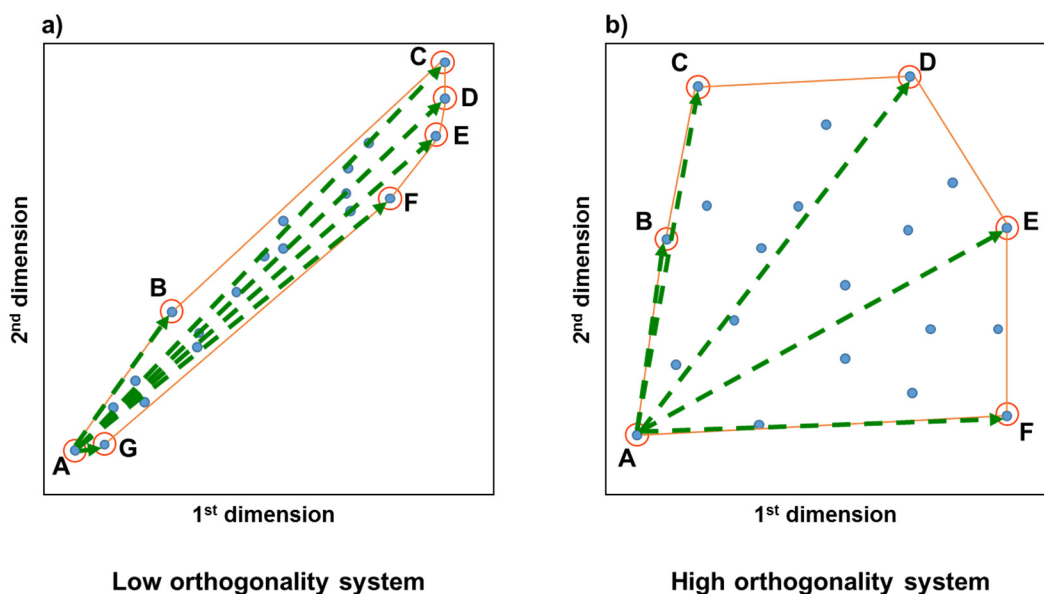
Figure S 6-3: An example for the orthogonality calculation according to the *Convex Hull* method. a) low orthogonality; b) high orthogonality.

The partial triangle surfaces $A_{triangle}$ can then be calculated as vector cross product according to Equations 6-7 to 6-9.

Equation 6-7: $A_{triangle} = \frac{1}{2} \, |\vec{a} \times \vec{b}|$

Equation 6-8: $A_{BC} = \frac{1}{2} \, \left| \overrightarrow{AB} \times \overrightarrow{AC} \right|$

Equation 6-9: $A_{BC} = \frac{1}{2} \, \left| (B_x - A_x) \times (C_y - A_y) - (C_x - A_x) \times (B_y - A_y) \right|$

The sum of all partial triangle surfaces $A_{triangle}$ hull is the total convex hull area (see Equation 6-10).

Equation 6-10:
$$A_{convex\ hull} = A_{BC} + A_{CD} + A_{DE} + A_{EF} + \cdots$$

The orthogonality value O is, therefore, the convex hull area contribution of the square surface area $A_{triangle}$, defined by the retention times of the first $(D1_{first}; D2_{first})$ and the last $(D1_{last}; D2_{last})$ eluted compound on both dimensions (see Equations 6-11 and 6-12).

Equation 6-11:
$$A_{theoretical} = (D1_{last} - D1_{first}) \times (D2_{last} - D2_{first})$$

Equation 6-12:
$$O = \frac{A_{convex\ hull}}{A_{theoretical}}$$

6.7.4 An example for the orthogonality calculation according to the *Asterisk* method
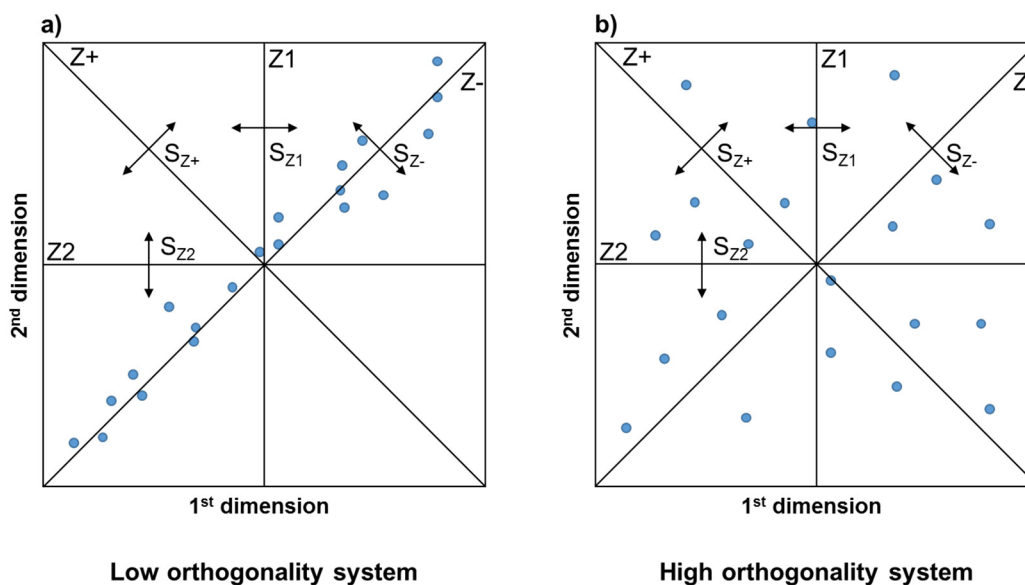
Figure S 6-4: An example for the orthogonality calculation according to the *Asterisk* method. a) low orthogonality; b) high orthogonality.

The spreading around the lines is calculated using Equations 6-7 to 6-9, where the calculations in the brackets are performed for every analyte individually, using the normalized fraction number ($^1t_{R,norm}$) in the first and the normalized retention time ($^2t_{R,norm}$) in the second dimension. σ is the standard deviation of all values obtained from the calculation in the brackets.

Equation 6-13: $\qquad\qquad S_{Z_-} = \sigma\{\,^1t_{R,norm} - \,^2t_{R,norm}\}$

Equation 6-14: $\qquad\qquad S_{Z_+} = \sigma\{\,^2t_{R,norm} - (1 - \,^1t_{R,norm})\}$

Equation 6-15: $\qquad\qquad S_{Z_1} = \sigma\{\,^1t_{R,norm} - 0.5\}$

Equation 6-16: $\qquad\qquad S_{Z_2} = \sigma\{\,^2t_{R,norm} - 0.5\}$

Based on the S_{Z_x} values, the Z_x parameters can be calculated according to Equations 6-17 to 6-20. They describe the use of separation space with respect to the corresponding Z_x line. Therefore, the main advantage of this method as suggested by the authors is the detection of peak clusters.

Equation 6-17:

$$Z_- = \left|1 - 2.5 \cdot \left|S_{Z_-} - 0.4\right|\right|$$

Equation 6-18:

$$Z_+ = \left|1 - 2.5 \cdot \left|S_{Z_+} - 0.4\right|\right|$$

Equation 6-19:

$$Z_1 = 1 - \left|2.5 \cdot S_{Z_1} \cdot \sqrt{2} - 1\right|$$

Equation 6-20:

$$Z_2 = 1 - \left|2.5 \cdot S_{Z_2} \cdot \sqrt{2} - 1\right|$$

All Z_x parameters are equally important and the orthogonality value A_O is calculated by Equation 6-21.

Equation 6-21:

$$A_O = \sqrt{Z_- \cdot Z_+ \cdot Z_1 \cdot Z_2}$$

6.7.5 An example for the orthogonality calculation according to the *Bing Counting* method
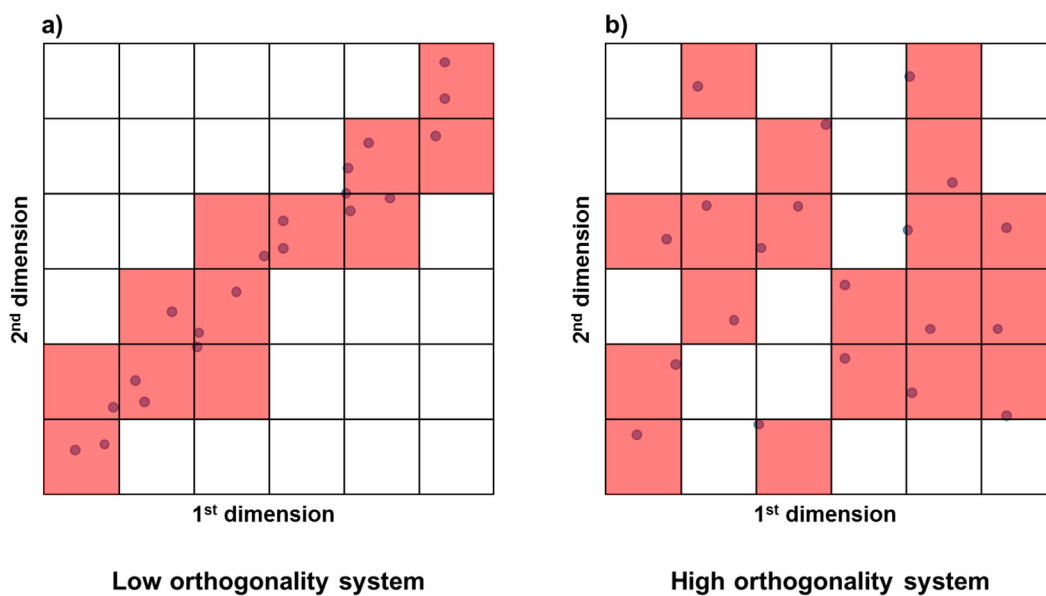
Figure S 6-5: An example for the orthogonality calculation according to the *Bing Counting* method. a) low orthogonality; b) high orthogonality.

6.7.6 Additional tables

Table S 6-1:   Detailed list of the compounds used for the reference standard.

Analyte	Purchased as	CAS No.	Purity*	Source	log D**
5,6-Dimethyl-1H-benzotriazole	5,6-Dimethyl-1H-benzotriazole monohydrate	4184-79-6	99%	Aldrich	2.34
5-Methyl-1H-benzotriazole	5-Methyl-1H-benzotriazole	136-85-6	≥ 98%	Fluka	1.83
Acetylsulfamerazine	N4-Acetylsulfamerazine	127-73-1	99%	IUTA***	0.51
Acetylsulfamethoxazole	N4-Acetylsulfamethoxazole	21312-10-7		LGC Standards	1.47
Azithromycin	Azithromycin	83905-01-5	≥ 95%	Sigma	-3.16
Benzotriazole	Benzotriazole	95-14-7	99%	Sigma-Aldrich	1.32
Bisoprolol	Bisoprolol fumarate	104344-23-2		LGC Standards	-0.47
Carbamazepine	Carbamazepine	298-46-4		Sigma	2.64
Citalopram	Citalopram hydrobromide	59729-32-7		Sigma	0.88
Clarithromycin	Clarithromycin	81103-11-9		LGC Standards	0.68
Clindamycin	Clindamycin hydrochloride	21462-39-5		Sigma	-1.93
Cyclophosphamide	Cyclophosphamide monohydrate	6055-19-2	≥ 97%	Sigma	-0.15
Diuron	Diuron	330-54-1	Pestanal	Fluka	2.97
Erythromycin	Erythromycin	114-07-8		Sigma-Aldrich	0
Fenofibrate	Fenofibrate	49562-28-9	≥ 99%	Sigma	5.46
Gemfibrozil	Gemfibrozil	25812-30-0		Sigma	4.42
Ibuprofen	Ibuprofen	15687-27-1	≥ 98%	Sigma	3.87
Ifosfamide	Ifosfamide	3778-73-2		Sigma	-0.15
Iohexol	Histodenz	66108-95-0		Sigma	-1.9
Iomeprol	Iomeprol	78649-41-9	96%	Dr. Ehrenstorfer	-1.4
Iopamidol	Iopamidol	60166-93-0	97%	Dr. Ehrenstorfer	-0.66
Iopromide	Iopromide	73334-07-3	≥ 99%	LGC Standards	-0.35
Metconazole	Metconazole	125116-23-6	Pestanal	Fluka	3.66
Metoprolol	(±)-Metoprolol (+)-tartrate	56392-17-7	≥ 98%	Sigma	-0.94
Metronidazole	Metronidazole	443-48-1		Sigma	-0.55
Naproxen	Naproxen	22204-53-1		Sigma-Aldrich	2.98
Paracetamol	Paracetamol	103-90-2		Fluka	0.87
Phenazone	Antipyrine	60-80-0		Fluka	1.12
Prednisolone	Prednisolone	50-24-8	≥ 99%	Sigma	1.19
Propyphenazone	Propyphenazone	479-92-5		LGC Standards	2.25
Roxithromycin	Roxithromycin	80214-83-1	≥ 90%	Sigma	0.29
Simvastatin	Simvastatin	79902-63-9	≥ 97%	Sigma	4.45
Sotalol	Sotalol hydrochloride	959-24-0		Dr. Ehrenstorfer	-2.79
Sulfadiazine	Sulfadiazine	68-35-9	≥ 99%	Sigma	0.33
Sulfadimidine	Sulfamethazine	57-68-1	≥ 99%	Sigma	0.51
Sulfamethoxazole	Sulfamethoxazole	723-46-6		Fluka	0.67
Sulfapyridine	Sulfapyridine	144-83-2	≥ 99%	Fluka	0.81
Tamoxifen	Tamoxifen citrate	54965-24-1		Fluka	3.28
Terbutryn	Terbutryn	886-50-0	Pestanal	Fluka	0.21
Tramadol	Tramadol hydrochloride	36282-47-0	≥ 99%	Sigma	-0.49
Trimethoprim	Trimethoprim	738-70-5	≥ 98%	Sigma	-2.83
Venlafaxine	Venlafaxine hydrochloride	99300-78-4	≥ 98%	Sigma	-0.2

Legend to Table S 6-1:

* Purity was at least pro analysi (p. a.) unless otherwise noted.

** log D values are predicted by ChemAxon – www.chemicalize.org

*** These standard has been prepared in-house according to the procedure described in the following article: Pfeifer T., Tuerk J., Bester K., Spiteller M. (2002) Rapid Commun Mass Sp 16(7):663–669.

Manufacturer information:

- Products from Aldrich, Fluka and Sigma were purchased from Sigma-Aldrich, Schnelldorf, Germany.

- Dr. Ehrenstorfer, Augsburg, Germany.

- LGC Standards, Wesel, Germany.

Table S 6-2:   Autosampler method for the first dimension.

#	Command	Description
1	Initialize	Autosampler device
2	Needle wash	Pre-wash – 1 x using wash solvent
3	Wait	For Gradient 1 ready to start
4	Get Sample	Pick up 10 μL : 2 mm from bottom
5	Start	Gradient 1
6	Valve	Injector inject
7	Wait	For Gradient 1 injection complete
8	Valve	Injector load and trigger to method of D2

Table S 6-3:   Autosampler method for the second dimension.

#	Command	Description
1	Start	Start Gradient 2
2	Wait	for Input 1 Low
3	Valve	Switch ISS-A valve to Load (6-1)
4	Wait	for Input 2 Low
5	Valve	Switch ISS-A valve to Load (1-2)
6	Wait	for Input 1 Low
7	Valve	Switch ISS-A valve to Load (6-1)
8	Wait	for Input 2 Low
9	Valve	Switch ISS-A valve to Load (1-2)
10	Wait	for Input 1 Low
11	Valve	Switch ISS-A valve to Load (6-1)
12	Wait	for Input 2 Low
13	Valve	Switch ISS-A valve to Load (1-2)
14	Wait	for Input 1 Low
15	Valve	Switch ISS-A valve to Load (6-1)
16	Wait	for Input 2 Low
17	Valve	Switch ISS-A valve to Load (1-2)
18	Wait	for Input 1 Low
19	Valve	Switch ISS-A valve to Load (6-1)
20	Wait	for Input 2 Low
21	Valve	Switch ISS-A valve to Load (1-2)
22	Wait	for Input 1 Low
23	Valve	Switch ISS-A valve to Load (6-1)
24	Wait	for Input 2 Low
25	Valve	Switch ISS-A valve to Load (1-2)
26	Wait	for Input 1 Low
27	Valve	Switch ISS-A valve to Load (6-1)
28	Wait	for Input 2 Low
29	Valve	Switch ISS-A valve to Load (1-2)
30	Wait	for Input 1 Low
31	Valve	Switch ISS-A valve to Load (6-1)
32	Wait	for Input 2 Low
33	Valve	Switch ISS-A valve to Load (1-2)
34	Wait	for Input 1 Low
35	Valve	Switch ISS-A valve to Load (6-1)

Table S 6-4:   MS Parameters - ESI Source.

Parameter	Value
Ion Source	Turbo Spray
Curtain gas / psi	10
Ion source gas 1 / psi	30
Ion source gas 2 / psi	70
IonSpray voltage floating / V	4500
Temperature / °C	350
Collision gas	Medium
Interface heater	On

Table S 6-5:   Detailed list of MS parameters for each compound. For each compound two mass transitions (_1, _2) were detected. Time: dwell time; Q1: precursor-ion mass; Q3: product-ion mass; DP: declustering potential; EP: entrance potential; CEP: collision cell entrance potential; CE: collision energy; CXP: cell exit potential.

Analyt	Q1 / Da	Q3 / Da	Time / ms	DP / Volt	EP / Volt	CEP / Volt	CE / Volt	CXP / Volt
5-Methyl-1H-benzotriazole_1	134.0	76.8	10	51	10	8	33	4
5-Methyl-1H-benzotriazole_2	134.0	79.1	10	51	10	8	27	4
5,6-Dimethyl-1H-benzotriazole_1	148.2	77.2	10	51	8	10	37	4
5,6-Dimethyl-1H-benzotriazole_2	148.2	93.1	10	51	8	10	27	4
Acetylsulfamethoxazole_1	295.9	134.1	10	71	5	20	31	4
Acetylsulfamethoxazole_2	295.9	65.0	10	71	5	20	63	4
Acetylsulfamerazine_1	307.1	134.2	10	51	6	24	33	4
Acetylsulfamerazine_2	307.1	65.1	10	51	6	24	57	4
Azitromycin_1	375.3	83.2	10	21	5.5	24	31	4
Azitromycin_2	375.3	158.3	10	21	5.5	24	29	4
Benzotriazole_1	120.1	65.0	10	46	8.5	12	29	4
Benzotriazole_2	120.1	92.1	10	46	8.5	12	23	4
Bisoprolol_1	326.3	116.1	10	51	4.5	16	25	4
Bisoprolol_2	326.3	74.2	10	51	4.5	16	37	4
Carbamazepine_1	237.1	194.3	10	56	4	14	25	4
Carbamazepine_2	237.1	193.3	10	56	4	14	43	4
Citalopram_1	324.9	109.1	10	46	4	16	33	4
Citalopram_2	324.9	262.3	10	46	4	16	27	4
Clarithromycin_1	748.6	158.4	10	51	8.5	32	37	4
Clarithromycin_2	748.6	83.2	10	51	8.5	32	71	4
Clindamycin_1	425.2	126.3	10	51	6	22	37	4
Clindamycin_2	425.2	377.4	10	51	6	22	25	6
Cyclophosphamide_1	261.0	140.1	10	51	8.5	14	29	4
Cyclophosphamide_2	261.0	106.2	10	51	8.5	14	23	4
Diuron_1	232.9	160.0	10	41	9	16	35	4
Diuron_2	232.9	133.1	10	41	9	16	51	4
Erythromycin_2	734.6	82.9	10	41	12	34	61	4

Analyt	Q1 / Da	Q3 / Da	Time / ms	DP / Volt	EP / Volt	CEP / Volt	CE / Volt	CXP / Volt
Erythromycin_1	734.6	158.3	10	41	12	34	39	4
Fenofibrate_1	360.9	139.0	10	61	6.5	20	41	4
Fenofibrate_2	360.9	233.1	10	61	6.5	20	23	4
Gemfibrozil_1	251.2	129.2	10	26	5.5	14	15	4
Gemfibrozil_2	251.2	83.1	10	26	5.5	14	19	4
Ibuprofen_1	207.2	161.2	10	21	7	15	15	4
Ibuprofen_2	207.2	119.1	10	21	7	15	29	4
Ifosfamide_1	261.1	92.1	10	46	4	26	35	4
Ifosfamide_2	261.1	154.2	10	46	4	26	33	4
Iohexol_1	822.0	804.1	10	56	9	34	31	4
Iohexol_2	822.0	375.2	10	56	9	34	63	6
Iomeprol_1	778.1	405.2	10	56	9	54	55	6
Iomeprol_2	778.1	288.2	10	56	9	54	91	4
Iopamidol_1	777.9	558.9	10	56	9	32	33	8
Iopamidol_2	777.9	387.1	10	56	9	32	53	6
Iopromide_1	791.9	300.1	10	51	9.5	34	73	4
Iopromide_2	791.9	573.0	10	51	9.5	34	35	6
Metconazole_1	320.1	70.0	10	61	7.5	18	39	4
Metconazole_2	320.1	125.2	10	61	7.5	18	45	4
Metoprolol_1	268.5	116.2	10	46	9	32	25	4
Metoprolol_2	268.5	56.0	10	46	9	32	41	4
Metronidazole_1	172.1	128.2	10	31	4.5	10	19	4
Metronidazole_2	172.1	82.2	10	31	4.5	10	35	4
Naproxen_1	231.1	185.2	10	46	9.5	18	21	4
Naproxen_2	231.1	115.0	10	46	9.5	18	77	4
Paracetamol_1	152.1	110.0	10	46	8	12	21	4
Paracetamol_2	152.1	64.9	10	46	8	12	39	4
Phenazone_1	189.1	56.1	10	36	9.5	16	37	4
Phenazone_2	189.1	77.2	10	36	9.5	16	59	4
Prednisolone_1	361.2	343.2	10	21	4	22	17	6
Prednisolone_2	361.2	147.3	10	21	4	22	31	4
Propyphenazone_1	231.2	56.1	10	56	7	16	47	4
Propyphenazone_2	231.2	189.2	10	56	7	16	27	4
Roxithromycin_1	837.6	158.3	10	51	7.5	36	47	4
Roxithromycin_2	837.6	116.2	10	51	7.5	36	65	4
Simvastatin_1	419.3	199.4	10	36	12	20	21	4
Simvastatin_2	419.3	143.1	10	36	12	20	61	4
Sotalol_1	273.2	255.3	10	26	5.5	16	17	4
Sotalol_2	273.2	133.3	10	26	5.5	16	35	4
Sulfadiazine_1	250.8	156.2	10	36	4	22	19	4
Sulfadiazine_2	250.8	92.1	10	36	4	22	33	4
Sulfadimidine_1	279.1	186.1	10	51	7.5	12	25	6
Sulfadimidine_2	279.1	124.1	10	51	7.5	12	27	4
Sulfamethoxazole_1	254.0	156.0	10	36	5	18	21	4
Sulfamethoxazole_2	254.0	92.0	10	36	5	18	37	4
Sulfapyridine_1	250.1	92.2	10	41	12	16	37	4
Sulfapyridine_2	250.1	156.1	10	41	12	16	21	4

Analyt	Q1 / Da	Q3 / Da	Time / ms	DP / Volt	EP / Volt	CEP / Volt	CE / Volt	CXP / Volt
Tamoxifen_1	372.3	72.1	10	56	8.5	22	39	4
Tamoxifen_2	372.3	70.2	10	56	8.5	22	65	4
Terbutryn_1	242.2	186.3	10	41	9.5	16	27	4
Terbutryn_2	242.2	68.0	10	41	9.5	16	55	4
Tramadol_1	265.1	58.1	10	31	6	22	39	4
Tramadol_2	265.1	59.2	10	31	6	22	31	4
Trimethoprim_1	291.2	123.2	10	41	6	24	33	4
Trimethoprim_2	291.2	230.4	10	41	6	24	33	4
Venlafaxine_1	278.6	58.2	10	26	7	26	31	4
Venlafaxine_2	278.6	121.1	10	26	7	26	41	4

Table S 6-6:   Detailed list of mean elution fraction numbers of the first dimension (10 mm PGC pre- and Cyano main-column) and mean retention times of the second dimension (RP-C$_{28}$). n=3.

Analyt	Mean fraction number of D1	RSD	Mean retention time of D2 / min.	RSD
5-Methyl-1H-benzotriazole	15	4%	0.259	2%
5,6-Dimethyl-1H-benzotriazole	18	0%	0.268	1%
Acetylsulfamethoxazole	16	0%	0.271	1%
Acetylsulfamerazine	14	2%	0.244	0%
Azithromycin	13	4%	0.244	3%
Benzotriazole	10	0%	0.247	1%
Bisoprolol	12	0%	0.259	0%
Carbamazepine	16	0%	0.293	0%
Citalopram	14	0%	0.273	1%
Clarithromycin	19	0%	0.290	1%
Clindamycin	12	0%	0.248	1%
Cyclophosphamide	11	5%	0.269	2%
Diuron	22	5%	0.324	3%
Erythromycin	16	0%	0.269	1%
Fenofibrate	25	0%	0.410	1%
Gemfibrozil	25	0%	0.373	2%
Ibuprofen	20	0%	0.334	0%
Ifosfamide	10	0%	0.274	1%
Iohexol	8	8%	0.184	3%
Iomeprol	7	0%	0.189	3%
Iopamidol	8	8%	0.200	3%
Iopromide	8	7%	0.216	2%
Metconazole	23	0%	0.361	3%
Metoprolol	10	6%	0.242	1%
Metronidazole	8	0%	0.220	2%
Naproxen	23	3%	0.326	2%
Paracetamol	10	6%	0.219	0%
Phenazone	9	7%	0.246	2%

Analyt	Mean fraction number of D1	RSD	Mean retention time of D2 / min.	RSD
Prednisolone	18	3%	0.278	3%
Propyphenazone	14	0%	0.310	1%
Roxithromycin	18	0%	0.275	0%
Simvastatin	23	0%	0.405	2%
Sotalol	6	0%	0.199	0%
Sulfadiazine	9	11%	0.235	3%
Sulfadimidine	10	0%	0.255	2%
Sulfamethoxazole	12	0%	0.272	0%
Sulfapyridine	10	6%	0.240	2%
Tamoxifen	19	0%	0.323	1%
Terbutryn	18	3%	0.307	3%
Tramadol	8	0%	0.245	0%
Trimethoprim	10	0%	0.225	2%
Venlafaxine	10	0%	0.262	0%

6.7.7 Simulated distribution pattern (6x6 bins)
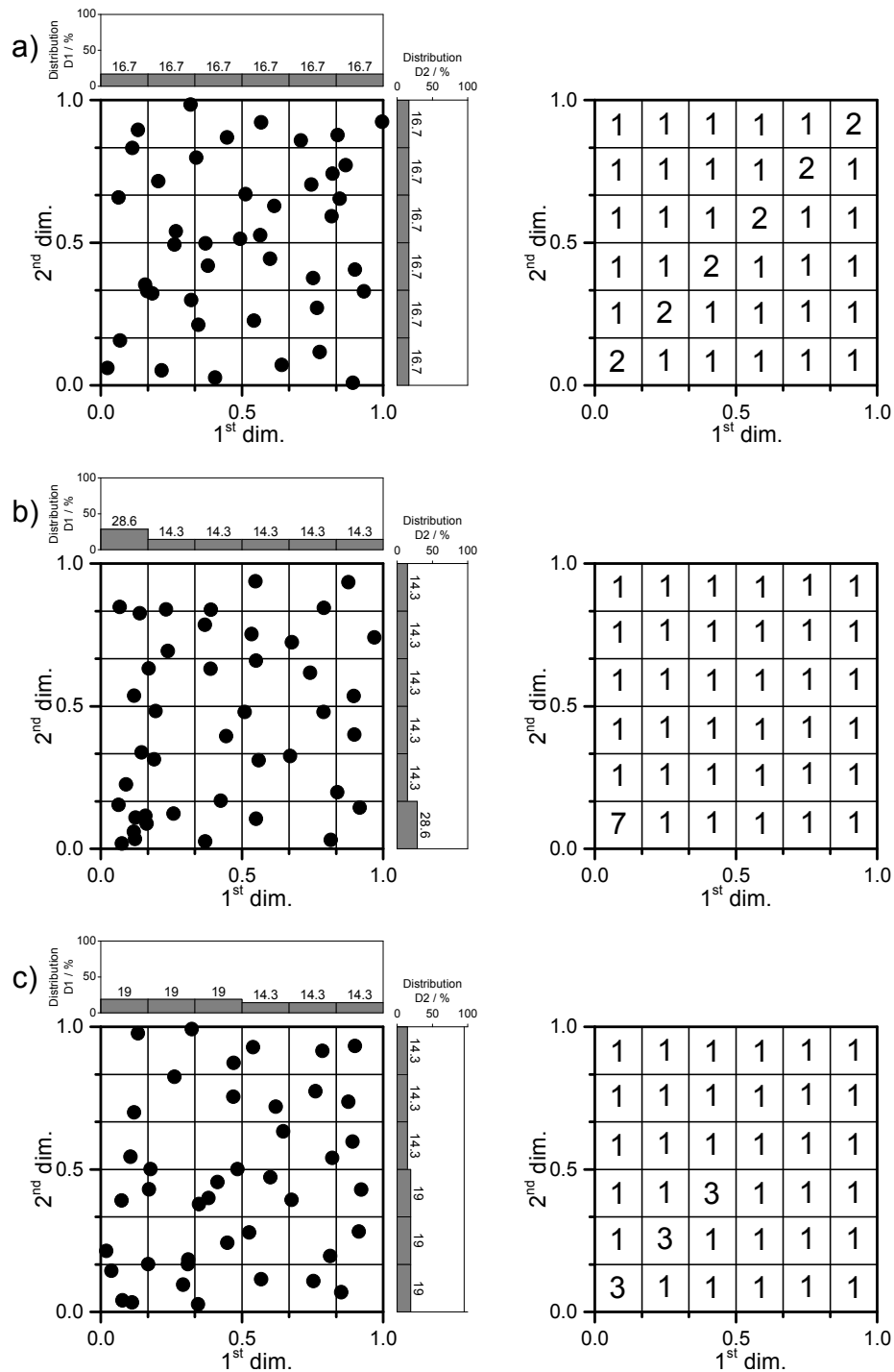
Figure S 6-6a-c: Comparison of different simulated distribution pattern. The left side shows the simulated dot-plot and the right side the distribution pattern (6x6 bins). For the simulation of the dot-plots a), b) and c) 42 data points were used.
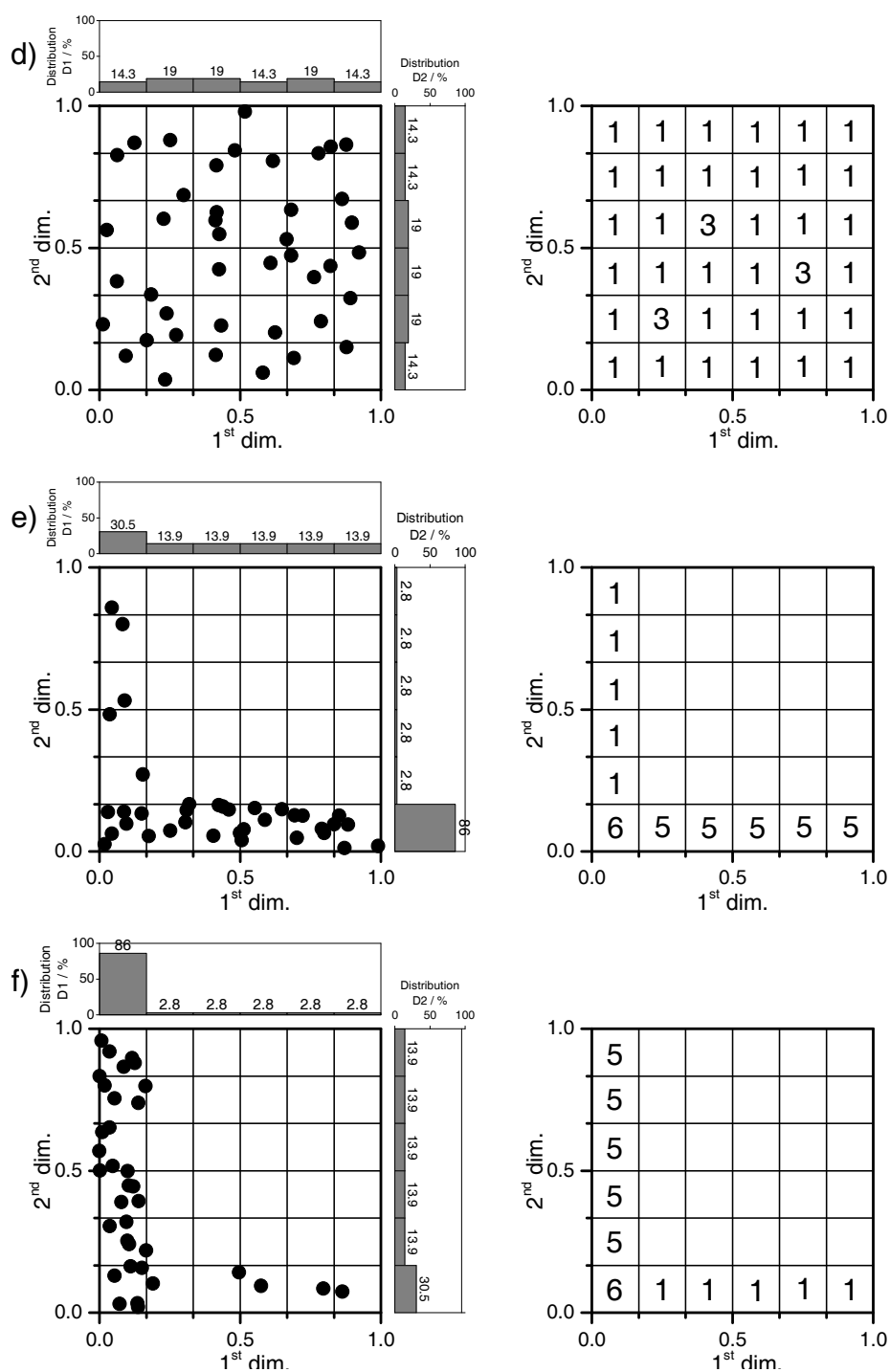
Figure S 6-6d-f: Comparison of different simulated distribution pattern. The left side shows the simulated dot-plot and the right side the distribution pattern (6x6 bins). For the simulation of the dot-plot d) 42 data points and for e) and f) 36 data points were used.
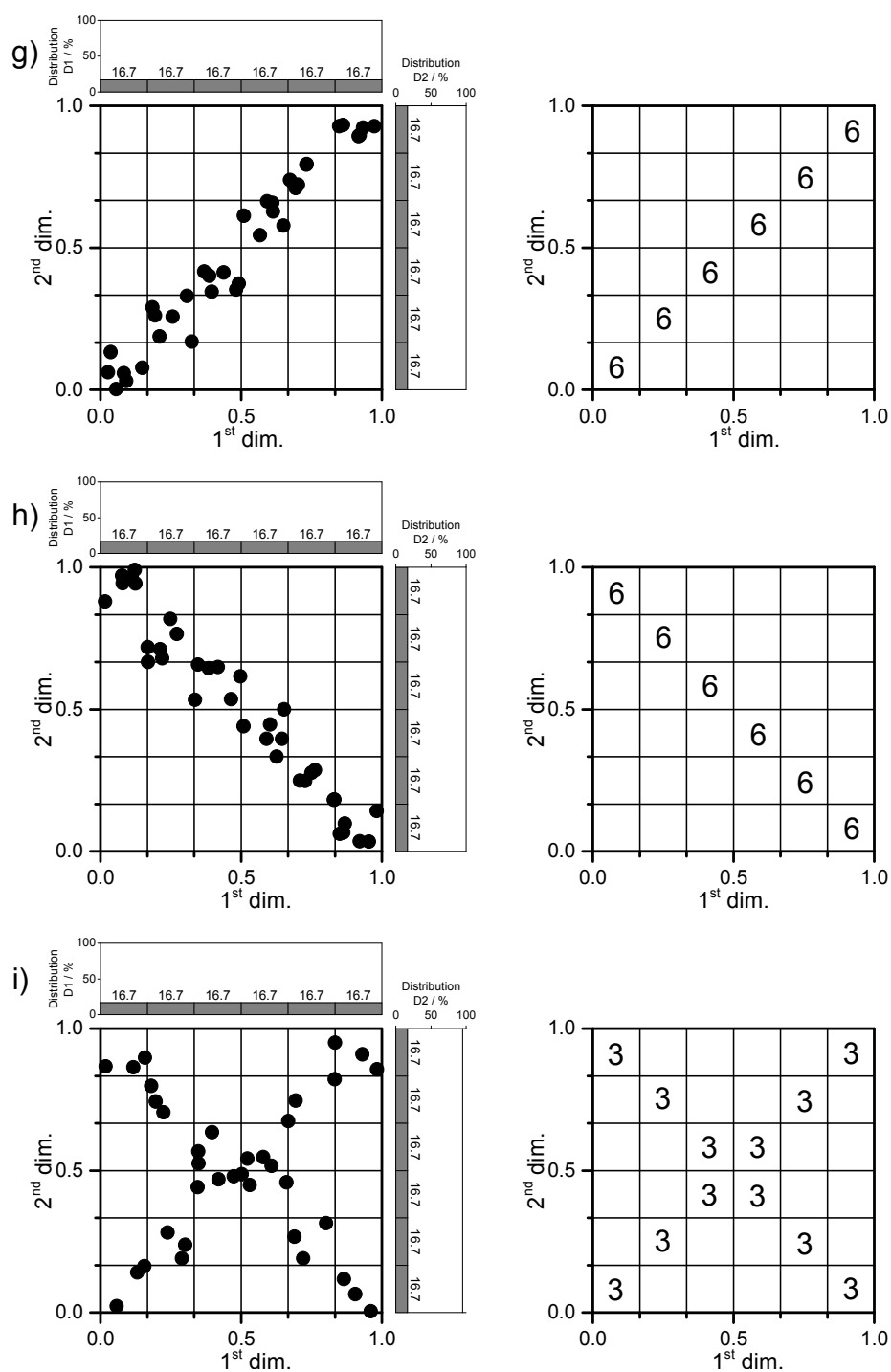
Figure S 6-6g-i: Comparison of different simulated distribution pattern. The left side shows the simulated dot-plot and the right side the distribution pattern (6x6 bins). For the simulation of the dot-plots g), h) and i) 36 data points were used.
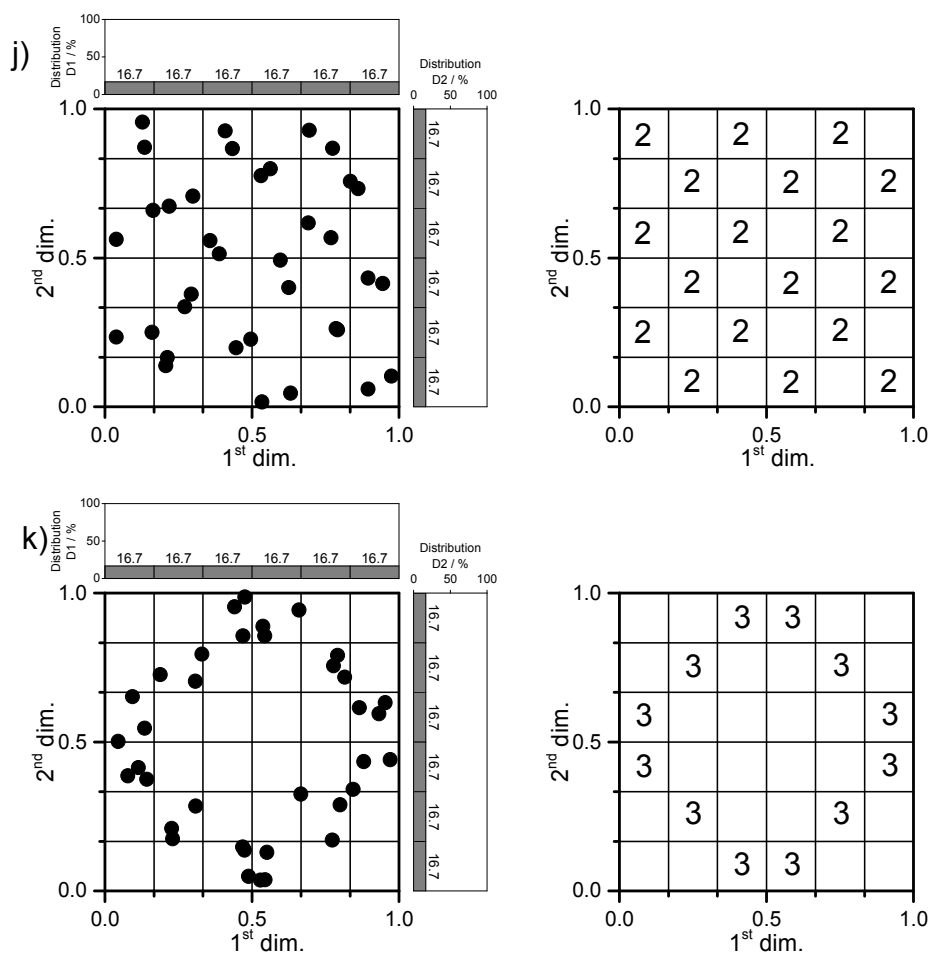
Figure S 6-6j-k: Comparison of different simulated distribution pattern. The left side shows the simulated dot-plot and the right side the distribution pattern (6x6 bins). For the simulation of the dot-plots j) and k) 36 data points were used.

Table S 6-7:   Evaluated data for the simulated data-plots of Figure S 6-6a-k (6x6 bins). The orthogonality values were calculated according to the *Bin Counting* method.

Cluster	SD_{first}	SD_{second}	SD_{total}	O
a	0	0	0	132
b	13	13	18	132
c	6	6	8	132
d	6	6	8	132
e	15	76	78	22
f	76	15	78	22
g	0	0	0	0
h	0	0	0	0
i	0	0	0	26
j	0	0	0	53
k	0	0	0	26

The results given in Table S 6-7 reveal the following findings.

1. Independent of the orthogonality value, the histograms and therefore the *SD* values provide information about clustering (see cluster Figure S 6-6a-f).

2. A good distribution across both dimensions is not a reason for a high orthogonality value (see clusters Figure S 6-6g-i and k).

3. A high orthogonality value does not exclude a clustering (see clusters Figure S 6-6b-d).

Additionally, nine different distribution pattern (5x5 bins) were simulated to demonstrate the applicability of the described concept of this work to a smaller data set of 25 compounds see (Figure S 6-7a-i and Table S 6-8).

6.7.8 Simulated distribution pattern (5x5 bins)
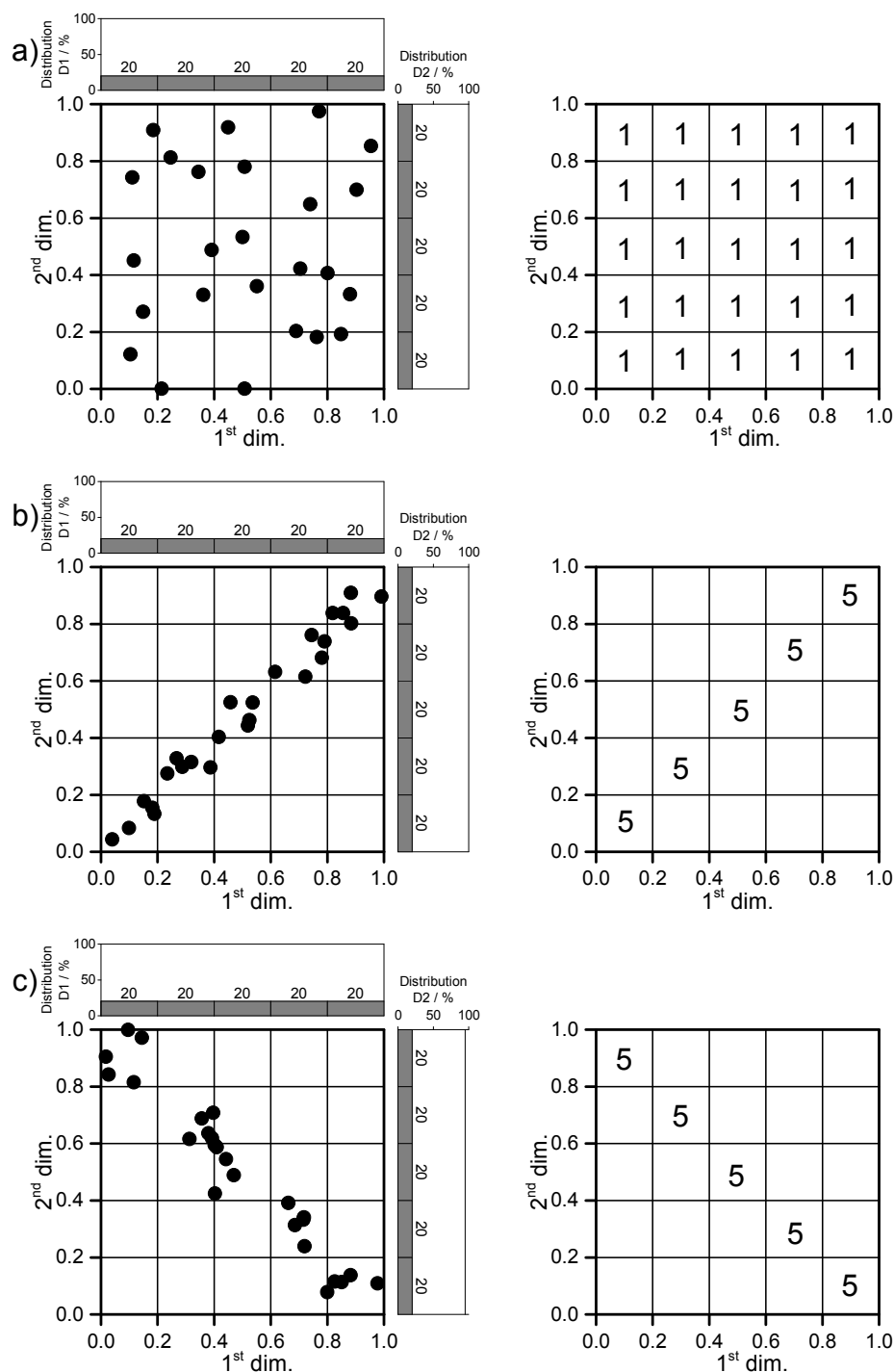
Figure S 6-7a-c: Comparison of different simulated distribution pattern. The left side shows the simulated dot-plot and the right side the distribution pattern (5x5 bins). For the simulation of the dot-plots a), b) and c) 25 data points were used.
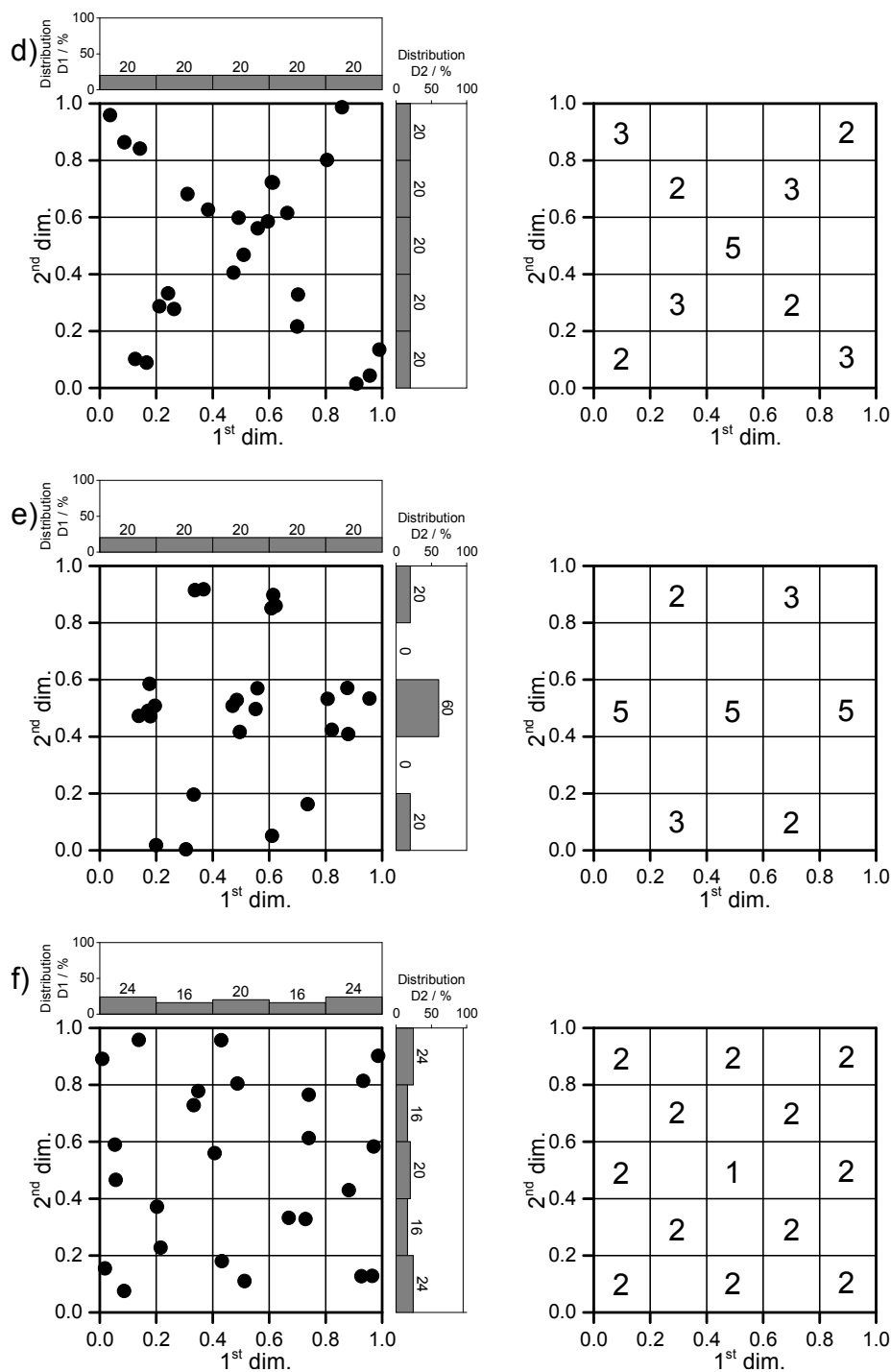
Figure S 6-7d-f: Comparison of different simulated distribution pattern. The left side shows the simulated dotplot and the right side the distribution pattern (5x5 bins). For the simulation of the dot-plots d), e) and f) 25 data points were used.
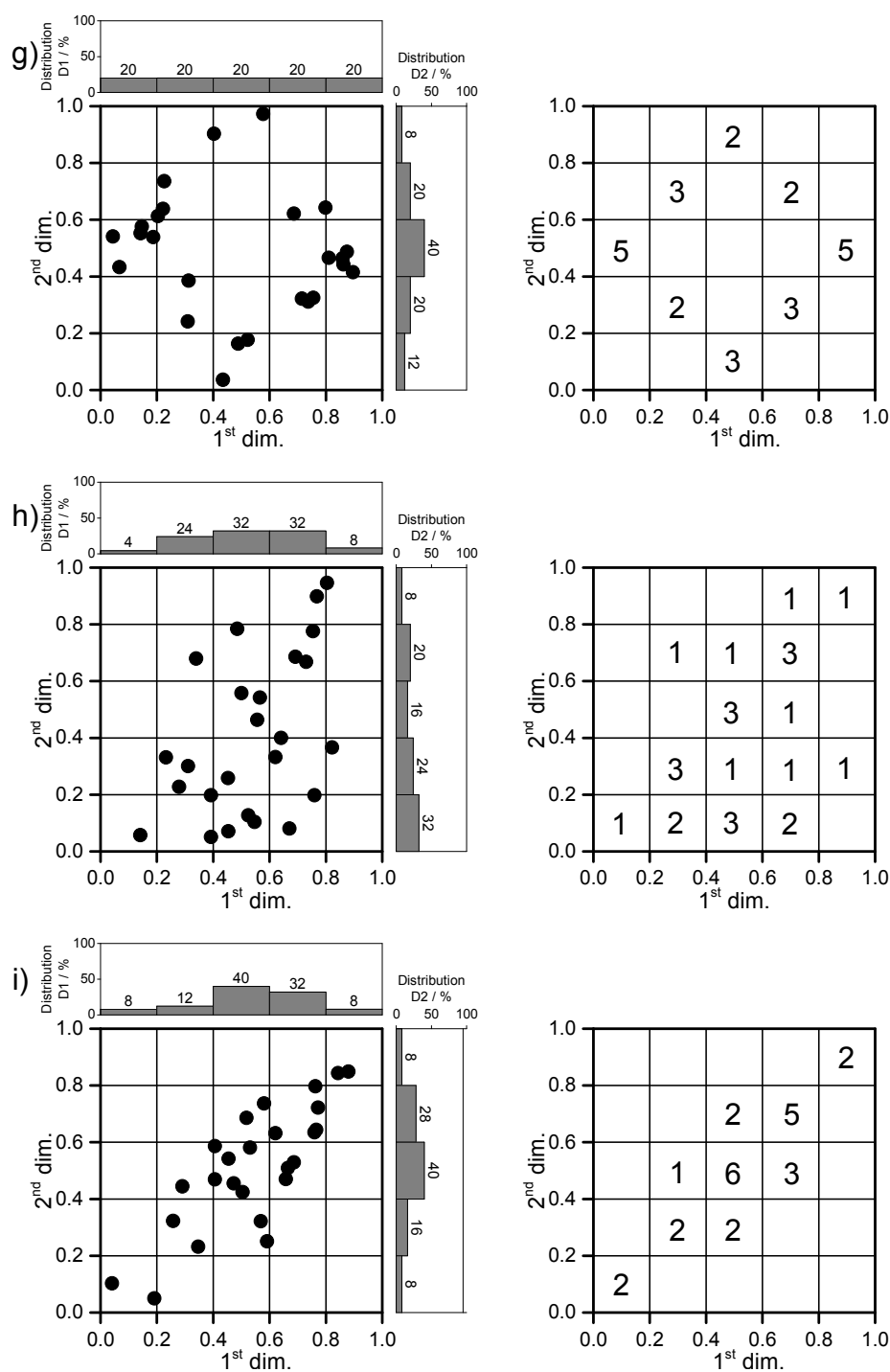
Figure S 6-7g-i: Comparison of different simulated distribution pattern. The left side shows the simulated dotplot and the right side the distribution pattern (5x5 bins). For the simulation of the dot-plots g), h) and i) 25 data points were used.

Table S 6-8:   Evaluated data for the simulated data-plots of Figure S 6-7a-k (5x5 bins). The orthogonality values were calculated according to the *Bin Counting* method.

Cluster	SD_{first}	SD_{second}	SD_{total}	O
a	0	0	0	127
b	0	0	0	0
c	0	0	0	0
d	0	0	0	25
e	0	49	49	13
f	8	8	11	51
g	0	25	25	19
h	27	18	32	63
i	30	28	41	25

The results given in Figure S 6-7a-i and Table S 6-8, confirmed the mentioned findings.

1.   Independent of the orthogonality value, the histograms and therefore the *SD* values provide information about clustering (see cluster Figure S 6-7e-i).

2.   A good distribution across both dimensions is not a reason for a high orthogonality value (see clusters Figure S 6-7b-d).

3.   A high orthogonality value does not exclude a clustering (see clusters Figure S 6-7h).

6.7.9 Comparison of peak distribution obtained with a 50 mm long PGC phase and 10 mm PGC / Cyano phases combination
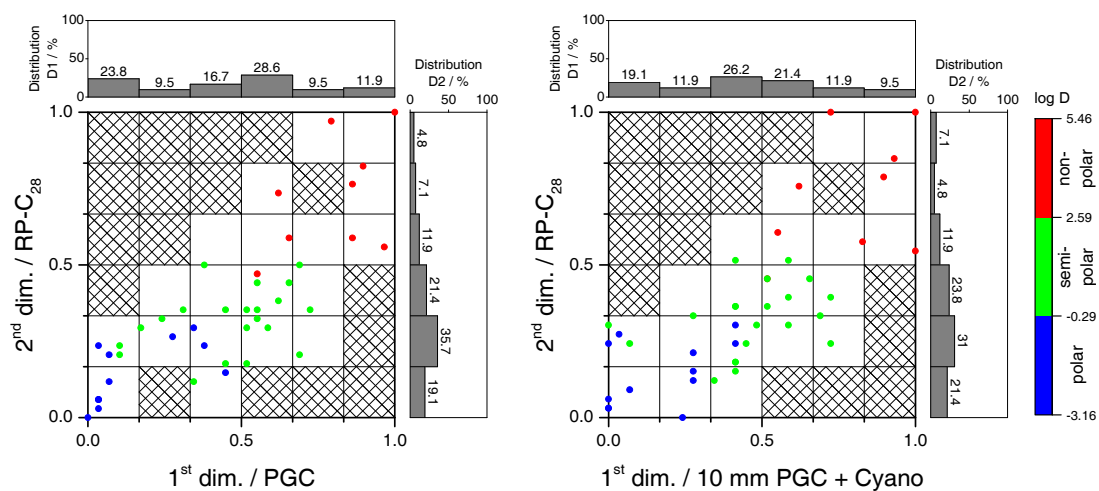
Figure S 6-8: Comparison of peak distribution across the normalized separation space obtained with a 50 mm long PGC phase (left) and 10 mm PGC / Cyano phases combination (right) in the first dimension.

Chapter 7   General conclusions and outlook

Based on the results of this work it was possible to eliminate weaknesses of the developed microscale 2D-LC system. The studies showed the enourmous potential of this system in comparison to classical 1D-LC and provided general procedures for the evaluation of complex data sets as well as orthogonality optimization.

The system comparison discussed in Chapter 3 showed that the additional selectivity of the microscale 2D-LC system can be of high importance for compound identification, which makes it suitable for non-target or suspected-target analysis of complex samples. The additional advantage of the microscale 2D-LC system is the reduced mobile phase comsumption, better hyphenation to mass spectrometry and less matrix introduction into the MS source.

The studies of this work demonstrate that PGC is a well suited stationary phase material for large volume injection of aqueous samples containing a broad range of polarity. Polar compounds can be focussed much better as on classical C18 material. However, some aspects must be considered when dealing with this material. For non-polar compounds the PGC phase results in exceptionally strong interactions and therefore pronounced tailing, especially for long columns. This work shows that it is more advantageous to use a short PGC pre-column in combination with an additional main column with a different selectivity instead of one single PGC main column.

The use of such a PGC pre-column concept with an additional main column with another selectivity in the first dimension of the microscale 2D-LC increases the system orthogonality due to the additional selectivity, which was confirmed by the orthogonality study of this work.

In terms of the total analysis time, a reduction from 104 minutes to 34 minutes could be achieved. This value is almost identical to the cycle times of one-dimensional screening methods used for the analysis of complex samples, where frequently a cycle time of about 30 minutes is used [1–4]. In contrast, the analysis time for the separation of complex samples by the two-dimensional separation is typically > 60 minutes [6–9]. The modulation time could be reduced from 60 to 30 seconds. For the developed microscale 2D-LC system, these values can be considered to be optimal. A further reduction of the modulation time down to 15 seconds results in a wrap around effect [5] which is the reason why it was not further explored in this work.

A common problem of multidimensional chromatography is the compatibility of the mobile pase of both dimensions. In contrast to reports in literature [10, 11], it is irrelevant wether an NPxRP system or RPxRP system is established in full gradient mode, since there will always be fractions with a high load of organic solvent, which decreases the band focussing on the second dimension. For a better compatibility of mobile phases an online dilution concept, which does not require an additional dilution pump and minimizes the risk of solvent incompatibility was developed. Applying such an online dilution concept based on serially coupled micro-LC columns, it is possible to dilute the injected solution and reduce the organic content, which counteracts the peak broadening. For a one dimensional separation this concept is applicable and allows to inject a twice higher sample volume without additional peak broadening. Applying the same concept on the second dimension of the microscale 2D-LC, a diadvantage is observed. The additional gradient delay volume resulting from the additional dilution column decreases the performance of the second dimension and increases the modulation time, which is necessary to prevent the wrap around effect. In consequence of that, the performance of the first dimension must be deteriorated to produce broader peaks on the first dimension to fulfill the M-S-F criterion. Therefore, this concept for online comprehensive 2D-LC cannot be generally used for all 2D separations. It is very well suited though for heart-cut 2D-LC or sLCxLC, where only a limited number of fractions are reanalyzed on the second dimension column.

Another aspect of this thesis was to further develop the concept of orthogonality for method development in 2D-LC. As described in the literature [12], it could be confirmed that the *Bin Counting* method provides realistic orthogonality values for small data sets, however, without the important information about the peak distribution. Therefore, the new concept is based on the *Bin Counting* method.

The new concept of the peak distribution across the separation space provides the information about peak distribution, possible clustering areas and the optimal selection of stationary phases in combination with the orthogonality value. Additionally, the effort to determine the optimum column combination is minimal, since each column of the first and each column of the second dimension needs only to be measured once in any desired combination. The optimal column combination can then be deduced according to the respective distribution across the first and second dimension.

Outlook

The multidimensional system in its current state offers options for further developments and improvements on the hardware as well as the software side. For example, the disadvantage of the pneumatic D2 syringe pumps is not eliminated. The new device generation from the same manufacturer is also based on pneumatic syringes and not continuous-flow pumps. Therefore, the pump refill procedure is still a disadvantage. However, alternative platforms from other manufacturers do not fulfill the necessary specifications and work with flow-splitters and/or have very large gradient delay volumes. Thus, an alternative splittless continuous-flow pump is still not commercially available and should be developed.

For better solvent compatibility and a reduction of the organic solvent transferred to the second dimension in an RPxRP system, a temperature gradient elution could be applied in the first dimension to prevent peak broadening in the second dimension. This concept can be a well suited alternative to the online dilution concept described in Chapter 5 and was already evaluated for a conventional 2D-LC system [15]. However, the mainly discussed disadvantage is the extended time (40 minutes) for the thermal re-equilibration. The re-equilibration time can be reduced by using nano- or micro-LC columns in combination with miniaturized column ovens, as a result of a lower thermal mass. Additionally, special column ovens with active cooling could be used to reduce the re-equilibration time.

Moreover, for mass spectrometric compound identification, information dependent acquisition (IDA) mode was used to collect MS/MS information. However, it became clear that modern mass spectrometers are not fast enough to obtain MS/MS information for all detectable ions (see Chapter 3). The all-ion fragmentation (AIF) mode can be an alternative approach to IDA and should be tested. Applying AIF mode, all ions will be fragmented without a prior ion isolation [13]. This method does not provide a specific MS/MS spectrum for an isolated ion. Rather, it provides an MS/MS spectrum of all fragments for all ions at the corresponding retention time [14]. An exact allocation of all fragments to the corresponding ions is not possible as well as the retrospective reconstruction of MS/MS spectra to the corresponding ion. Therefore, the sample must be measured at first in scan mode to get the retention time of the ions and then only in AIF mode to obtain the retention time of the fragments. The analyte identification can be done by retention time matching of ions and the corresponding suspected fragments. If the retention time of all suspected fragments is exactly the same, the probability

that they belong to the suspected compound or ion is very high. This approach does not provide an absolute confirmation and the possible identification of unknowns should be proved by reference standards, but it provides much more information for compounds of low intensity, which cannot be selected if IDA is used.

The evaluation of the highly complex data sets is still very difficult and time consuming. Especially for the current miniaturized 2D-LC system there is no commercially available data processing software, which can handle the data files. In this context, future research should be focused on data evaluation algorithms, which allow an automated data processing like peak finding/detection and identification. New data processing concepts based on one-dimensional non-target analysis of unknown samples [4] should be evaluated for the two-dimensional approach as well. First efforts for the visualization are already presented in Chapter 2. The implementation of this concept in an alternative (~ 15x) faster and resource efficient Python environment is already under development by the author of this thesis. Additionally it is based on the open source data formats mzML and/or mzXML. The advantage of open source formats is the independence from manufacturers' software. This program will be finished within the next months, but it can be used only for data visualization (2D-LC-TIC-Plot) and not for automated peak finding or extracted ion chromatograms (2D-LC-EIC-Plot). However, these data evaluation algorithms should be further developed to handle the big data in an acceptable time to make the miniaturized 2D-LC system suitable for routine analysis.

The future hardware developments should be focused on the hyphenation of the microscale 2D-LC to the ion mobility spectrometry (IMS), which can be used as an additional separation dimension. Stephan et al. already introduced the hyphenation of IMS as a fourth dimension within an LC+LC-IM-qTOF-MS system with impressive results regarding to peak capacity and orthogonality [16, 17]. Additionally, the microscale LC+LC approach should be evaluated, which could counteract the dilution resulted by the modulation of the LCxLC approach. Higher signal intensity on the second dimension and therefore higher probability for compound detection as well as a simplified data evaluation could be the advantageous aspects of this approach.

7.1 References

1. Schlüsener MP, Kunkel U, Ternes TA. Quaternary Triphenylphosphonium Compounds: A New Class of Environmental Pollutants. Environ Sci Technol; 2015;49(24):14282–91

2. Vom Eyser C, Palmu K, Otterpohl R, Schmidt TC, Tuerk J. Determination of pharmaceuticals in sewage sludge and biochar from hydrothermal carbonization using different quantification approaches and matrix effect studies. Anal Bioanal Chem; 2015;407(3):821–30

3. Vom Eyser C, Schmidt TC, Tuerk J. Fate and behaviour of diclofenac during hydrothermal carbonization. Chemosphere; 2016;153:280–6

4. Bader T, Schulz W, Kümmerer K, Winzenbacher R. General strategies to increase the repeatability in non-target screening by liquid chromatography-high resolution mass spectrometry. Anal Chim Acta; 2016.

5. Gassner O. Optimierung eines Nano x Mikro 2D-HPLC-Systems zur Abwasseranalytik mit splitlos gekoppeltem MS. Master thesis, Fachbereich Chemie, Hochschule Niederrhein / University of Applied Sciences: Krefeld, Germany, 2016

6. Sarrut M, D'Attoma A, Heinisch S. Optimization of conditions in on-line comprehensive two-dimensional reversed phase liquid chromatography. Experimental comparison with one-dimensional reversed phase liquid chromatography for the separation of peptides. J Chromatogr A; 2015:48–59

7. Willmann L, Erbes T, Krieger S, Trafkowski J, Rodamer M, Kammerer B. Metabolome analysis via comprehensive two-dimensional liquid chromatography: identification of modified nucleosides from RNA metabolism. Anal Bioanal Chem; 2015.

8. Donato P, Rigano F, Cacciola F, Schure M, Farnetti S, Russo M, Dugo P, Mondello L. Comprehensive two-dimensional liquid chromatography–tandem mass spectrometry for the simultaneous determination of wine polyphenols and target contaminants. J Chromatogr A; 2016:54–62

9. Malik MI, Lee S, Chang T. Comprehensive two-dimensional liquid chromatographic analysis of poloxamers. J Chromatogr A; 2016:33–41

10. Carr PW, Stoll DR. Two-Dimensional Liquid Chromatography - Principles, Practical Implementation and Applications. Online resource: http://www.agilent.com/cs/library/primers/public/5991-2359EN.pdf. Accessed 9 October 2016

11. Jandera P. Comprehensive Two-Dimensional Liquid Chromatography - Practical impacts of theoretical considerations. A review. Cent Eur J Chem; 2012;10(3):844–75

12. Gilar M, Fridrich J, Schure MR, Jaworski A. Comparison of orthogonality estimation methods for the two-dimensional separations of peptides. Anal Chem; 2012;84(20):8722–32

13. Zhu X, Chen Y, Subramanian R. Comparison of information-dependent acquisition, SWATH, and MS(All) techniques in metabolite identification study employing ultrahigh-performance liquid chromatography-quadrupole time-of-flight mass spectrometry. Anal Chem; 2014;86(2):1202–9

14. Leendert V, Van Langenhove H, Demeestere K. Trends in liquid chromatography coupled to high-resolution mass spectrometry for multi-residue analysis of organic micropollutants in aquatic environments. TrAC-Trend Anal Chem; 2015;67:192–208

15. Holland BJ, Conlan XA, Francis PS, Barnett NW, Stevenson PG. Overcoming solvent mismatch limitations in 2D-HPLC with temperature programming of isocratic mobile phases. Anal Methods; 2016;8(6):1293–8

16. Stephan S, Jakob C, Hippler J, Schmitz OJ. A novel four-dimensional analytical approach for analysis of complex samples. Anal Bioanal Chem; 2016;408(14):3751–9

17. Stephan S, Hippler J, Köhler T, Deeb AA, Schmidt TC, Schmitz OJ. Contaminant screening of wastewater with HPLC-IM-qTOF-MS and LC+LC-IM-qTOF-MS using a CCS database. Anal Bioanal Chem; 2016;408(24):6545–55

Chapter 8   Appendix

8.1 List of abbreviations and symbols

1D	one-dimensional
$^1t_{R,norm}$	normalized fraction number in the first dimension
2D	two-dimensional
$^2t_{R,norm}$	normalized retention time in the second dimension
3D	three-dimensional
5-FU	5-fluorouracil
A	aqueous mobile phase
AC-S	Acetyl-sulfamerazine
AIF	all ion fragmentation
A_O	Orthogonality according to the *Asterisk* method
$A_{S,0.1}$	peak asymmetry factor at 10% height
ASCII	american standard code for information interchange
A_x	surface
B	organic mobile phase
B_{max}	maximum bin number
BS	size of the bins
C18	octadecylsilane
C28	octacocylsilane
CA	California
CC-LVI	coupled column large volume injection
CE	collision energy
CEP	collision cell entrance potential
cm	centimeter
CN	cyano
col.	column
cps	counts per second
CXP	cell exit potential

D1	first dimension
$D1_{first}$	retention time of the first eluted compound on the first dimension
$D1_{last}$	retention times of the last eluted compound on the first dimension
D2	second dimension
$D2_{first}$	retention time of the first eluted compound on the second dimension
$D2_{last}$	retention times of the last eluted compound on the second dimension
Da	dalton (atomic mass unit)
$d_{c,1}$	inner diameter of the first dimension column
$d_{c,2}$	inner diameter of the second dimension column
dim.	dimension
DOI	digital object identifier
DP	declustering potential
D_x	percentage distribution of segment x
$D_{x\,(orthogonal)}$	percentage distribution of segment x for a fully orthogonal system
e. g.	exempli gratia
EP	entrance potential
ESI	electrospray ionization
etc.	et cetera
eV	electronvolt
FA	formic acid
FEN	fenofibrate
FS	fused-silica
F_X	fraction number
GC	gas chromatography
GCxGC	comprehensive two-dimensional gas chromatography
HILIC	hydrophilic interaction chromatography
HPLC	high-performance liquid chromatography
HRMS	high resolution mass spektrometry

i.d.	inner diameter
IDA	information dependent acquisition
IEC	ion-exchange chromatography
k	retention factor
kpsi	1000 psi
LC	liquid chromatography
LC-LC	heart-cut 2D-LC
LCxLC	comprehensive 2D-LC
LC+LC	large fractions 2D-LC
log D	octanol-water distribution coefficient
log P	logarithmic octanol-water partition-coefficient
LVI	large volume injection
M	molecule
mAU	milli absorbance units
μg	microgram
mg	milligram
μL	microliter
μLC	micro-LC
mL	milliliter
min	minutes
MRM	multiple reaction monitoring
ms	milliseconds
M-S-F	Murphy–Schure–Foley criterion
MW	molecular weight
m/z	mass-over-charge ratio
n_c	peak capacity
n_{c1}	peak capacities of the first dimension
n_{c2}	peak capacities of the second dimension
$n_{c,2D}$	total peak capacity
$NC_{area,x}$	number of compounds eluting inside the respective segment

NC_{total}	total number of compounds
ng	nanogram
nL	nanoliter
nm	nanometer
NP	normal phase (chromatography)
O	orthogonality
o.d.	outer diameter
p. a.	pro analysi
PEEK	polyether ether ketone
PFP	pentafluorophenyl
pg	picogram
PGC	porous graphitic carbon
pH	"potentia Hydrogenii" – negative decimal logarithm of the hydrogen ion activity
ppm	parts per million
psi	pound-force per square inch
puris.	purissimum
Q1	precursor-ion mass
Q3	product-ion mass
R^2	coefficient of determination
ref.	reference
RP	reversed phase (chromatography)
RSD	relative standard deviation
$RT_{i(norm)}$	normalized fraction number of the first dimension or normalized retention time of the second dimension
RT_{max}	fraction number or retention time of the most retained compound
RT_{min}	fraction number or retention time of the least retained compound
s	second
SC-LVI	single column large volume injection
SD	distribution as the square root of the sum of the squares of the differences between the respective D_x values and $D_{x\ (orthogonal)}$
SEC	size-exclusion chromatography

sLCxLC	selected heart-cup 2D-LC
S/N	signal-to-noise
SPE	Solid-phase extraction
S_X	one segment of the elution window
S_{Z_x}	spread of peaks according to *Asterisk* method
t_g	gradient time
TIC	total ion current
ToF	Tome-of-flight
t_R	retention time
t_x	elution time
UV	Ultraviolet (spectroscopy)
V	volt
v	volume percent
Vis	visible (spectroscopy)
Vm	volume
$w_{0.1}$	peak width at 10% height
$\bar{w}$	mean peak width
WIFF	Sciex raw data file format
XIC	extracted ion chromatogram
z	number of transferred fractions on the second column
ZIM	Zentrales Innovationsprogramm Mittelstand
Z_x	definition of lines according to *Asterisk* method
°C	degree Celsius
>	greater-than
<	less-than
*.txt	text file
$[M+H]^+$	protonated molecule
σ	standard deviation
Δ	delta
$\Delta\, i.d.$	relative difference of the column inner diameters of the two coupled LC dimensions

$\Delta\,t_R$ retention time deviation

8.2 List of Figures and Figures S

8.3 List of Tables and Tables S

8.4 Publications

Articles in peer-reviewed journals

Haun, J.; Leonhardt, J.; Portner, C.; Hetzel, T.; Tuerk, J.; Teutenberg, T.; Schmidt, T. C. *Online and Splitless NanoLC × CapillaryLC with Quadrupole/Time-of-Flight Mass Spectrometric Detection for Comprehensive Screening Analysis of Complex Samples.* Analytical Chemistry 2013, 85 (21), 10083-10090.

Leonhardt, J.; Hetzel, T.; Teutenberg, T.; Schmidt, T. C. *Large volume injection of aqueous samples in nano liquid chromatography using serially coupled columns.* Chromatographia, January 2015, 78 (1 – 2), 31 – 38.

Leonhardt, J.; Teutenberg, T.; Tuerk, J.; Schluesener, M. P.; Ternes, T. A.; Schmidt, T. C. *A comparison of one-dimensional and microscale two-dimensional liquid chromatographic approaches coupled to high resolution mass spectrometry for the analysis of complex samples.* Analytical Methods, 2015, 7, 7697 – 7706.

Teutenberg, T.; Schmidt, T. C.; Haun, J.; Leonhardt, J. *Conceptual Framework of Miniaturized Online LC x LC Coupled to Hybrid High Resolution Mass Spectrometry.* LCGC Europe, accepted 2016.

Leonhardt, J.; Teutenberg, T.; Buschmann, G.; Gassner, O.; Schmidt, T. C. *A new method for the determination of peak distribution across a two-dimensional separation space for the identification of optimal column combinations.* Analytical and Bioanalytical Chemistry, doi:10.1007/s00216-016-9911-3, online available since 09/13/2016.

Other articles

Teutenberg, T.; Haun, J.; Leonhardt, J.; Portner, C. *Potenziale und Anwendung der umfassenden zweidimensionalen Flüssigkeitschromatografie.* Analytik News, publication date: 03/02/2012. URL: http://www.analytik-news.de/Fachartikel/2012/10.html.

Teutenberg, T.; Leonhardt, J.; Haun, J.; Wiese, S.; Wenkel, N. *Mikro-LC - Nur das ewige Talent?* GIT Labor-Fachzeitschrift 2012, Issue 04/2012, 246-248.

Teutenberg, T.; Leonhardt, J.; Haun, J.; Portner, C. *Die zweite Dimension – Neue Entwicklungen in der 2D-Flüssigkeitschromatographie.* LaborPraxis 2012, Issue 10/2012. URL: http://www.laborpraxis.vogel.de/analytik/chromatographie/hplc/articles/382538

Teutenberg, T.; Leonhardt, J.; Wiese, S. *Method Development for Fast Separation of Polycyclic Aromatic Hydrocarbons Using Micro-LC – The Importance of the Dwell Volume.* The Column, Volume 8, Issue 13 (2012) 9-12.

Teutenberg, T.; Leonhardt, J.; Hetzel, T.; Freihoff, S.-D.; Tuerk, J. Bettermann, H.; Fischer, B. *Do we really need chromatography? The role of chromatography and different detection techniques in the context of mass spectrometry.* Separation 1/2013, 8-12.

Teutenberg, T.; Türk, J.; Leonhardt, J.; Hetzel, T.; Freihoff, S.-D.; Bettermann, H.; Fischer, B. *Brauchen wir die Chromatographie wirklich? Die Rolle der Chromatographie und anderer Nachweistechniken im Kontext der MS.* GIT Labor-Fachzeitschrift, 11, 2013, 690-695.

Teutenberg, T.; Freihoff, S.-D.; Hetzel, T.; Leonhardt, J. *Warten auf die Zukunft? Nano-, Mikro- und zweidimensionale HPLC zeigen sich heute schon stark.* q&more, 01.14, 36 – 40.

Teutenberg, T.; Leonhardt, J. *Peak versus Peak capacity – The role of comprehensive two-dimensional liquid chromatography.* GIT Separation 2/2014, 20 – 21.

Teutenberg, T.; Leonhardt, J. *Miniaturisierte zweidimensionale Chromatographie gekoppelt mit Massenspektrometrie – Wie weit ist die Praxis noch von der Theorie entfernt?* chrom+food FORUM, Issue 03/2015, 40-42.

Teutenberg, T.; Hetzel, T.; Loeker, D.; Leonhardt, J.; Schulze, P. *Steht die Ampel auf Grün? - Der Weg der Mikro-LC in die Routineanalytik.* GIT Labor-Fachzeitschrift, 5-6, 2016, 18-21.

Teutenberg, T.; Hetzel, T.; Loeker, D.; Leonhardt, J. *Von der Farbschreibung zur modernen Chromatographie – Ein historischer Überblick.* GIT Labor-Fachzeitschrift, 10, 2016, 49-50.

Books chapters

Teutenberg, T.; Leonhardt, J. *2D-Chromatography - potentialities and limitations.* In: Kromidas S. (editor) *The HPLC-Expert II: Find and Optimize the Benefits of your HPLC/UHPLC.* Wiley; 2017, ISBN: 978-3-527-33972-3

Tuerk, J.; Boergers, A.; Leonhardt, J.; Portner, C.; Gehrmann L.; Teutenberg, T. *Target analysis, suspected-target and non-target screening for evaluation and comparison of full-scale ozonation at three wastewater treatment plants.* In: Drewes J. E. and Letzel T. (editors) *Towards Harmonized Strategies and Workflows to Assess Transformation Products of Chemicals of Emerging Concern by Non-Target and Suspect Screening.* ACS Books, Washington, DC, USA, 2017

Oral presentations

Leonhardt, J.; Haun, J.; Teutenberg, T.; Portner, C.; Hetzel, T.; Tuerk, T. *Development of a comprehensive two-dimensional nano-/capillary-LC system with mass-spectrometric detection for the screening analysis of complex samples.* AFWC Meeting, Antwerp, Belgum, 03/19 – 03/21/2014.

Leonhardt, J. *New developments related to LCxLC based on the Eksigent NanoLC 425.* AFWC Meeting, Koblenz, Germany, 04/28 – 04/30/2015.

Leonhardt, J.; Teutenberg, T.; Schmidt, T. C. *Entwicklung und Optimierung von miniaturisierten multidimensionalen chromatographischen Methoden und deren Kopplung mit der Massenspektrometrie.* 26. Doktorandenseminar des AK Separation Science, Fachgruppe „Analytische Chemie", Gesellschaft Deutscher Chemiker (GDCh), Hohenroda, Germany, 01/10 – 01/12/2016.

Leonhardt, J. *Development and optimization of miniaturized chromatographic methods and the hyphenation to mass spectrometry.* AFWC Meeting, Langenau, Germany, 04/05 – 04/07/2016.

Leonhardt, J.; Teutenberg, T.; Schmidt, T. C. *Development of a non-target time-of-flight mass spectrometric detection method for a miniaturized two-dimensional liquid chromatographic approach.* NonTarget 2016, Monte Verità, Ascona, Switzerland, 05/29 – 06/03/2016.

Poster presentations

Leonhardt, J.; Teutenberg, T.; Haun, J.; Portner, C.; Wolff, M. *Development of a comprehensive two-dimensional nano-/capillary-LC system with mass-spectrometric detection for the screening analysis of complex samples.* Analytica Conference 2012, Munich, Germany, 04/17 – 04/20/2012.

Leonhardt, J.; Teutenberg, T.; Wiese, S.; Wolff, M. *Method development using micro-LC for separation of environmentally and pharmaceutically relevant substances.* Analytica Conference 2012, Munich, Germany, 04/17 – 04/20/2012.

Leonhardt, J.; Teutenberg, T.; Haun, J.; Portner, C.; Wolff, M. *Development of a comprehensive two-dimensional nano-/capillary-LC system with mass-spectrometric detection for the screening analysis of complex samples.* 36th International Symposium on Capillary Chromatography (ISCC), Riva del Garda, Italy 05/27-06/01/2012.

Leonhardt, J.; Teutenberg, T.; Wiese, S.; Wolff, M. *Method development using micro-LC for separation of environmentally and pharmaceutically relevant substances.* 36th International Symposium on Capillary Chromatography (ISCC), Riva del Garda, Italy 05/27-06/01/2012.

Leonhardt, J.; Teutenberg, T.; Haun, J.; Portner, C.; Wolff, M. *Development of a comprehensive two-dimensional nano-/capillary-LC system with mass-spectrometric detection for the screening analysis of complex samples.* 29th International Symposium on Chromatography (ISC), Torún, Poland, 09/09-09/13/2012.

Leonhardt, J.; Hetzel, T.; Teutenberg, T.; Schmidt, T. C. *Serially coupled columns for large volume injection in nano-liquid chromatography.* ANAKON 2013, Essen, Germany, 03/04-03/07/2013.

Leonhardt, J.; Hetzel, T.; Teutenberg, T.; Schmidt, T. C. *Serially coupled columns for large volume injection in nano-liquid chromatography.* 39th International Symposium on High Performance Liquid Phase Separations and Related Techniques (HPLC 2013), Amsterdam, Netherlands, 06/16-06/20/2013.

Leonhardt, J.; Teutenberg, T.; Türk, J.; Schmidt, T. C.; Schlüsener, M. P.; Ternes, T. A. *A General strategy to compare One- and Two-dimensional Liquid Chromatographic approaches coupled to High Resolution Mass Spectrometry.* 30th International Symposium on Chromatography (ISC 2014), Salzburg, Austria, 09/14 – 09/18/2014.

Leonhardt, J.; Buschmann, G.; Loeker, D.; Wiese, S.; Teutenberg, T.; Bohrisch, J.; Schmidt, T. C. *Trenn- und Sorptionsmaterialien auf Basis von modifizierten Perlcellulosen.* ANAKON 2015, Graz, Austria, 03/23 – 03/26/2015

Hetzel, T.; Leonhardt, J.; Loeker, D.; Teutenberg, T.; Bohrisch, J. *Analytical characterization of stationary phases packed with pearl cellulose particles.* 31st International Symposium on Chromatography (ISC 2016), Cork, Ireland, 08/28/2016 – 09/01/2016

8.5 Curriculum vitae

Der Lebenslauf ist in der Online-Version aus Gründen des Datenschutzes nicht enthalten.

For reasons of data protection, the curriculum vitae is not included in this online document.

.

Curriculum vitae

Der Lebenslauf ist in der Online-Version aus Gründen des Datenschutzes nicht enthalten.

For reasons of data protection, the curriculum vitae is not included in this online document.

Curriculum vitae

Der Lebenslauf ist in der Online-Version aus Gründen des Datenschutzes nicht enthalten.

For reasons of data protection, the curriculum vitae is not included in this online document.

8.6 Erklärung (Declaration)

Hiermit versichere ich, dass ich die vorliegende Arbeit mit dem Titel

"Development and optimization of multidimensional methods based on online comprehensive microscale liquid chromatography and mass spectrometry."

selbst verfasst und keine außer den angegebenen Hilfsmitteln und Quellen benutzt habe, und dass die Arbeit in dieser oder ähnlicher Form noch bei keiner anderen Universität eingereicht wurde.

Essen, 30.09.2016

Juri Leonhardt

8.7 Acknowledgements